

**INVESTIGATION INTO THE PRODUCTION OF A
PARTICLE-IN-PARTICLE SYSTEM FOR THE TREATMENT
OF HEPATOCELLULAR CARCINOMA BY
TRANSARTERIAL CHEMOEMBOLIZATION**

Patrick Michael McCarry

December 2014

A thesis submitted to the department of Chemical Engineering

The University of Birmingham

for the Degree of Doctor of Philosophy

UNIVERSITY OF
BIRMINGHAM

University of Birmingham Research Archive

e-theses repository

This unpublished thesis/dissertation is copyright of the author and/or third parties. The intellectual property rights of the author or third parties in respect of this work are as defined by The Copyright Designs and Patents Act 1988 or as modified by any successor legislation.

Any use made of information contained in this thesis/dissertation must be in accordance with that legislation and must be properly acknowledged. Further distribution or reproduction in any format is prohibited without the permission of the copyright holder.

SUMMARY

Transarterial Chemoembolization (TACE) has become a leading therapy in patients suffering from intermediate to advanced hepatocellular carcinoma (HCC), the fifth most common cancer making it a major health issue worldwide. TACE is a non-surgical transarterial therapy that involves injection of embolizing particles and chemotherapeutic agents directly to the tumour site. Once administered through the hepatic artery, the particles block the blood flow to the tumour starving it of oxygen while also allowing targeted delivery of the anti-cancer drugs. Several therapies have proven to increase survival in people suffering from HCC where drug eluting beads (DEBs) have become a frequently used method. DEBs allow anti-cancer drugs to be loaded onto preformed beads where they are held tightly through electrostatic interactions between the drug and beads allowing high loadings and controlled release to be achieved. Despite their success, DEBs are limited to drugs that interact with the embolizing material's functional groups. Also, the embolizing beads must be calibrated to a patient's blood vessel size where smaller sized beads will display faster release rates than larger beads, potentially resulting in high toxicity peaks for some patients. In order to overcome these disadvantages, a Particle-in-Particle (PIP) system is proposed which will be produced of two main components, a drug delivery component and an embolizing component. Small microparticles (1 – 3 μm) are to be manufactured to suit a specific drug with high drug loadings and the ability to control the release rate, where they will function as the drug delivery component of the PIP system. These microparticles are then to be encapsulated into larger microparticles (100 – 1000 μm) which will act as the embolizing component of the PIP system.

Initially experiments exploring materials that were capable of controlling the release rate of small molecular weight hydrophilic drugs were investigated using verapamil hydrochloride as

the model drug. Various water soluble polymers that effectively encapsulated the compound were explored however, they were incapable of controlling the drug release of the drug. By incorporation of an inorganic material into an organic polymer, stronger gels were produced that dramatically decreased the release rate of the hydrophilic compound compared to the single organic polymer. Drug loadings and release rates could be tailored from days to weeks by adjustment of the concentration of organic polymer and inorganic material.

This organic-inorganic blend was processed into drug delivery microparticles where the effects of the processing parameters in the water in oil (w-o) emulsion and spray drying methods were investigated. In the w-o emulsion method, effects of polymer concentration, mixing speed, surfactant concentration and crosslinker concentration were assessed by light microscopy and laser diffraction where various microparticle sizes could be obtained by adjustment of the processing parameters. Production of spherical particles was seen to be highly dependent on the formation of a stable emulsion with sufficient surfactant and high crosslinking concentrations, and particle size was seen to be dependent on polymer concentration and mixing speed. Despite spherical particles being formed, the o-w emulsion method failed to encapsulate any of the hydrophilic compound. Spray drying was investigated as an alternate method since it is known to yield high entrapment efficiencies. The effects of polymer concentration, inlet temperature and feed flow rate were investigated by SEM and laser diffraction. Again, adjustment of the parameters allowed particle size to be adjusted where the feed flow rate and polymer concentration were found to highly effect particle size. Effects of polymer concentration and drug concentration on drug loading and release rate were also analysed by UV spectroscopy where alteration of the parameters allowed varied loadings and release rates to be achieved.

Production of the embolizing particle system was investigated using the w-o emulsion and nozzle vibrating methods. In the w-o emulsion method, effects of mixing speed on particle

size was analysed with light microscopy and laser diffraction where smaller spheres were produced with increased mixing speeds. Once optimum embolizing particles were produced, the drug delivery particles were loaded yielding the PIP system, where the effects of drug delivery particle loading were investigated by UV spectroscopy. This PIP system displayed similar release rates to the un-encapsulated drug delivery particles due to the embolizing materials high porosity. This allowed PIP systems of various sizes to poses similar release rates indicating that the effect of particle size on drug release rate had been decoupled, overcoming a pitfall with current TACE therapies. The system could also be used for a variety of other drugs by tailor making the inner drug delivery particles to a desired compound. A microencapsulation method that has seen limited attention in the literature based on nozzle vibrating technology was also investigated. In this method, the effects of nozzle vibration, electrode voltage and nozzle size were analysed by light microscopy and laser diffraction where spherical particles with narrow distributions within the TACE range could be produced under mild processing methods. Despite this method being highly attractive for TACE, the drug delivery particles previously produced were too large and aggregated to pass though the nozzle. An alternate to the PIP system was investigated where the organic/inorganic drug delivery blend investigated was processed using the microencapsulation device to produce a drug delivery system for the controlled release of the hydrophilic drug where effects of polymer concentration and nozzle size on drug loading and release rate was investigated. This microencapsulation device along with the organic-inorganic blend investigated gave an interesting approach to the development of a microparticle system for controlled release of hydrophilic drugs, that was well suited for TACE and other drug delivery applications.

ACKNOWLEDGEMENTS

Firstly I would like to thank my former lead supervisor Dr Rachel Bridson for giving me this opportunity and for her guidance during the first year of this project. I would also like to thank Prof Liam Grover for taking me into his research group after Dr Bridsons early departure along with my co-supervisor Dr Richard Greenwood for their help and support.

I would like to thank my former research colleague Dr Ian Lee for all of his support and drug delivery expertise that was of great assistance throughout this whole project. I would also like to thank Elaine Mitchel, David French and Ronnie of Biochemical Engineering along with Receptionist Lynn Draper for their assistance over the last three years. I would also like to thank my friends and family for the much needed help and support.

Finally I would like to acknowledge the EPSRC for funding this project along with Simon Mortimer of Buchi Switzerland for providing free trials on the Buchi B-290 Mini Spray Dryer and Buchi B-395 Pro MicroEncapsulator.

Table of Contents

CHAPTER 1 - INTRODUCTION TO HEPATOCELLULAR CARCINOMA	13
1.1 Introduction	13
1.2 Causes and risk factors in HCC	13
1.3 Surveillance and diagnosis of HCC	14
1.4 Staging of HCC	17
1.5 Curative treatments for HCC.....	19
1.5.1 Resection	19
1.5.2 Ablation	20
1.5.3 Transplantation	21
1.6 TACE	21
1.6.1 Conventional TACE	22
1.6.2 Drug eluting beads.....	24
1.7 Proposal of a new microparticle drug delivery system for TACE	26
 CHAPTER 2 - POLYMERS IN DRUG DELIVERY	 30
2.1 Introduction.....	30
2.1.1 Hydrogels in drug delivery applications	31
2.2 Alginate.....	33
2.3 Pectin.....	37
2.4 Carrageenan	38
2.5 Gellan	41
2.6 Inorganic materials in drug delivery	42
2.7 Verapamil Hydrochloride	43
2.8 Conclusion	45
 CHAPTER 3 - MATERIAL SCREENING	 46
3.1 Introduction.....	46
3.2 Materials and Methods.....	47
3.2.1 Materials	47
3.2.2 Production of the alginate and pectin beads	47

3.2.3 Production of the Gellan and Carrageenan (kappa/iota) beads	48
3.2.4 Production of the alginate/sodium silicate.....	48
3.2.5 Swelling of the polymer beads	49
3.2.6 Drug loading and encapsulation efficiency	50
3.2.7 Drug release	51
3.3 Results and Discussion	51
3.3.1 Production of the Polymer beads	51
3.3.2 Swelling of the polymer beads	53
3.3.3 Drug loading and Encapsulation efficiency of the polymer beads	55
3.3.4 Drug release from the polymer beads	58
3.4 Conclusions	62
 CHAPTER 4 - MICROPARTICLES FOR DRUG DELIVERY APPLICATIONS	63
4.1 Introduction to Microparticle Drug Delivery Systems	63
4.2 Particle production methods	66
4.2.1 Emulsions	66
4.2.2 Ionic gelation/polyelectrolyte formation	70
4.2.3 Spray Drying.....	71
4.3 Particle Characterization methods	76
4.3.1 Imaging	76
4.3.2 Particle sizing	77
4.3.3 Drug loading, Encapsulation and Drug release	78
4.3.4 Swelling	79
4.3.5 Zeta potential	79
 CHAPTER 5 - PRODUCTION OF THE DRUG DELIVERY PARTICLES	81
5.1 Introduction	81
5.2 Materials	82
5.3 Methods.....	82
5.3.1 Water in oil emulsion method	82
5.3.2 Spray Drying.....	83
5.3.3 Particle Characterization.....	85
5.3.3.1 <i>Light microscopy</i>	85

5.3.3.2 SEM	85
5.3.3.3 Particle sizing	86
5.3.3.4 Drug loading and encapsulation efficiency	86
5.3.3.5 Drug release	86
5.4 Results and Discussion	86
5.4.1 Water in oil emulsion method	86
5.4.1.1 Effect of alginate concentration on particle size and formation	87
5.4.1.2 Effect of mixing speed on particle production	91
5.4.1.3 Effect of surfactant concentration on particle production	94
5.4.1.4 Effect of calcium chloride concentration on particle production	98
5.4.1.5 Effect of sodium silicate concentration on particle production	100
5.4.1.6 Drug loading	103
5.4.2 Spray drying method	104
5.4.2.1 Effect of alginate concentration on particle production	104
5.4.2.2 Effect of inlet temperature on particle production	110
5.4.2.3 Effect of alginate flow rate on microparticle production	112
5.4.2.4 Drug loading and encapsulation efficiency of the alginate microparticles ..	115
5.4.2.5 Drug release from the alginate microparticles	117
5.4.2.6 Effect of alginate: sodium silicate ratio on particle production	118
5.4.2.7 Drug loading and encapsulation of the alginate sodium silicate particles ..	118
5.4.2.8 Drug release from the alginate sodium silicate microparticles	124
5.5 Conclusion	126

CHAPTER 6 - PRODUCTION OF THE EMBOLIC PARTICLES AND ENCAPSUALTION OF THE DRUG DELIVERY PARTICLES

6.1 Introduction	128
6.2 Particle-in-Particle systems for drug delivery applications	129
6.3 Production of the embolizing particles by nozzle vibrating technology	132
6.4 Materials	135
6.5 Methods	135
6.5.1 Production of the embolic particles by the w-o emulsion	135
6.5.2 Production of embolic particles by nozzle vibrating technology	136
6.5.3 Particle characterization	140

6.6 Results and Discussion	140
6.6.1 Emulsion method.....	140
6.6.1.1 <i>Particle production</i>	140
6.6.1.2 <i>Drug loading and encapsulation efficiency</i>	143
6.6.1.3 <i>Drug release from PIP system</i>	147
6.6.2 Production of the embolic particles by a nozzle vibration method	149
6.6.2.1 <i>Effect of vibration frequency on microsphere production</i>	149
6.6.2.2 <i>Effect of electrode voltage on particle production</i>	152
6.6.2.3 <i>Effect of nozzle size on particle production</i>	155
6.6.2.4 <i>Drug loading and encapsulation</i>	157
6.6.2.5 <i>Drug release</i>	159
6.6.2.6 <i>Microcapsule formation</i>	162
6.7 Conclusion	168
 CHAPTER 7 - CONCLUDING REMARKS AND FUTURE WORK	170
 REFERENCES	177

List of Figures

Figure 1.1	HCC surveillance guidelines
Figure 1.2	Treatment algorithm for HCC
Figure 1.3	Spherical embolizing particles for TACE
Figure 1.4	Loading of anti-cancer drugs onto DEBs
Figure 1.5	Proposed PIP for TACE
Figure 2.1a	Chemical Structure of Alginate
Figure 2.1b	Egg box configuration for alginate gelation
Figure 2.2	Chemical structure of Pectin
Figure 2.3a	Chemical structure of Carrageenan – Kappa, Iota and Lambda
Figure 2.3b	Gel formation for thermoresponsive polymers
Figure 2.4	Chemical structure of Gellan
Figure 2.5	Chemical structure of Verapamil hydrochloride
Figure 2.6	Chemical structure of Doxorubicin hydrochloride
Figure 3.1a	Alginate and pectin beads
Figure 3.1b	Gellan and carrageenan beads
Figure 3.1c	Alginate – sodium silicate beads
Figure 3.2	Calibration curve for verapamil hydrochloride
Figure 3.3	Percentage drug release from the polymer beads
Figure 3.4a	Percentage drug release of the alginate-sodium silicate beads over the initial 8 hours
Figure 3.4b	Percentage drug release of the alginate-sodium silicate bead over 8 weeks
Figure 4.1	Microparticle systems in drug delivery – microspheres and microcapsules
Figure 4.2	Controlled delivery vs traditional delivery
Figure 4.3	Particle production by the emulsion method
Figure 4.4	HLB balance
Figure 4.5	Particle production by spray drying
Figure 4.6	Atomizers in spray drying
Figure 4.7	Particle size distribution plot showing volume distribution
Figure 5.1	Light microscope images of the alginate particles in o-w emulsion showing effect of alginate concentration
Figure 5.2	Size distribution of the alginate particles in o-w emulsion showing effect of alginate concentration
Figure 5.3	Light microscope images of the alginate particles in o-w emulsion showing effect of mixing speed
Figure 5.4	Size distribution of the alginate particles in o-w emulsion showing effect of mixing speed
Figure 5.5	Light microscope images of the alginate particles in o-w emulsion showing effect of surfactant concentration
Figure 5.6	Size distribution of the alginate particles in o-w emulsion showing effect of surfactant concentration
Figure 5.7	Light microscope images of the alginate particles in o-w emulsion showing effect of calcium chloride concentration
Figure 5.8	Light microscope images of the alginate particles in o-w emulsion showing effect of sodium silicate concentration

Figure 5.9	Size distribution of the alginate particles in o-w emulsion showing effect of sodium silicate concentration
Figure 5.10	SEM of the alginate particles produced by spray drying showing effect of alginate concentration
Figure 5.11	Size distribution of the alginate particles produced by spray drying showing effects of alginate concentration
Figure 5.12	SEM of the un-crosslinked alginate particles
Figure 5.13	SEM of the alginate particles produced by spray drying showing effect of inlet temperature
Figure 5.14	Size distribution of the alginate particles produced by spray drying showing effects of inlet temperature
Figure 5.15	SEM of the alginate particles produced by spray drying showing effect of flow rate
Figure 5.16	Size distribution of the alginate particles produced by spray drying showing effects of flow rate
Figure 5.17	Drug release profiles of the alginate particles
Figure 5.18	SEM of the alginate-silicate particles showing effect of silicate concentration
Figure 5.19	Size distribution of the alginate- silicate particles produced by spray drying showing effects of silicate concentration
Figure 5.20	SEM of the un crosslinked alginate-silicate particles showing effect of silicate concentration
Figure 5.21	Percentage drug release of the alginate silicate spray dried particles showing the effect of alginate concentration
Figure 5.22	Percentage drug release of the alginate silicate spray dried particles showing the effect of silicate concentration
Figure 5.23	Percentage drug release of the alginate silicate spray dried particles showing the effect of drug concentration
Figure 6.1	A PIP system used for TACE
Figure 6.2	Liquid break up by nozzle vibration
Figure 6.3	Buchi microencapsulator
Figure 6.4	Droplet formation from buchi microencapsulator
Figure 6.5	Carrageenan embolic spheres
Figure 6.6	Size distributions for carrageenan embolic spheres
Figure 6.7	Light microscope images of the PIPs
Figure 6.8	Light microscope images of the small PIPs
Figure 6.9	Percentage drug release of the PIPs loaded with 2 % drug delivery particles
Figure 6.10	Percentage drug release of the PIPs loaded with 5 % drug delivery particles
Figure 6.11	Light microscope images of the alginate spheres produced with the microencapsulator showing the effect of vibrating frequency
Figure 6.12	Size distribution of the alginate spheres produced with the microencapsulator showing the effect of vibration frequency
Figure 6.13	Light microscope images of the alginate spheres produced with the microencapsulator showing the effect of electrode strength
Figure 6.14	Size distribution of the alginate spheres produced with the microencapsulator showing the effect of electrode strength
Figure 6.15	Light microscope images of the alginate spheres produced with the microencapsulator showing the effect of nozzle size
Figure 6.16	Size distribution of the alginate spheres produced with the

	microencapsulator showing the effect of nozzle size
Figure 6.17	Percentage drug release showing effect of alginate concentration
Figure 6.18	Percentage drug release showing effect of silicate concentration
Figure 6.19	Percentage drug release showing effect of nozzle size
Figure 6.20	Light microscope mages of the alginate microcapsues showing the effect of oil flow rate
Figure 6.21	Light microscope mages of the alginate microcapsues showing the effect of alginate flow rate
Figure 6.22	Light microscope mages of the alginate microcapsues showing the effect of nozzle size
Figure 6.23	Size distributions of the alginate microcapsules

List of Tables

Table 1.1	Global causes of HCC
Table 1.2	Child pugh score pointing system
Table 1.3	Child pugh score staging system
Table 2.1	Chemical properties of Verapamil hydrochloride and Doxorubicin hydrochloride
Table 3.1a	Swelling of the polymer beads
Table 3.1b	Swelling of the alginate-sodium silicate beads
Table 3.2a	DL and EE of the polymer beads
Table 3.2b	DL and EE of the alginate-sodium silicate beads
Table 4.1	Effect of process parameters in emulsions
Table 5.1	Parameters in the water and oil emulsion
Table 5.2	Parameters in spray drying
Table 5.3	Size data of the alginate particles produced with the w-o emulsion showing effects of alginate concentration
Table 5.4	Size data of the alginate particles produced with the w-o emulsion showing effects of mixing speed
Table 5.5	Size data of the alginate particles produced with the w-o emulsion showing effects of surfactant concentration
Table 5.6	Size data of the alginate particles produced with the w-o emulsion showing effects of sodium silicate concentration
Table 5.7	Size data of the alginate particles produced by spray drying showing effects of alginate concentration
Table 5.8	Size data of the alginate particles produced by spray drying showing effects of inlet temperature
Table 5.9	Size data of the alginate particles produced by spray drying showing effects of flow rate
Table 5.10	DL and EE of the spray dried alginate particles showing effect of alginate concentration
Table 5.11	Size data of the alginate particles produced by spray drying showing effects of silicate concentration
Table 5.12	DL and EE of the alginate silicate particles by spray drying showing

	alginate concentration effect
Table 5.13	DL and EE of the alginate silicate particles by spray drying showing silicate concentration effect
Table 5.14	DL and EE of the alginate silicate particles by spray drying showing drug concentration effect
Table 6.1	Proces parameters investigated for particle formation with the buchi encapsulator
Table 6.2	Parameters investigated for microcapsule formation
Table 6.3	Parameters investigated for drug loaded alginate microspheres
Table 6.4	Size data for carrageenan embolic spheres
Table 6.5	DL and EE of the PIPs loaded with 2 % drug delivery particles
Table 6.6	DL and EE of the PIPs loaded with 5 % drug delivery particles
Table 6.7	Particle size data for alginate spheres by nozzle vibration showing effects of vibration frequency
Table 6.8	Particle size data for alginate spheres by nozzle vibration showing effects of electrode strength
Table 6.9	Particle size data for alginate spheres by nozzle vibration showing effects of nozzle size
Table 6.10	DL and EE of the alginate spheres showing effect of alginate concentration
Table 6.11	DL and EE of the alginate spheres showing effect of silicate concentration
Table 6.12	DL and EE of the alginate spheres showing effect of nozzle size
Table 6.13	Size data of the alginate microcapsules

CHAPTER 1

INTRODUCTION TO HEPATOCELLULAR CARCINOMA

1.1 Introduction

Hepatocellular carcinoma (HCC) is ranked as the 5th most common cancer world-wide with approximately 750,000 new cases arising each year making it a major health issue worldwide (Parkin *et al* 2001). Most HCC cases end in fatality which has ranked it as the 3rd leading cause of cancer related death (Ferlay *et al* 2008). Hot spots around the globe are Asia, Africa, Europe and North America where the western regions have seen an increase due to the spread of the hepatitis C virus (HCV), alcoholism, obesity and poor lifestyle choices (El-Serag 2011). The introduction to this thesis highlights the main causes of HCC along with how the condition can be monitored and treated. Emphasis is given to transarterial chemoembolization (TACE), a non-surgical palliative treatment for intermediate HCC where current therapies are reviewed and a new concept of a particle-in-particle (PIP) system is proposed as a new treatment method.

1.2 Causes and risk factors in HCC

Many HCC conditions initially develop from carriers of the hepatitis B virus (HBV), HCV and conditions that arise from poor lifestyle habits such as alcoholism and obesity. Causes also vary from global locations around the world (Table 1.1) (Sherman 2010). In Asia and Africa carriers of HBV can be at high risk of developing HCC whereas in Europe and North America carriers of HCV and alcoholics can have a potentially high rate of developing the disease (Alazawi *et al* 2010, Sherman 2010). Men are known to be at higher risk of developing HCC opposed to women, especially those that have a high body mass index (Calle *et al* 2003). Carriers of HBV or HCV that also abuse alcohol are known to have an

even higher risk of developing HCC (Donato *et al* 2008). Unlike other cancers, HCC can possess two simultaneous conditions, the tumour and an underlying scarring known as cirrhosis, which can make HCC a difficult condition to monitor and treat. Cirrhosis can be caused by the same factors that cause HCC (HCV/alcoholism etc) and up to 80 % of HCC conditions begin from a cirrhotic liver. If left untreated the scarred liver can result in liver failure and then progress into the more serious HCC condition resulting in a number of tumours developing on top of the scarred tissue.

Region	HBV	HCV	Alcohol	Other
Europe	10-15 %	60-70 %	20 %	10 %
North America	20 %	50 %	20 %	< 10 %
Asia and Africa	70 %	20 %	10 %	< 10 %

Table 1.1 – Global causes of HCC (Sherman 2010)

1.3 Surveillance and diagnosis of HCC

Surveillance of HCC has shown to reduce the fatality rate. By screening patients known to be at high risk (carriers of HBV/HCV and people with a family history of the disease) the condition can be monitored and action taken with the potential to catch the condition in its early stage, allowing patients to live a disease free life (Crosswell *et al* 2010). A study in China where patients were monitored against un-monitored patients saw survival rates at 1, 3 and 5 years was 66 %, 53 % and 46 % for the monitored patients against 31 %, 7 % and 0 % for the un-monitored patients (Zhang *et al* 2004). Like other cancers, early detection is the best method for long term survival, however only 30 % of HCC cases are caught at the early stages since no cancer related symptoms become recognisable until the intermediate/late stages have developed (Lencioni 2012). Organisations such as the American Association for the Study of Liver Disease and the European Association for the Study of the Liver have published guidelines to help clinicians monitor and diagnosis HCC (Figure 1.1). Patients that

are carriers of HBV, HCV or have developed cirrhosis are considered high risk patients where screening is recommended once every 6 months (Bruix *et al* 2005). Methods of screening include ultrasonography, assessment of the level of alpha fetoprotein (AFP), computed tomography and magnetic resonance imaging (MRI) where ultrasound is the preferred method and AFP is the most widely used serological test (Singal *et al* 2009). Nodules less than 2 cm are often hard to discover making the diagnosis difficult, whereas nodules greater than 2 cm allow a diagnosis to be made (Parikh *et al* 2007). Combination of ultrasound with AFP is known to be more effective in finding nodules however the cost of the procedure is increased when AFP levels greater than 400 ng/mL show indications of the presence of HCC. Nodules less than 1 cm have a 50 % chance of being malignant however ultrasound every 6 months is recommended to monitor the condition and take the required action if the condition progresses to increase survival (Parikh *et al* 2007).

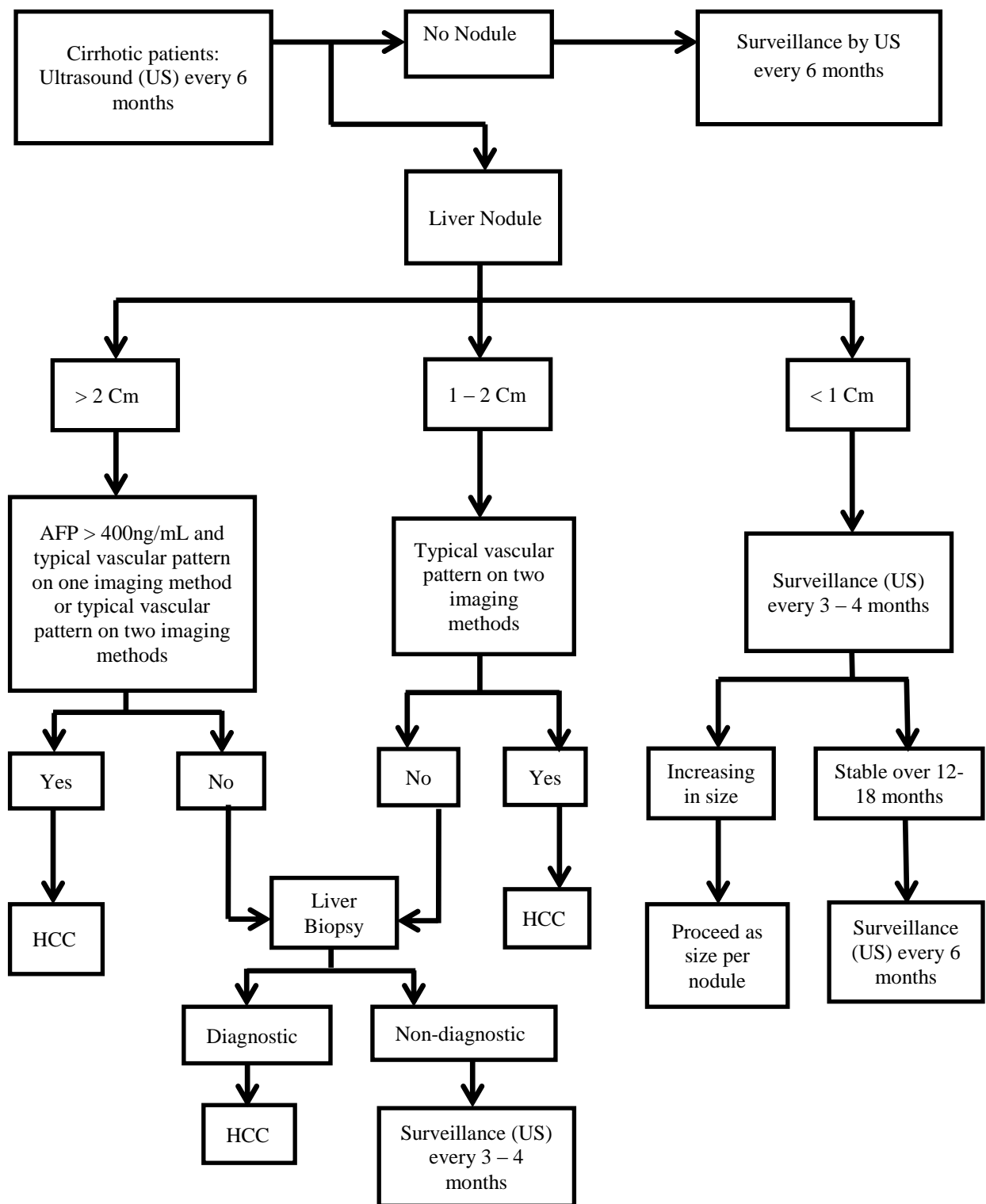


Figure 1.1 – HCC surveillance guidelines

1.4 Staging of HCC

Several staging systems have been established in order to determine the severity of the HCC condition where the Barcelona Cancer of the Liver Clinic system (BCLC) has become the most frequently used method. An algorithm (Figure 1.2) is used where the most effective treatment is picked. The BCLC system splits HCC into the early, intermediate and advanced stages where various treatments can be chosen depending on the HCC stage. The early stage shows good liver reserve, excellent performance status along with a limited tumour burden where this stage is open to possible curative treatments with high survival rates. The intermediate stage shows moderate liver reserve, excellent performance status with multi nodular tumours where non curative methods are chosen, where TACE is the treatment of choice. Finally, the advance stage shows moderate liver reserve, vascular invasion, extra hepatic spread and a venerable performance. TACE can be offered at this late stage where it has seen limited success in improving patient survival, however at this stage the HCC is often beyond achieving effective treatment from the current therapies, therefore the best possible care is given (Parikh *et al* 2008).

Before a treatment method can be picked, the function of the liver is assessed and a stage is assigned depending on the status of the condition by the child pugh scoring system. During this assessment, parameters including the levels of bilirubin and albumin, prothrombin time, encephalopathy and presence of ascites are assessed where points are calculated to give the child pugh score of A-C (Table 1.2 and 1.3). Stage A shows good function allowing curative treatment methods to chosen, stage B shows a vulnerable performance status where TACE is commonly chosen and C shows poor function where transplantation is offered to specially selected patients (Forner *et al* 2010 and Parikh *et al* 2008). Also the degree of vascular invasion and extra hepatic spread must also be evaluated before treatments methods can be

picked. For example, small tumours can meet the criteria for transplantation, however if the condition has spread outside of the liver, the limited number of organs would likely rule these patients out for a transplant since it would have a higher reoccurrence rate, therefore other therapies such as TACE will be offered (Parikh *et al* 2008).

In terms of possible curative treatments, transplantation, resection and ablation are possible treatments which have strict criteria that are assessed and will be describe in further detail in the next section. Curative treatments are only open to patients with early stage HCC which accounts to only 30 % of all cases since no cancer related symptoms are seen until the intermediate stage is reached and the screening process for small tumours previously discussed is a challenging process. In intermediate HCC, palliative treatment methods such as TACE is frequently offered which accounts for approximately 50% of HCC cases.

Chemical Parameters	1 point	2 points	3 points
Encephalopathy	none	1 - 2	3-4
Ascites	none	slight	Moderate
Albumin (g/dL)	> 3.5	2.8 – 3.5	< 3.5
Prothrombin time prolonged (sec)	1-4	4-6	> 6
Bilirubin (mg/dL)	1-2	2 - 3	> 3

Table 1.2 – Pointing system for determining the child pugh score

Child Pugh Score	Liver function	Total points
A	Good	5-6
B	Moderate	7-8
C	Poor	10-15

Table 1.3 – The child pugh score staging system

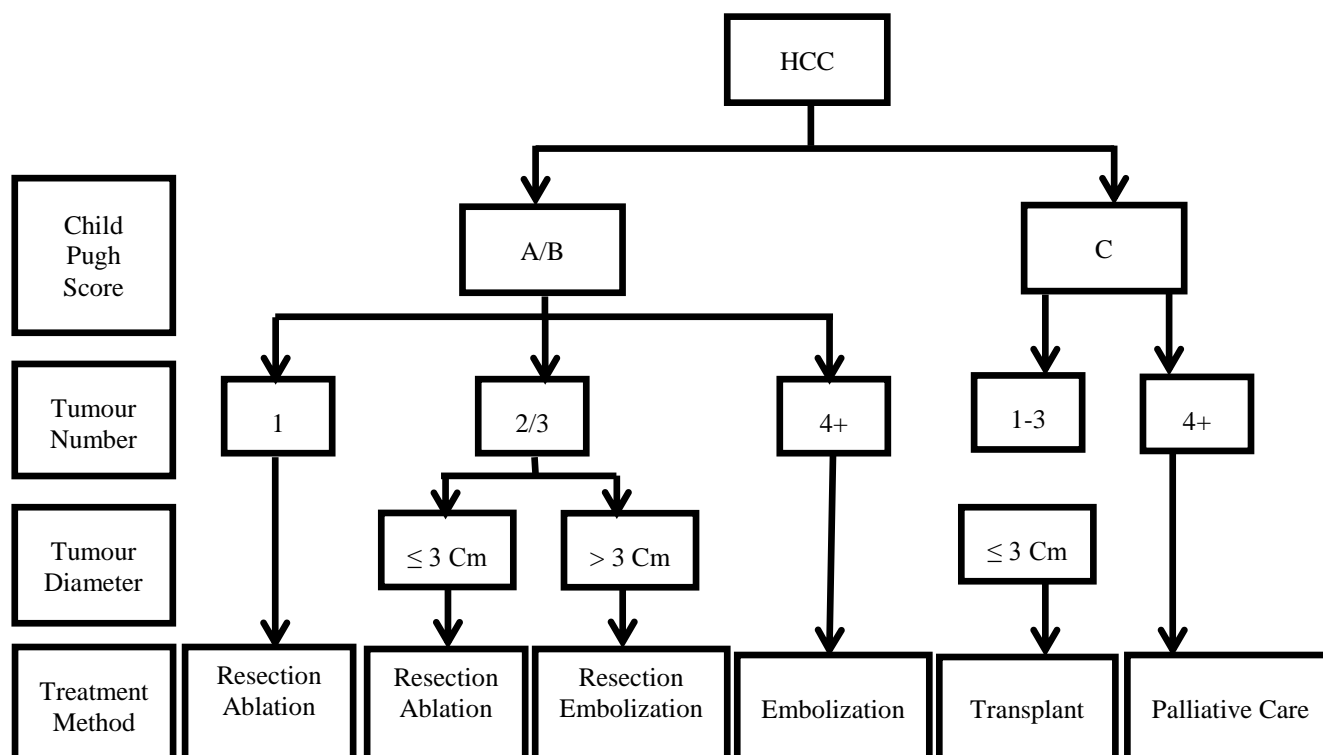


Figure 1.2 – Treatment algorithm in determining the most effective treatment for HCC

1.5 Curative treatments for HCC

As discussed, before a treatment method for HCC is chosen, the condition must be assessed so that the most effective treatment for the patient can be applied. Potential curative treatments include transplantation, resection and ablation. Non-curative methods have shown to increase patient survival where methods such as TACE are used in approximately 50 % of HCC cases.

1.5.1 Resection

Resection is a surgical procedure that involves removal of a section of the liver and is the treatment of choice in patients with HCC that do not display cirrhosis, which can make the procedure more challenging and dangerous for the patient (Belghiti *et al* 2000). In cases where the underlying cirrhosis is present, patients are carefully selected to avoid

complications such as liver failure or increased risk of death. Patients in the child pugh class A (single tumour, good liver reserve and good performance status) are the main class to undergo resection since their livers will still show good function. However, patients in Class B (multiple nodules and moderate liver reserve) are not entirely ruled out for resection although the reoccurrence rates can be relatively high. These patients are carefully selected based on the survival and reoccurrence rates compared to other therapies such as ablation and embolization. The reoccurrence rate at 2 and 5 years is 50 % and 70 % after resection (Imamura *et al* 2003). In cases where the cancer reoccurs, transplantation can be offered when the procedure has failed. This method allows an efficient use of the limited number of organs available for transplantation (Maluccio *et al* 2012).

1.5.2 Ablation

Ablation is another potentially curative treatment that induces tumour necrosis for early stage HCC in tumours ranging from 2-3 cm with similar survival rates to resection. In tumours greater than 3 cm ablation is less effective, however, the method can be combined with embolization to improve response rates (Yan *et al* 2008). The two types of ablation are thermal and chemical ablation. Thermal ablation applies radiofrequency by a needle that is inserted into the tumour tissue causing tumour necrosis. Advantages of radiofrequency are that it is a non-surgical method with low complication rates, low cost and the procedure can be repeated (Willet *et al* 2012). In terms of the tumour size, tumours greater than 5 cm are considered too big for ablation. Also the method is limited to a maximum of 3 tumours (Lam *et al* 2008). Complications of the radiofrequency procedure can include pain and haemorrhage. Chemical ablation involves an injection of 95 % ethanol to the tumour which is a low cost procedure with a low chance of complications. Disadvantages include the need for repeat procedures and an inability to achieve complete necrosis in large tumours which

has led to radiofrequency being a favourable therapy (Livraghi *et al* 1999). Thermal ablation gives better control and survival over the ethanol injection however its side effects are more frequent. Both ablation therapies are effective since the tumour is a soft tissue surrounded by a hard cirrhotic liver which insulates the tumour tissue. Also the hard cirrhotic liver prevents the alcohol from leaking out of the tumours tissue once administrated (Shiina *et al* 2012). 5 year survival in patients with child pugh score A is at 50 – 75% (Willet *et al* 2012) and like resection, transplantation can be offered if ablation fails making efficient use of organs.

1.5.3 Transplantation

Transplantation is the most effective procedure with the potential to cure both the cancer and the underling cirrhosis. Due to the shortage of organs, criteria have been stabilised where the Milan criteria is the most frequently used. The criteria state that a patient with a single tumour measuring less than 5 cm or 3 tumours measuring 3 cm or less are eligible for transplantation. 5 year survival has a rate of 75 % with a reoccurrence of less than 15 % (Mazzaferro *et al* 1996). Due to the limited number of organs patients are often referred to a waiting list which will often see a high drop-out rate due to patient death or tumour progression no longer making the treatment possible (Lolvet *et al* 1999). Bridging therapies such as ablation and embolization have been frequently used for patients awaiting transplantation to prevent tumour progression and has shown success (Graziadei *et al* 2003).

1.6 TACE

As discussed, most HCC cases arise in the intermediate to advanced stages where potential curative treatments are no longer possible. TACE is a palliative non-surgical arterial based technique applied to intermediate to advanced HCC where it is used in more than 50 % of HCC conditions (Lencioni 2012). When HCC arises, the tumour receives the majority of its blood supply by the hepatic artery. TACE therapies take advantage of this feature by using

it as a delivery route allowing targeted drug delivery directly to the tumour site. Anti-cancer agents are delivered to treat the tumour along with embolizing particles which block the blood flow to the tumour starving it of oxygen, preventing tumour growth and also preventing wash out of the drugs.

1.6.1 Conventional TACE

The conventional TACE procedure involves injection of chemotherapeutic agents which are emulsified with Lipidol, an oily medium composed of long-chained ethyl esters derived from poppy seed oil which increases the solution viscosity aiding delivery and imaging. Doxorubicin is a frequently used single drug and doxorubicin, cisplatin and mitomycin C is a frequently used cocktail in the conventional TACE procedure (Osaga *et al* 2012). The drug solutions and emulsion are prepared and blended in the clinic prior to treatment then administered to the patient via a micro catheter. Following the administration of the anti-cancer agents, embolizing particles are then administered where gelatin or polyvinyl alcohol (PVA) particles are common choices (Table 1.4). Gelatin particles are cheap and biodegradable and are available in the size range of 40 – 60 μm (Makuuchi *et al* 1985), however the size and morphology of these particles are irregular with wide size distributions which can result in aggregation (Osaga *et al* 2009). PVA particles are available in a larger size range of 50 – 1200 μm , however these particle also display irregular shapes and are also non-degradable. Disadvantages of the conventional TACE method include high reoccurrence rates following treatment, no control over the drug release rate, potential for high concentrations of drug to enter the system circulation and the need for two injections.

Category	Device	Composition
Conventional particles	Gelport PVA	Porous gelatin Non spherical PVA
Bland beads	Emosphere Bead Block Contour SE Embozene	Trisacryl polymer embedded with gelatin Spherical PVA Spherical PVA Polyphosphazene-coated PMMA
Drug eluting beads	DC/LC bead Quadrasphere/Hepasphere	PVA modified with sulfonate sodium salt Super absorbent polymer

Table 1.4 – Embolic devices used in TACE

To overcome the aggregation issues with non-spherical gelatin and PVA particles, spherical particles with smooth hydrophilic surfaces have become the standard choice of embolizing agents for TACE (Figure 1.3). They avoid aggregation and can be easily passed through a microcatheter and allow easier targeted delivery to the tumour sight by choosing the optimum particle size (Osaga *et al* 2012).

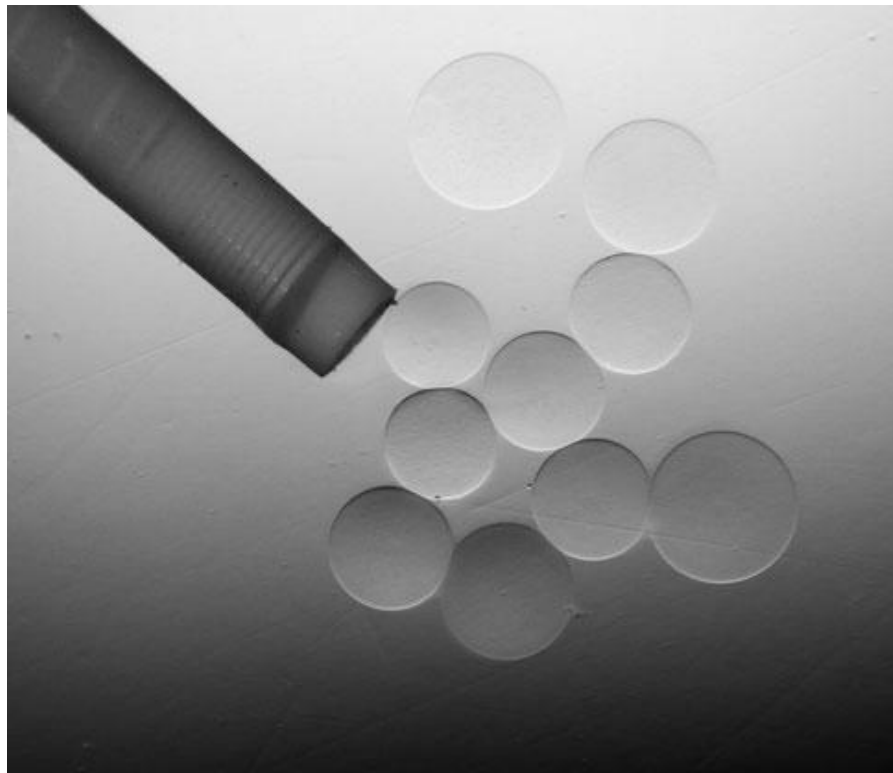


Figure 1.3 – Spherical embolizing particles for TACE (Osaga *et al* 2012)

Several beads have been developed specifically for bland embolization, where HCC is treated purely by the embolizing particles with no anti-cancer agents allowing no chemotherapeutic related side-effects to arise after the treatment has been applied. Emosphere is a brand of embolizing beads produced from trisacryl gelatin and are available in the size range of 40 – 120, 100 – 300, 300 – 500, 500 – 700, 700 – 900 and 900 – 1200 μm (Osaga *et al* 2012). In most cases, a single bead can block a vessel, effectively embolizing the tumour (Laurent *et al* 2004). Contor and Bead Block are other devices that have come to market available in the size ranges of 100 – 300, 300 – 500, 500 – 700, 700 – 900 and 900 – 1200 μm and the beads have less resistance in the blood vessels than Emosphere beads (Osaga *et al* 2012 and Laurent *et al* 2006). Another bead Emozene is a polyphosphazene coated polymethymethacrylate bead. The particle size is available in a narrower size range of 40, 75, 100, 250, 400, 500, 700, 900, 1100 and 1300 μm . Each size has a specific colour to allow visibility and allow the bead size to be easily distinguished. The coating of polyphosphazene on the bead acts as an anti-inflammatory for when long periods of exposure to the embolic material is needed to reduce patient discomfort (Stampfl *et al* 2011).

1.6.2 Drug eluting beads

The major disadvantage of conventional TACE is its inability to control drug release and target drug delivery directly to the tumour with limited tumour response. Since the 1990s this pitfall of conventional TACE have been overcome where drug eluting beads (DEBs) have become a favourable choice in patients suffering from intermediate HCC. During the TACE procedure, a drug solution is added to blank DEBs where a typical loading of doxorubicin can reach a maximum loading of 37 mg/mL in 20 minutes (Figure 1.4) (Liapi *et al* 2007). The beads are then administered to the patient via a micro catheter which takes approximately 1.5 hours (Liapi *et al* 2007). The DEBs are calibrated between 100 – 1000 μm allowing targeted

delivery to the tumour where the procedure can be completed in a single injection compared to two injections that are required for conventional TACE. DEBs also allow high loadings and controlled release of the therapeutic compound over time, a particularly important feature for anti-cancer drugs which can display narrow therapeutic windows.

Two brands of beads based on PVA are available, the DC bead (in Europe) and the LC bead (in the US). The DC bead is a PVA based bead that has been modified with sulfonate groups that gives the bead a strong negative charge (Osaga *et al* 2012). This allows positively charged drugs such as doxorubicin to be loaded onto the preformed beads and the ability to release the drug slowly over a period of days to weeks depending on the size of the bead (Liapi *et al* 2007). The size ranges of the DC beads that are available are 100 – 300, 300 – 500, 500- 700 and 700 – 900 μm . Indication of the loading can be confirmed since the dry beads undergo a colour change from blue to red once the doxorubicin is loaded.

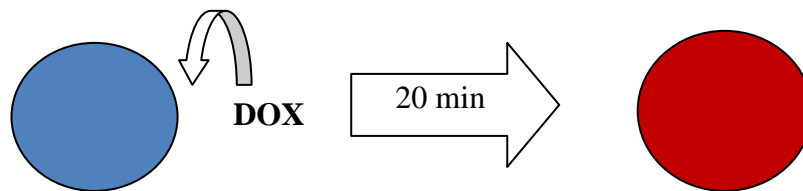


Figure 1.4 – Loading of anti-cancer drugs to DEBs. The drug solution is added to the dry beads where drug molecules bind to the embolic device. DEBs typically display a negative charge and can load positively charged drugs such as doxorubicin with high loadings and controlled release capabilities.

Another two brands of DEBs are Hepasphere and Quadrasphere which are produced from vinyl alcohol and sodium acrylate copolymer. During the TACE procedure, the dry beads are added to a drug solution in saline and expand up to four times their dry bead size, which are available from 50 – 100, 100 – 150 and 150 – 200 μm . Like the DC bead they are also negatively charged and can load the positively charged doxorubicin in 20 minutes where 50 mg of the drug can be loaded on to 25 mg of dry beads then be released in a controlled

state overtime. Negative or neutrally charged drugs can also be loaded into the beads, however in-vitro studies have shown the drug release rate to be rather fast where all of the drug is released within a 24 hour period (Maeda *et al* 2010).

DEBs have shown to greatly improve survival with improved tumour response compared to conventional TACE. The major disadvantage of DEBs is that when controlled release of the therapeutic is required, the DEBs are limited to positively charged drugs, since the strong interactions between the drug and material allow the controlled rate to be achieved. Also, DEBs are specifically calibrated to a patient's blood vessel size. Patients with varying blood vessel widths will require different sized particles resulting in various release rates where the smaller sized DC beads release doxorubicin within 24 hours and the larger DC beads control the release rate over 14 days (Maeda *et al* 2010). This is a particular disadvantage since patients with narrow blood vessels with require more treatments and can potentially be exposed to peaks in drug toxicity resulting in unwanted side-effects. Finally, DEBs fall short if multiple drugs are to be administrated since the drug is loaded to pre-formed beads and the beads have a limited loading capacity.

1.7 Proposal of a new microparticle drug delivery system for TACE

As discussed, many current therapies have proven to cure/reduce tumour burden for patients that suffer from HCC. Specifically for TACE, the DEBs have emerged as a dominant therapy in the treatment of intermediate HCC, where the DC bead has been a major player for the delivery of doxorubicin, a commonly used drug to treat HCC. However, the DEBs have several setbacks that limit the use to specific drugs and patients with various blood vessel widths will receive the drug at different rates.

A new delivery system is proposed in an attempt to overcome the limitation to one class of drugs and also to decouple the effect of particle size on drug release rate, allowing a single

release profile to be available to all patients. This new system will be composed of microparticles encapsulated into larger microparticles yielding a particle-in-particle (PIP) system (Figure 1.5). The PIP system will have two key functions that current TACE therapies lack. The first function of the PIP system is a drug delivery/chemotherapy component, composed of small microparticles approximately 1 – 3 μm in diameter for delivery of the drug. The second function of the PIP system is the embolization component, composed of larger spherical microparticles with porous structures in the 100 – 1000 μm size range allowing effective embolization and targeted delivery to the tumour site. The small drug delivery particles are to be designed to encapsulate a desired drug with high drug loadings and controlled release characteristics, allowing multi drugs to be encapsulated into the PIP system. A key feature of the embolizing particles is a particle with a high porosity allowing PIPs of various sizes to display the same release pattern and also where the encapsulated drug delivery particles show no interaction with the embolizing material which could potentially result various drug release patterns. This will allow patients with various blood vessels widths to receive similar release rates for a wide range of drugs which will stay in the same therapeutic window range, a function that current DEBs for TACE lack. The embolic particles are also to be produced from a biocompatible and biodegradable polymer so that the particles degrade overtime avoiding accumulation in the blood vessels, since many treatments may be needed over the patients life span.

It is to this authors knowledge that there is currently no other particle based drug delivery system capable of decoupling the effect of particle size on drug release rate for TACE or in any other drug delivery application. Also it is believed that there are no other current PIP systems designed to encapsulate a specific or multiple drugs for TACE. Therefore this new PIP system will have great potential to not only deliver current drugs used for TACE but also any new drugs that are could prove to be more effective with all the benefits that the current

DEBs display. The ability for the PIPs to display identical release rates can also reduce the peaks in drug toxicity reducing side effects along with the number of treatments thereby improving patient quality of life.

Since these particles are to be delivered by the parental route, formation of a sterile product is critical where some methods of manufacturing could possibly allow a sterilization step to be avoided. Like with the DEBs these PIPs would be stored in the dry state allowing greater stability during storage and preventing the drug leaking out over time. They would then be suspended in saline and administered to the patient via a micro catheter in the clinic under local anaesthetic. Like some of the embolization devices discussed, the PIPs will display smooth spherical surface, with narrow size ranges allowing the PIPs to be administered with ease, and allow targeted delivery directly to the tumour site. Use of Lipidol as used in conventional TACE could also aid delivery and imaging of the beads post treatment. Finally, current DEBs available are mainly non resorbable systems. Materials investigated in this work will be mainly from natural biodegradable polymers. Since patients suffering from intermediate HCC may need multiple treatments over their life span, the PIPs produced in this work must be able to breakdown and be removed from the body once the delivery of the drug has been completed.

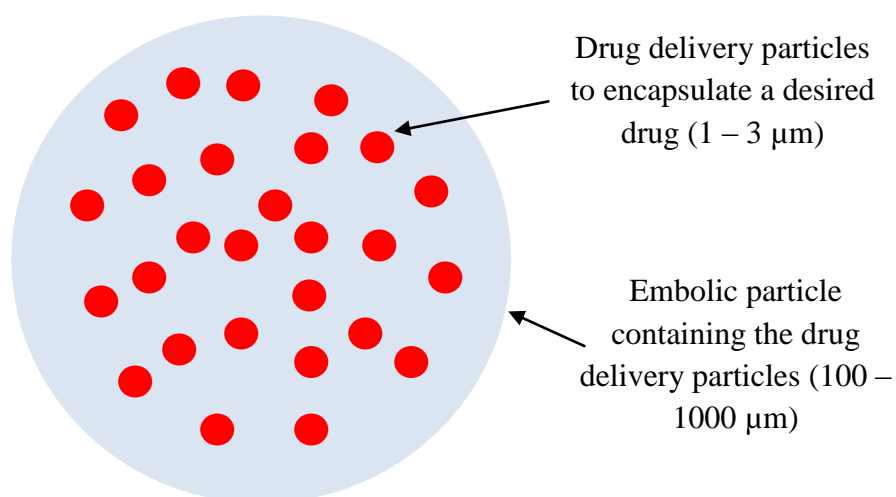


Figure 1.5 – The proposed PIP system composed of microparticles encapsulated into microparticles. The inner drug delivery particles are to be tailored to a desired drug with high drug loadings and controlled release capabilities. These drug delivery particles are then encapsulated into larger microparticles which will act as the embolic device allowing embolization of the tumour and targeted delivery to the tumour site.

The body of this thesis explores various aspects of polymer science and particle production processes that have been reported within the field of drug delivery. More specifically the following chapters explore;

- Possible materials capable of controlled release where small molecular weight hydrophilic drugs with chemistry similar to doxorubicin are to be delivered.
- Particle production processes for particles that display high drug loadings and controlled release of the encapsulated drug.
- Materials and methods that allow porous embolic particles (100 – 1000 μm) to be produced.
- Particle production processes that allow the drug delivery particles to be uniformly distributed within the embolizing particles
- Production methods of PIPs that allow the effect of particle size to be decoupled from drug release rate.

CHAPTER 2

POLYMERS IN DRUG DELIVERY

2.1 Introduction

Polymer Science is an area that has seen extensive research within the food, cosmetics and pharmaceutical industries. For pharmaceutical applications, polymers have been a favoured choice as drug delivery systems since they are biocompatible and biodegradable. Release from such systems is by diffusion of drug molecules from a polymer matrix into an external volume of media, or by degradation of the polymer as it enters a particular environment. Polymers can be produced from natural sources such as plants and animals or be synthetically man made (Kunal *et al* 2009). Natural polymers such as alginate, chitosan and gelatin generally have more complex structures than synthetic polymers, and their properties can vary greatly depending on the source from which they are produced (Enderle *et al* 2005). They are a class that are open to a wide range of functional groups and chemical characteristics making them an interesting choice as drug delivery vehicles. Natural polymers also carry hydrophilic characteristics along with low costs making them an attractive choice for encapsulation of hydrophilic drugs allowing the water soluble compounds to be well mixed and processed into a solid matrix with the drug uniformly distributed. The disadvantage of natural polymers is a risk of microbial contamination from the animal or plant source (Kunal *et al* 2009). Synthetic (also argued as semi-synthetic) polymers such as polylactic acid (PLA), polycaprolactone (PCL) and poly (lactic-co-glycolic acid) (PGLA) can be tailor made to suit a specific application and batches of the produced material can have more like for like chemical characteristics compared to natural polymers. They can also be easier to process than natural polymers since they often do not require

crosslinking to form a drug delivery system. However, they carry a higher cost and often require the use of environmentally unfriendly solvents such as dichloromethane when fabricating them into drug delivery systems.

2.1.1 Hydrogels in drug delivery applications

In modern drug delivery technology development scientists look to improve upon existing drug delivery methods by developing sustained release systems that control the rate a drug enters the blood stream (Brannon-Peppas 1997). This method of drug delivery can avoid overdosing, reduce the required dose of drug and decrease the number of unwanted side effects. Many of these controlled drug delivery systems are composed from hydrogels. Hydrogels consist of three dimensional polymer networks that retain large volumes of water. Hydrogels make attractive delivery systems since they can be made of the similar building blocks that mimic living tissue and can therefore display lower toxicity and a better biocompatibility than other materials (Gupta *et al* 2002). Hydrogels are produced by crosslinking functional groups along the polymer backbone which increase the rigidity and density of the network which can be a physical or chemical process (Hoffmann 2002). Physical crosslinking processes involve a change in the polymers physical state though methods such as temperature changes and UV/gamma radiation producing the three dimensional gel network (Moffat and Mara 2004, Taleb 2008). Chemical crosslinking requires addition of a chemical agent to the polymer solution that induces hydrogel formation (Moffat and Mara 2004, Taleb 2008). Chemical crosslinking is generally an easier process to control over physical crosslinking since the experimental parameters such as polymer concentration, crosslinking agent concentration and crosslinking time can be adjusted to fit a desired requirement (Peppas 1987, Kashyap *et al* 2005). Also, chemical crosslinking can be completed by two methods known as zero length and non-zero length crosslinking. Zero

length crosslinking involves binding two different polymer chains of opposite charge through interaction of oppositely charged functional groups. For example the negative carboxylic acid groups in alginate can bind to the positive amine groups in chitosan to form the gel. Non-zero length crosslinking involves binding the functional groups in a single polymer to form a gel, for example crosslinking of alginates carboxylic acids groups with calcium ions (Petite *et al* 1994, Kao *et al* 2004).

When designing a drug delivery system, the choice of material is often dependent on the drug to be encapsulated. The polymer and manufacturing method used must allow the chemical nature of the drug to be preserved, for example when encapsulating sensitive drugs such as proteins, use of materials that require harsh solvents or high temperatures may not be ideal. The physical properties of the drug must also be addressed. If a hydrophilic drug is to be encapsulated, methods such as the oil in water emulsion will not be ideal as a large quantity of the drug can be lost to the water based continuous phase, resulting in low drug loadings. Some materials are chosen to allow electrostatic interactions between the polymer and drug allowing a drug delivery system to hold the drug more effectively, resulting in higher encapsulation efficiencies and controlled release rates. Bonferoni *et al* (2007) produced a particulate system from the positively charged polysaccharide chitosan to encapsulate salicylic acid, a negatively charged drug where the interactions between polymer and drug allowed controlled release to be achieved. Mahesh *et al* (2007) produced a drug delivery system composed of alginate and an anionic surfactant Aerosol OT by a double emulsion method. The anionic surfactant introduced stronger functional groups to interact with a range of positively charged drugs including doxorubicin and verapamil hydrochloride that were released over a 30 day period with high drug loadings and encapsulation efficiencies.

The choice of drug investigated in this thesis will be given to small molecular weight hydrophilic drugs, since their encapsulation into microparticles for controlled release has seen

limited attention in the literature where they are known to display rapid release rates due to their water loving nature. Many anti-cancer drugs possess a positive charge, particularly the commonly used doxorubicin, which belongs to the class of drugs are explored in this thesis. Water soluble polymers make an attractive choice of materials for the entrapment of hydrophilic compounds since they are open to a wide variety of functional groups that can interact with the drug molecule, and since both dissolve well in water, the drug can be well mixed and encapsulated throughout a solid particle matrix once processed. Natural polymers that display a negative charge are the class of materials investigated since they can allow interaction with the positive charge of the drug molecule which can potentially allow high loadings and a sustained release rate to be achieved. This can be particularly challenging for hydrogel based systems encapsulating hydrophilic drugs since the gels are known to swell rapidly in water where the encapsulated contents can be instantly released. Therefore strong interactions between the material and drug will be of great importance in order for the hydrogel system to effectively retain the drug making it capable of controlled release. Several of these commonly used water soluble polymers are discussed along with some of their current uses as microparticle based drug delivery vehicles.

2.2 Alginate

Alginate (Figure 2.1a) is an anionic linear polysaccharide derived from brown seaweed that consists of D mannuronic acid (known as the M unit) and L guluronic acid (known as the G unit) units along the polymer backbone, where these units are arranged in a random distribution (GG, MM, MG, GM) depending on the alginate source (Draget *et al* 1996). One characteristic that makes alginate an attractive material in drug delivery is its ability to form instant gels upon addition to solutions of divalent ions such as calcium chloride. The gel forms through crosslinking of the G unit carboxyl groups and the calcium ions which has

become known as the egg box configuration, which is a mild process making it an attractive method for the encapsulation of sensitive drug molecules (Ostberg *et al* 1994) (Figure 2.1b). The G and M units vary in alginate sources and the ratio of the M/G units is known to influence the gel strength. Alginate containing a high G content produces strong but brittle gels while alginate with a high M content forms weaker flexible gels (Kakita *et al* 2008). In drug delivery applications alginate with a high G content is desirable since the stronger gel will have more potential to produce a denser polymer network once crosslinked, potentially allowing a sustained release rate to be achieved. Along with the M/G ratio, the solution concentration and molecular weight can produce gels with variable drug release properties where gels produced from solutions of high molecular weight and high concentrations can yield strong gels however the solutions will be highly viscous making them difficult to process (Lee *et al* 2011). Calcium ions can induce alginate gelation by two methods. The first is an external gelation method. When alginate solutions come into contact with calcium chloride solutions, gelation occurs from the exterior of the hydrogel where the alginate carboxyl groups are crosslinked with the calcium ions. Gelation can also be induced from the interior of the gel where calcium carbonate solutions are mixed in with the alginate solution. By addition of glacial acetic acid, calcium ions are released from the alginate/calcium carbonate blend where the gel is from the interior. Factors effecting gel strength are the concentration of alginate and crosslinking solution and crosslinking time (Kunal *et al* 2009).

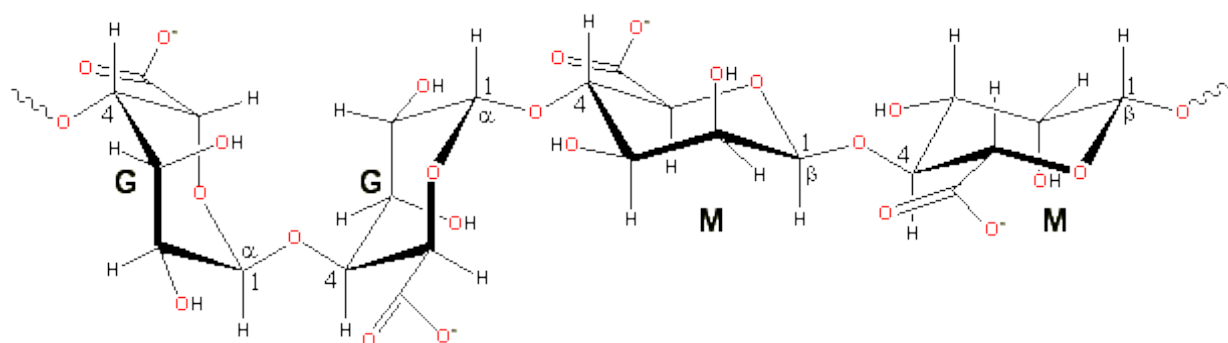


Figure 2.1a – Chemical structure of Alginate (Mahesh *et al* 2007)

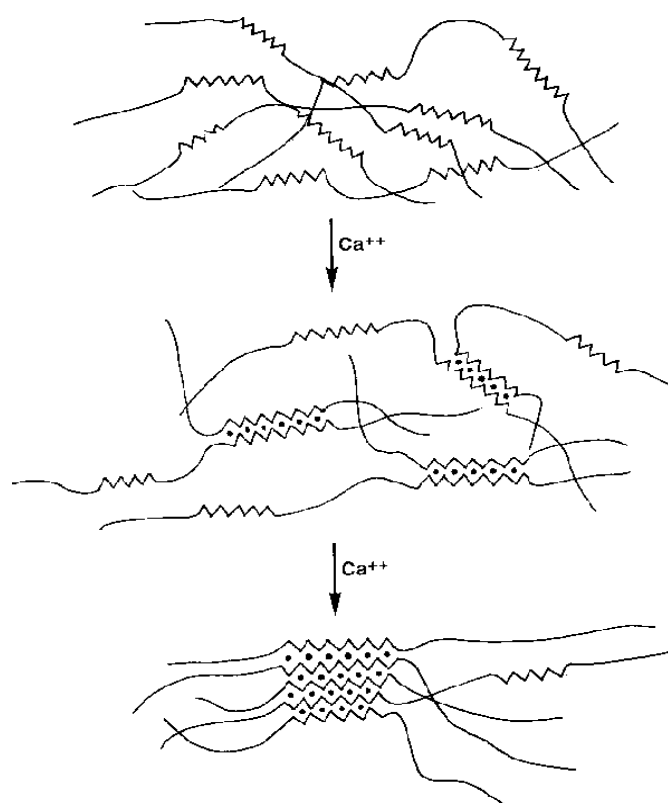


Figure 2.1b – Egg box configuration for Alginate gelation (Mahesh *et al* 2007)

Various methods have been investigated for alginate gelation. One of the commonly used methods is by the syringe droplet method where solutions of alginate are added to a bath of calcium chloride where the alginate forms instant gel beads upon entry into the crosslinking solution. This particle production method generates large beads greater than 1 mm in diameter, which can be considered too large for some drug delivery applications. The size of the beads can be to a some degree controlled by use of a needle with a narrow diameter, however this limits the choice of alginate to low concentration/molecular weight/viscosity solutions as solutions too viscous would not pass through the needle. On the other hand, due to the beads greater diameter and therefore lower surface area, the method allows hydrogels with greater controlled release capabilities to be produced. Alginate has also been formed into micro sized drug delivery systems by use of water in oil emulsions. When processing by

an emulsion method, an alginate solution mixed with a drug to be encapsulated is emulsified in an oil and suitable surfactant. Micro sized droplets are produced which can be crosslinked into solid particles by gradually adding a solution of calcium chloride to the emulsion. By varying mixing speed, alginate concentration and the surfactant concentration, the size of the droplets can be tailored from micro to nano sized droplets. Another attractive technique for microparticle production method is by use of nozzle vibrating technology where a vibration is applied to a flowing polymer jet which breaks to the jet down into droplets of a uniform size once passed through a nozzle or needle allowing particles or beads of a more uniform size to be produced. These techniques will be discussed in further detail in later chapters of this thesis.

Encapsulation of small molecular weight hydrophilic drugs in alginate hydrogels in the literature is limited due to the polymers high porosity and rapid swelling characteristics. Alginate has been used for the encapsulation of poorly/slightly water soluble drugs where Soni *et al* (2010) produced alginate microparticles by a water-in-oil emulsion method where the alginate particles sustained the release of theophylline over 8 hours from particles with a Dv_{50} of approximately 10 μm . Alginate has also been used to encapsulate proteins and large molecules due to its mild gel formation process which avoids use of solvents and conditions that can potentially denature the protein to be encapsulated. Mobus *et al* (2012) spray dried zinc crosslinked alginate microsphere to encapsulate insulin for delivery to the lungs. The particles had a Dv_{50} of 4 μm and controlled the rate of the large molecule over 48 hours. To extend controlled release capabilities of some drug delivery systems, alginate has been used in conjunction with positively charged polymers such as chitosan as a coating technique known as a layer-by-layer approach, where the additional layers can potentially make the diffusion process of a drug more challenging (Liu *et al* 2013).

Publications for controlled release of small molecular weight hydrophilic drugs using alginate as a carrier particle are limited. Several publications have discussed addition of materials that enhance interactions between the drug and carrier particles and produce stronger gels with reduced porosity. Mahesh *et al* (2007) combined alginate with the anionic surfactant Aerosol OT which contains sulfonate groups (function groups responsible for making the DC bead capable of controlled release) to prolong the release rate of several positively charged drugs, including verapamil hydrochloride and doxorubicin. The addition of the sulfonated agent sustained the drug release over a 30 day period. The drug loadings of several negatively charged drugs were also investigated where the loadings were less than that of the positively charged drugs however no drug release studies were performed with the negatively charged compounds.

2.3 Pectin

Pectin (Figure 2.2) is a linear polysaccharide obtained from the walls of most plants such as citrus fruit and apples. Its polymer chain consists of repeating 1 – 4 linked D-galacturonic acid units which contain carboxyl groups along the backbone in the form of smooth and hairy regions giving the molecule a negative charge (Luishu *et al* 2003). Like alginate, pectin forms instant gels in the presence of calcium ions though the egg box configuration, making it attractive for drug delivery applications. The galacturonic groups in pectin are partly esterified with methyl groups which can vary in pectin types and influence the properties of the polymer where this characteristic is known as the degree of esterification (DE). Pectin with a DE below 50 % is classed as low DE pectin and pectin with a DE above 50 % is classed as high DE pectin (Luishu *et al* 2003). High DE pectin has less carboxyl groups available in the polymer backbone and giving it a lower water permeability than low DE pectin making it an ideal coating agent where it has been used in oral dosage forms to reduce

water permeability (Wong *et al* 2002). As for drug delivery matrixes pectin with a low DE is an ideal choice since they have a greater number of carboxyl groups available for interaction with calcium ions, allowing denser gels to be produced. As with alginate factors influencing gel strength are the concentration of polymer used, crosslinking time and concentration and polymer molecular weight (Wong *et al* 2002).

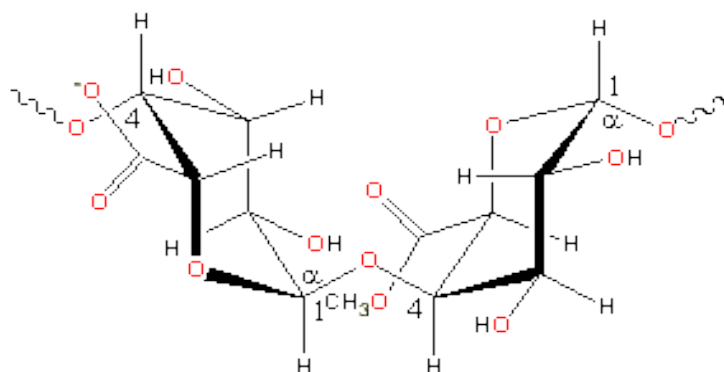


Figure 2.2 – Chemical structure of Pectin (Luishu *et al* 2003)

Pectin has been used to produce gels by similar methods as discussed with alginate. Pectins main applications have been as a drug carrier for delivering drugs to the colon by the oral route since it is degraded by the colonic micro-flora (Wong *et al* 2002). Vaidya *et al* (2009) produced a pectin based microparticle system containing metronidazole where the pectin particles were coated with Eudragit S100, a pH responsive polymer that protects the encapsulated drug along the upper gastrointestinal tract until it reaches the colon site allowing the full load of drug to be released. The drug was displayed a controlled release using in-vitro testing in conditions simulating the colon over 18 hours.

2.4 Carrageenan

Carrageenan (Figure 2.3a) is a family of sulfonated linear polysaccharides that are derived from red marine algae where its use has been used as a thickener in the food industry. Their linear primary structure is based on alternating 1,3 linked D galactose and 1,4 linked

D galactose which are linked with 1,3 and 1,4 glycosidic linkages, with varying degrees of sulfation (Mayur *et al* 2004). They are a family of polymers that depending on the number of sulfonate groups in the polymer backbone, form gels with strong or elastic characteristics. In the heated state the polymer exists as a random distribution of coils. Upon cooling, the polymer chains arrange into double helical junction zones (Figure 2.3b) that become closer as the temperature decreases resulting in gel formation (Mayur *et al* 2004). Addition of cations, potassium for kappa carrageenan and calcium for iota carrageenan give a more ordered structure, reinforcing the gel (Mayur *et al* 2004). Three types of carrageenan are commonly used in industry, kappa, iota and lambda carrageenan. Kappa carrageenan contains one sulfonate group in the backbone and forms strong gels that can be reinforced with potassium ions. Iota carrageenan has two sulphate groups in the backbone and forms soft elastic gels at lower temperatures than kappa carrageenan. Lambda carrageenan has three sulphate groups in the backbone which cannot form a gel where it is used as a thickener in the food industry (Mayur *et al* 2004).

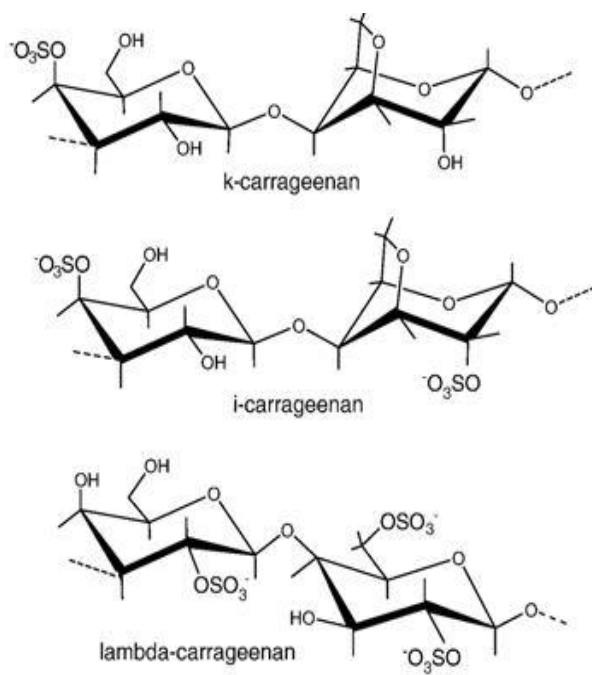


Figure 2.3a – Chemical structure of kappa, iota and lambda carrageenan (Janna *et al* 2011)

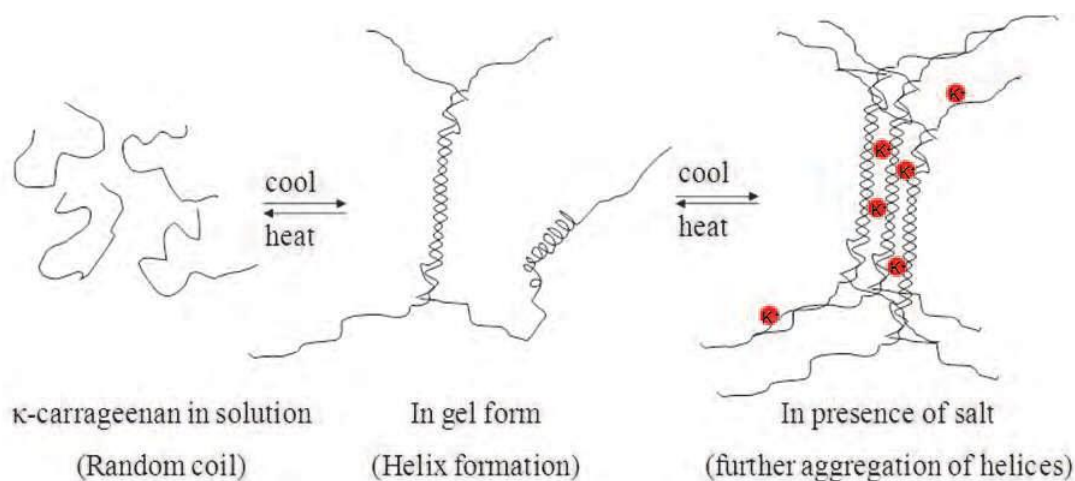


Figure 2.3b – Gel formation of thermoresponsive polymers. In the heated state the polymer chains are in a randomised coil formation. Upon cooling the chains form double helix junctions leading to the gel formation (Mayur *et al* 2004).

In drug delivery applications, kappa carrageenan is known to be an ideal choice since it forms strong gels. However, production of micro sized particle systems has seen limited attention, since the material needs temperatures up to 90 °C in order to form a processable solution which will degrade some drugs during the encapsulation process. Also, common particle production methods such as emulsions and spray drying will require these high temperatures for vast amounts of time limiting their use to fabricate microparticle systems. Most delivery systems discussed in the literature produce large gel beads produced by the syringe droplet method where hot solutions of the polymer/drug blend are added to cold solutions of potassium chloride. Sipahigil *et al* (2001) produced large kappa carrageenan beads encapsulating verapamil hydrochloride given beads containing 3 % w/v carrageenan and 1 % w/v drug. The large beads sustained the release of the hydrophilic compound over 5 hours in phosphate buffered saline (pH 7.4) where the beads had entrapment efficiencies up to 70 %. Carrageenan was chosen since it possesses sulfonate groups in the polymer backbone which are the functional groups in the DC bead that make it capable of controlling the release rate of

doxorubicin. The strong interaction between the verapamil and carrageenan could potentially give the drug delivery system high loadings and controlled release characteristics.

2.5 Gellan

Gellan (Figure 2.4) is an anionic linear polysaccharide that is fermented from the microbe *Pseudomonas elodea*. It is made up of repeating units of one L rhamnose, one D glucuronic acid and two D glucose units (Hasheminya *et al* 2003). Like carrageenan, gellan is also a thermo responsive polymer where gels are formed upon cooling followed by crosslinking with calcium ions due to the presence of carboxyl groups along the polymer backbone. Gellan has two main forms with high or low acyl content, which has a strong influence on the materials gelling characteristics. Low acyl gellan dissolves in water at temperatures around 90 °C and can be processed into hydrogels that form strong gels in the presence of calcium ions, therefore making it ideal for drug delivery applications (Liang *et al* 2006). The high acyl form of gellan forms weaker gels because of the bulky acetyl and glyceryl groups which prevent close association between gellan polymer chains in the double helical formation making it less ideal as a drug delivery system for controlled release (Liang *et al* 2006).

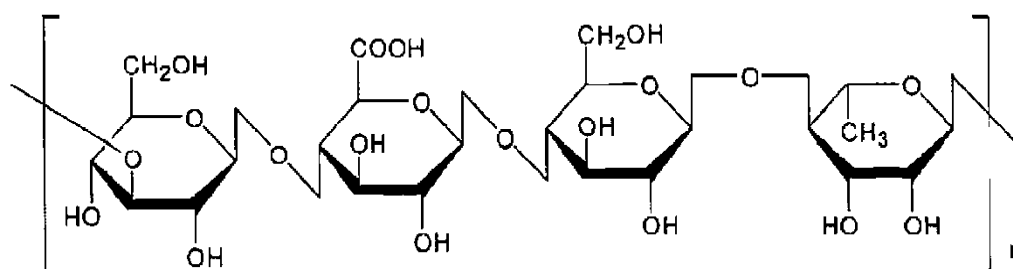


Figure 2.4 – Chemical structure of Gellan (Janna *et al* 2011)

Gellan like carrageenan has also been processed into large gel beads by the syringe droplet method by dropping hot solutions into hot solutions of calcium chloride. Verma *et al* (2011) encapsulated rifabutin, a low water soluble drug into the large beads where the drug was released over a 4 hour period.

2.6 Inorganic materials in drug delivery

Despite the field of drug delivery being a polymer dominated area of research, inorganic based delivery systems have also become a growing area of interest in the field. Inorganic systems have several advantages over organic polymers. Firstly, they have slower degradation rates and do not swell to the extent of polymer based systems upon contact with an aqueous environment (Lovino *et al* 2005). These characteristics of inorganic delivery systems can make them a more beneficial choice for controlled release where other systems fall short due to the rapid swelling and degradation rate. Also inorganics can have a greater biocompatibility over some polymers (particularly synthetics) which can break down into acidic compounds during degradation, which often result in irritation of tissue. (Lui *et al* 2006). The disadvantage to inorganic drug delivery systems is that they can remain in the body for long periods of time or permanently due to their slow degradation time.

Several reviews have demonstrated the significance of inorganics in drug delivery. Wang *et al* (2010) produced a carboxyl methyl chitosan/calcium carbonate nanoparticle hybrid by an ionic gelation method where preformed particles were loaded with doxorubicin and showed controlled release characteristics over a 30 day period. Also, Assifaoui *et al* (2012) produced calcium pectinate hydrogel beads by the syringe droplet method where the beads were then coated with silica by a sol-gel process. The coated beads reduced swelling and the drug release rate of theophylline compared to the pure gel beads. Finally Birdi *et al* (2012) produced an alginate/sodium silicate hybrid bead by the syringe droplet method where the

presence of the sodium silicate dramatically decreased the beads degradation rates to the pure alginate beads; however no drug release studies were investigated. Since a drug delivery system capable of controlled release is required, encapsulating drugs into an inorganic matrix can have the potential to produce a system where the diffusion of the drug is more challenging therefore improving its controlled release capability. The sodium silicate used in the study by Birdi was also investigated as a material to bind into the alginate hydrogels crosslinking mechanism since it greatly reduced the beads degradation, where it was believed it could have potential to improve the systems capabilities for controlled release.

2.7 Verapamil Hydrochloride

The model drug used in this thesis was verapamil hydrochloride, a small molecular weight negatively charged basic drug (Figure 2.5), since it displays similar chemical characteristics to doxorubicin (Figure 2.6), a commonly used drug for TACE. The main chemical property of interest is that the drug is positively charged allowing interaction with the negatively charged polymers during the encapsulation process. This is believed to be of great significance so that small microparticles can bind to the drug molecule producing a system with high drug loadings and controlled release abilities. Small microparticle hydrogel systems will exhibit a high surface area that can rapidly swell making them liable to rapid release rates which can makes this aim of controlled release for hydrophilic drugs particularly challenging.

In an ideal world, doxorubicin would have been investigated however the anti-cancer drug is highly toxic and was too dangerous for the lab environment where the research was performed. Also, the molecule was too expensive for this research. Therefore verapamil, a safer cheaper compound was chosen for the investigation. The properties of the verapamil and doxorubicin are detailed in Table 2.1.

	Verapamil Hydrochloride	Doxorubicin Hydrochloride
Form	White powder	Red powder
Molecular weight (g/mol)	491.06	543.5
pKa	8.6	8.4
pH	5.6	6.5
Water solubility (25 °C)	83 mg/mL	10 mg/mL

Table 2.1 – Chemical properties of Verapamil Hydrochloride and Doxorubicin Hydrochloride

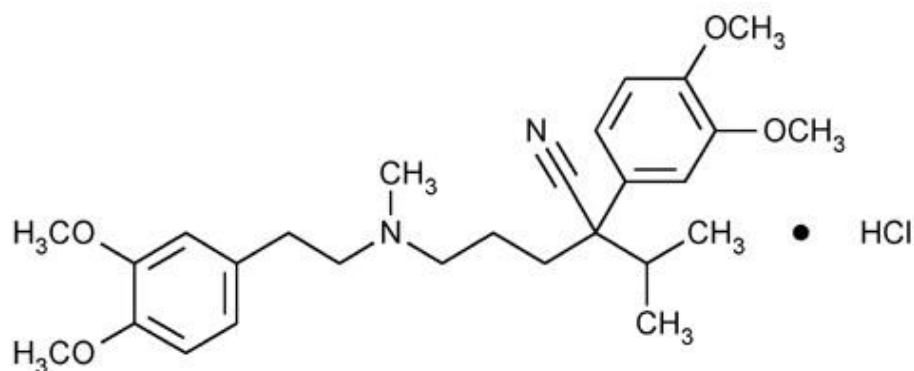


Figure 2.5 – Chemical structure of Verapamil hydrochloride (Sigma Aldrich)

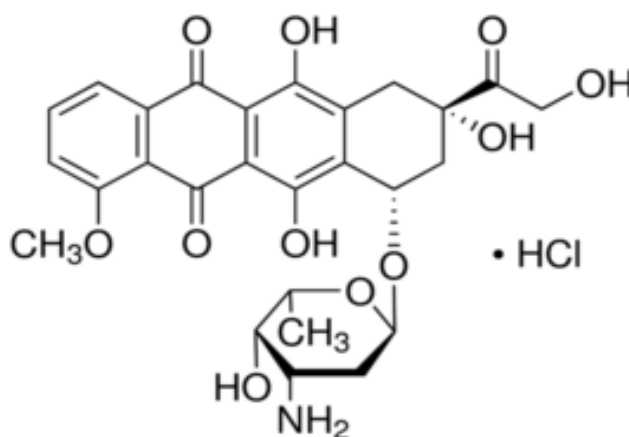


Figure 2.6 Chemical structure of doxorubicin hydrochloride (Sigma Aldrich)

Verapamil is used to treat high blood pressure and heart disorders as a calcium channel blocker where it relaxes the muscles in the heart. It has been investigated in several reviews based on microparticle drug carriers. The first, which inspired the concept of polymer/drug interactions in this thesis, was by the work of Mahesh *et al* (2007) who encapsulated the drug into alginate/Aerosol OT nanoparticles by a double emulsion method, where the system gave

high loadings and controlled release rates. Mahesh also investigated doxorubicin where the two drugs were released at similar rates. Zhang *et al* (2014) produced an alginate-chitosan hybrid particle system by the solvent extrusion method. Large microparticles 1 – 1.5 mm were produced where the particles displayed a release over 12 hours. Paspatis *et al* (2006) encapsulated verapamil hydrochloride into large alginate beads with chitosan coatings where the chitosan coating slightly sustained the release compared to the alginate beads.

2.8 Conclusion

This chapter detailed various water soluble polymers that display negative charges allowing them to interact with positively charged small molecular weight hydrophilic drugs. These interactions can potentially allow small microparticle systems that display high surface areas to be capable of controlled release of a water loving molecule, an area that has seen limited attention in the literature. These interactions will be of great significance since hydrogel based drug delivery systems are known to swell when exposed to water which can lead to rapid or instant drug release rates. Therefore the ability for the gel to not only encapsulate but retain the drug effectively in the formulation is critical. The reviewed materials are to be investigated for the ability to load and control the release of verapamil hydrochloride as the model drug.

CHAPTER 3

MATERIAL SCREENING

3.1 Introduction

The initial experiments investigated in this chapter were to explore various negatively charged water soluble polymers for their drug loading and controlled release characteristics, of verapamil hydrochloride, a small molecular weight cationic hydrophilic drug. Development of drug delivery systems for hydrophilic drugs with high loadings and controlled release characteristics is challenging due to the hydrophilic nature of the drug. Large masses of the drug can be lost during the production process and the drug delivery systems containing hydrophilic compounds are often subject to the burst effect, where large masses of the drug are released in an uncontrolled manner. Therefore, in order to fabricate a system capable of controlled release, materials that would allow interaction with the drug were of key interest. Also, introduction of inorganic materials into the polymer gels to increase the gel strength in an attempt to slow down the drug release rates were also investigated. Large gel beads were produced by the syringe droplet method. This method allowed a fast hydrogel production method to allow screening of the effectiveness of the investigated polymers for their controlled release capabilities.

The objectives of these initial experiments were to;

- Investigate various water soluble polymers for their controlled release abilities where polymers that display a negative charge were of interest.
- Investigate various mixtures of materials that can potentially prolong the drug release rate as opposed to single polymer systems.

- Characterise the materials for their drug loading, encapsulation and drug release capabilities of verapamil hydrochloride.

3.2 Materials and Methods

3.2.1 Materials

Alginic acid sodium salt (ID # 180947, MW 120,000 – 190,000 g/mol, viscosity (1 %) 15-20 cP, M/G 1.56), kappa carrageenan (ID # 22048, viscosity (0.3%) 5-25 mPa.s), iota carrageenan (ID # C1138) and sodium silicate were supplied by Sigma Aldrich UK. Gellan (Gelzan MW 3×10^5 Daltons) and low DE pectin (MW 60,000 – 130,000 g/mol) were supplied by CP Kelco. Calcium chloride, potassium chloride and phosphate buffered saline (PBS) were supplied by Fisher Scientific UK. Verapamil hydrochloride was supplied by Cambridge Bioscience. All aqueous solutions were produced using double distilled water.

3.2.2 Production of the alginate and pectin beads

Alginate and pectin beads were produced by the syringe droplet method using a syringe fitted with a 14 G needle (Sugawara *et al* 1994). Solutions and were produced as follows. Polymer solutions at 6 % w/v were produced by mixing the materials in distilled water overnight at 50 °C. A 2 % w/v solution of verapamil hydrochloride was produced by dissolving the drug in distilled water with mild heating. To produce the polymer-drug solution, equal volumes were well mixed with gentle heating producing a slightly cloudy solution with a final concentration of 3 % w/v polymer and 1 % w/v verapamil hydrochloride. A 3 % w/v solution was chosen since higher polymer concentrations will give denser gels once crosslinked and can potentially display improved controlled release characteristics. Also, the polymer concentrations investigated would be used to produce the small microparticle system in the next chapter. Concentrations above 3 % would be too viscous to process into small

microparticles therefore 3 % was used as a standard concentration for all materials investigated. A 1 M calcium chloride solution was chosen as the crosslinking solution by dissolving the calcium chloride dihydrate in distilled water. Since verapamil belongs to the hydrophilic class of drugs, a strong crosslinking concentration was chosen to minimise the crosslinking period of the beads to reduce drug loss during the fabrication process. To prepare the beads, 2 mL of the polymer-drug solution was added drop wise to 20 mL of the 1 M calcium chloride solution and the beads were then left to crosslink for a 1 hour period in a fridge. The beads were then filtered and dried overnight and stored in vials for analysis.

3.2.3 Production of the Gellan and Carrageenan (kappa/iota) beads

Gellan, kappa carrageenan and iota carrageenan beads were also produced by the syringe droplet method using a syringe and a 14 G needle. Solutions were produced as follows. 6 % w/v gellan and carrageenan were produced by adding the polymers to pre heated distilled water at 120 °C and mixed overnight. The beads were then produced as with the alginate beads above. Crosslinking solutions of 1 M potassium chloride for kappa carrageenan and 1 M calcium chloride for gellan and iota carrageenan were produced by mixing the crosslinking agents in distilled water. Beads were produced by adding 2 mL of the polymer-drug solutions dropwise to 20 mL of the corresponding crosslinking solutions in an ice bath. All beads were left for 1 hour to harden in a fridge followed by filtration and oven drying overnight. The beads were then stored in vials for analysis. The polymer and drug solutions were mixed and added to the crosslinking agents quickly as the high polymer concentrations would cause the polymer solutions to gel quickly once removed from the heat source.

3.2.4 Production of the alginate/sodium silicate

Alginate/sodium silicate beads were also produced by the syringe droplet method. Solutions were produced as follows. A 6 % w/v alginate solution was produced by mixing the polymer

overnight. Several concentrations of 4 %, 8 %, 12 %, 16% and 20 % w/v sodium silicate were produced by dissolving the powder in distilled water at 80 °C. A 4 % w/v verapamil hydrochloride solution was produced by dissolving the drug in distilled water with mild heating. To produce the polymer-ceramic-drug solution, 5 mL of the alginate and 2.5 mL of the verapamil hydrochloride solution were added and well mixed with mild heating. This was followed by addition of 2.5 mL of the desired sodium silicate concentration. The combination of materials was well mixed yielding a 10 mL solution composed of 3 % w/v alginate, 1% w/v verapamil hydrochloride along with 1 - 5% w/v sodium silicate. A 1 M calcium chloride was prepared as the crosslinking agent. To prepare the beads, 2 mL of the mixture was added through a syringe fitted with a 14 G needle to 20 mL of the calcium chloride solution and were crosslinked for a one hour period in a fridge. Again, beads were filtered, oven dried and stored in vials for analysis.

Blank beads in all of the above formulations were prepared and used as the blank sample in the drug loading and release studies for the drug content analysis with UV spectroscopy.

3.2.5 Swelling of the polymer beads

The polymer beads were analysed for their swell characteristics (Equation 3.1) (Nagasawa *et al* 2004). 1 gram of the beads was suspended in 10 mL of double distilled water and left to hydrate for 24 hours. Excess water was removed by drying the beads on a paper towel and the hydrated mass was recorded. The mean was determined from three independent studies and swelling (S) was determined by;

$$S = W_2 - W_1 / W_2 \times 100$$

Equation 3.1 – Hydrogel swelling

Where W_1 is the initial dry mass and W_2 is the hydrated mass.

3.2.6 Drug loading and encapsulation efficiency

The drug loading (DL) and encapsulation efficiency (EE) of the beads were determined by measuring the mass of drug lost to the crosslinking solutions (Equation 3.2a and b) (indirect DL method) (Mitra *et al* 2014). A 1 mL sample was removed from the crosslinking solutions and spun down in eppendorf tubes to separate any solid polymer masses from the drug solution. 750 µL of the supernatant was removed and the verapamil hydrochloride content was assessed with UV spectroscopy (Jasco V-530) at 278 nm (Mahesh *et al* 2007) where a mass of drug was determined from a calibration curve of verapamil hydrochloride prepared by serial dilution.

All drug samples were run against a blank sample obtained from the 1M crosslinking solution used to prepare the blank beads.

DL and EE was determined by;

$$DL = [(D_1 - D_2) / P] \times 100$$

Equation 3.2a – DL of the hydrogel beads

$$EE = [(D_1 - D_2) / D_1] \times 100$$

Equation 3.2b –EE of the hydrogel beads

Where D_1 is the initial mass of drug used in bead preparation, D_2 is the mass of drug lost to the crosslinking solution and P is the mass of material used in bead preparation. All drug loading and encapsulation studies were performed three times where the mean average was determined \pm standard deviation (SD).

3.2.7 Drug release

The polymer beads were subject to in vitro release in PBS as the release media at 37 °C. 50 mg of beads were suspended in 100 mL of PBS (pH 7.4) in 250 mL conical flasks plunged with polystyrene foam plugs and mixed in an incubator at 100 rpm. 1 mL samples were taken on an hourly basis over the first 12 hours of the drug release study followed by a daily basis. For each 1 mL of release media removed, 1 mL of fresh PBS was replaced. All samples were spun down in eppendorf tubes at 10,000 rpm for 1 minute using a centrifuge then 750 µL of the supernatant was analysed for verapamil content by UV spectroscopy at 278 nm. Blank beads were used as a control in all polymer formulations. All drug release studies were performed three times where the mean average mass was determined \pm SD.

3.3 Results and Discussion

3.3.1 Production of the Polymer beads

The polymer beads were prepared by the syringe droplet method (Sugawara *et al* 1994), (Figure 3.1a, b and c). All polymers, upon addition to the hardening bath form instant spherical gel beads though various gelling mechanisms. The alginate, pectin and alginate-sodium silicate beads form instant gels upon contact with the calcium chloride solution where the carboxyl groups (and oxygen atoms in sodium silicate complex) in the polymer backbone are externally crosslinked by divalent calcium ions though the egg box configuration. When fabricating alginate and pectin into drug delivery systems, the degree of crosslinking within the beads can have a great influence on the gel strength. Alginate with a high G/M ratio, high molecular weight and high concentration can produce strong beads with a high degree of crosslinking, however when too high, these solutions would become highly viscous making them difficult to process. The 3 % solution was chosen since it was considered to be strong enough to produce strong hydrogels while still being processable into small microparticles to

be investigated in chapter 5. As for the Gellan, Kappa and Iota carrageenan, the gel beads are formed through a sol-gel transition. In their heated states, the polymer chains exist as a random entanglement of coils that upon cooling form double helical junctions forming the solid beads. Addition of the relative ions, calcium for gellan and iota carrageenan and potassium for kappa carrageenan to the hardening solutions increases the gel strength by allowing the helical structures to pack tighter, forming stronger gels. Kappa carrageenan has one sulfonate group in its structure and forms strong brittle gels whereas iota carrageenan has two sulfonate groups and forms weaker elastic gels. The iota gels were of a more disordered structure than the spherical kappa carrageenan beads due to this weaker elastic gel structure.

The polymers investigated in this study have been developed into a range of drug delivery hydrogels by the syringe droplet method for the encapsulation of many drugs, proteins and cells due to its mild and fast bead preparation procedure (Kim *et al* 2005, Xu *et al* 2007, Stabler *et al* 2001). Kishore *et al* (2012) produced an alginate hydrogel bead system for the encapsulation and controlled release of an antibiotic rifampicin where effective drug loadings and controlled release was achieved. Pasparakis *et al* (2006) produced a verapamil hydrochloride loaded alginate/chitosan hydrogel system for controlled release applications where interactions between the negatively charged alginate and positively charged chitosan prolonged release from the beads. Also, Mrunalini *et al* (2010) produced a gellan hydrogel system by ionotropic gelation for the controlled delivery of an acid soluble drug amoxicillin for delivery to the stomach. Despite its fast and mild preparation procedure, the beads produced are too large for many drug delivery applications however the method provided a good procedure to assess the various materials abilities to load and release the encapsulated drugs.

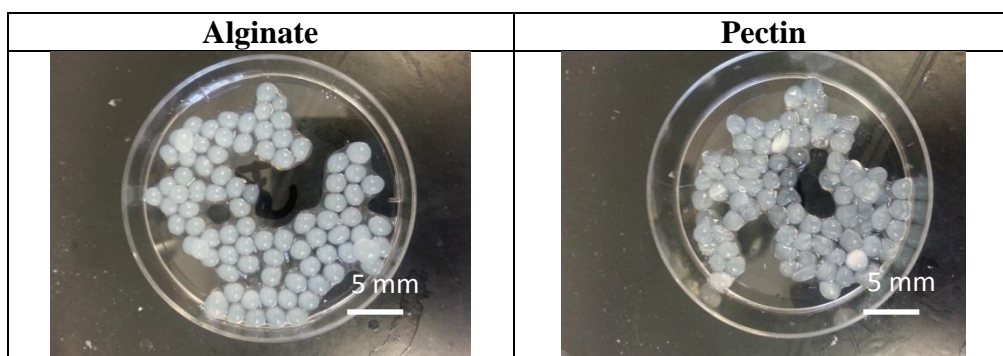


Figure 3.1a – Alginate and Pectin beads formed by the syringe droplet method

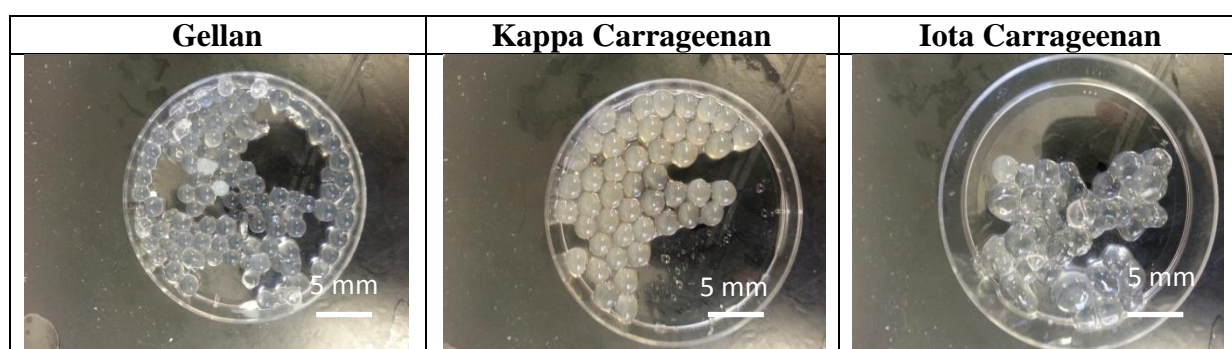


Figure 3.1b – Gellan, kappa and iota carrageenan beads



Figure 3.1c – Alginate/sodium silicate beads

3.3.2 Swelling of the polymer beads

The polymer beads were analysed for their swellability where the variation in the dry and hydrated masses were assessed (Table 3.1a and 1b). Alginate, pectin and gellan all displayed

similar swelling characteristics where the change in mass was approximately 50 % the initial weight of the dry beads. Each of these polymers contains carboxyl groups in the backbone and gel through interactions between the carboxyl groups and calcium ions. Since identical polymer and crosslinking concentrations were used to form the gels, it is believed that this similarity resulted in similar water uptakes of the alginate, gellan and pectin gel beads. Iota and kappa carrageenan had slightly varied swelling characteristics where iota carrageenan took on a higher water mass than kappa carrageenan. This is believed to be due to the fact that iota carrageenan forms a softer elastic gel with higher hydrophilic character since it contains two sulfonate groups, while kappa carrageenan forms a stronger rigid gel with one sulfonate group, resulting in iota carrageenan taking on a higher mass of water.

Swelling of hydrogel system is dependent on the density of the polymer network which is a result of a combination of the polymer concentration, cross linker concentration and crosslinking time used to produce the hydrogel. Surajit *et al* (2010) have investigated several formulation parameters in the production of calcium pectinate beads which included polymer concentration, crosslinking concentration and crosslinking time on the swelling rates where increasing these parameters generally decreases swelling due to the increased gel density.

The addition of the sodium silicate into the alginate saw a fairly significant reduction of swelling in the hydrated mass compared to the alginate beads swelling of 54 %. Upon increasing the silicate concentrations from 1 – 5 %, the beads saw a decrease in swelling from 24 % <p 0.068> - 19 % <p 0.066> - 17 % <p 0.056> - 13 % <p 0.048> - 11 % <p 0.047> respectively. Since this is the first swelling study on this organic-inorganic blend, the reduced water intake is believed to be due to several factors. Firstly, it is seen from the image of the beads in figure 3.1c that the presence of the sodium silicate gives the beads a colour change from an off white in the alginate beads alone to an opaque white when the mineral is present. The silicate is believed to interact with the alginate and calcium ions with a greater

degree of crosslinking increasing the gel strength, reducing the water intake compared to alginate alone. Birdi *et al* (2012) discuss this interaction within the crosslinking mechanism producing stronger gels where the degradation rate was dramatically decreased and the colour change confirms some degree of interaction within the beads. Also, silica has a nano-porous microstructure while alginate is highly porous. Presence of the sodium silicate reduces the beads porosity, which can also reduce the water intake of the beads. Finally it is known that inorganic materials do not swell to the degree that organic polymers do where the presence of the sodium silicate prevents the gel from swelling to the extent of the alginate beads.

Polymer	Alginate	Pectin	Gellan	Iota Cag	Kappa Cag
Swelling (%)	54	48	43	63	47
<i>St Dev</i>	5.2	3.4	6.3	8.4	6.2
<i>RSD (%)</i>	9.6	7.1	14.7	13.1	13.2

Table 3.1a – Swelling of the polymer beads

Na Silicate	1 %	2 %	3 %	4 %	5 %
Swelling (%)	24	19	17	13	11
<i>St Dev</i>	2.1	3.6	2.7	1.3	1.9
<i>RSD (%)</i>	8.6	18.9	15.9	10	17.3

Table 3.1b – Swelling of the alginate-sodium silicate beads

3.3.3 Drug loading and Encapsulation efficiency of the polymer beads

All polymer bead formulations were loaded with verapamil hydrochloride as a model drug. Verapamil hydrochloride was chosen as it is a small molecular weight hydrophilic drug with a positive charge like doxorubicin hydrochloride, a commonly used hydrophilic drug for TACE. The DL and EE (Table 3.2a) of the polymer beads was determined by the indirect method where drug masses were determined from the drug lost to the crosslinking solutions by a calibration curve of verapamil hydrochloride (Figure 3.2). From the polymer beads, DL of 9.7 %, 11.2 % and 8.7 % and EE of 29.2 %, 33.6 % and 26.1 % were determined for alginate, pectin and gellan respectively. As for carrageenan, DL of 22 % and 17.5 % and EE

of 65.6 % and 52.7 % for kappa and iota carrageenan respectively were determined. Alginate, pectin and gellan are carboxylated polymers while carrageenan is a sulfonated polymer. The DL (22 %) <p 0.025> and EE (65.6 %) <p 0.020> in kappa carrageenan was significantly higher compared to the carboxylated polymer alginate with a DL of 9.7 % and EE of 29.2 %. The sulfonate groups give the polymer a stronger negative charge than the carboxylated polymers and they are stronger acidic functional groups that allow them to interact and bind strongly to positive basic drugs such as verapamil hydrochloride allowing higher drug retention. As for the variations of DL and EE with kappa and iota carrageenan, higher DL and EE were determined for kappa carrageenan. Kappa carrageenan forms strong gels while iota carrageenan forms gels that are soft and elastic, where the weaker gel can be less effective at retaining the drug during the production process. Despite iota carrageenan having two sulfonate functional groups that potentially allows it to interact with higher masses of drug, kappa carrageenan's stronger gel strength allowed it to retain larger masses of drug during the production process which makes it the favoured choice for drug delivery systems.

The addition of the sodium silicate to the alginate saw some interesting trends (Table 3.2b). Firstly the DL compared to the 3 % alginate beads (DL 9.7 %), the presence of the sodium silicate in the hydrogel beads greatly increased DL at low concentrations, however this became less significant with increasing sodium silicate concentration within the 3 % alginate beads where a DL of 19.4 % <p 0.025>, 16.2 % <p 0.04>, 15.3 % <p 0.06>, 13 % <p 0.07> and 12.05 % <p 0.1> was determined for 1 – 5 % sodium silicate respectively. As for EE, the silicate significantly increased the efficiency as the silicate content increased where an EE of 75.9 % <p 0.03>, 81.3 % <p 0.02>, 91.7 % <p 0.01>, 90 % <p 0.01> and 96.5 % <p 0.01> was determined for 1 – 5 % sodium silicate respectively.

For increasing silicate concentrations, decreasing drug loading and increasing encapsulation efficiencies were determined as detailed above. The sodium silicate interacts with the crosslinking mechanism of the alginate and calcium ions producing a stronger gel with a higher degree of crosslinking. Since the mass of drug within the varying material formulations stays constant while the mass of sodium silicate increases, the drug delivery system can see a general decrease in DL with the increasing material-drug ratio. As for EE, the literature has reported that higher polymer concentrations prevents the internal drug from leaking out into the crosslinking bath during production due to the increased density and reduced porosity resulting in higher EE. This is also seen with the alginate-sodium silicate beads where higher masses of silicate are believed to allow stronger crosslinks to be produced, preventing high masses of drug from diffusing out of the beads during production. Tavakol *et al* (2013) investigated the effects of polymer and crosslinking concentration on alginate-carboxymethyl chitosan beads where higher concentrations displayed greater drug retention during the manufacturing process resulting in a greater EE.

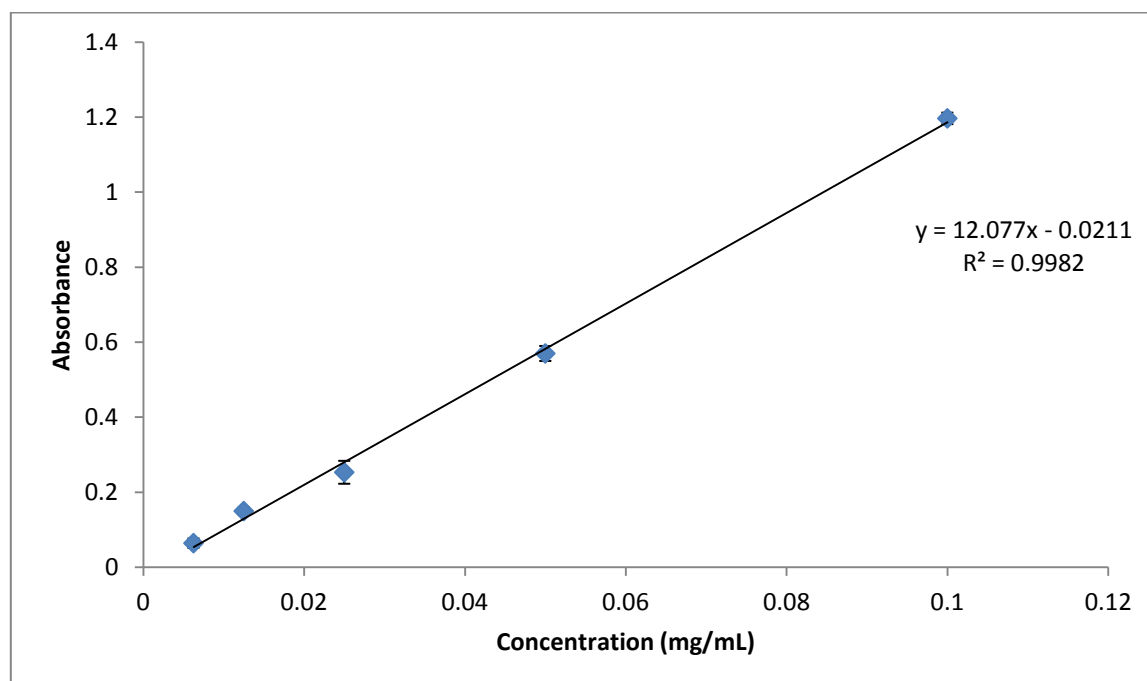


Figure 3.2 – Calibration curve of Verapamil Hydrochloride

	Alginate	Pectin	Gellan	Cag (kappa)	Cag (iota)
DL (%)	9.7	11.2	8.7	22.0	17.5
<i>St Dev</i>	0.6	0.7	0.5	0.6	0.6
<i>RSD (%)</i>	6.2	6.3	4.5	2.7	3.4
EE (%)	29.2	33.6	26.1	65.6	52.7
<i>St Dev</i>	1.6	1.9	1.6	1.2	1.9
<i>RSD (%)</i>	5.5	1.4	6.1	1.8	3.6

Table 3.2a – DL and EE of the polymer beads

	1% Si	2% Si	3% Si	4% Si	5% Si
DL (%)	19.4	16.2	15.3	13	12.0
<i>St Dev</i>	0.3	0.5	0.7	0.3	0.2
<i>RSD (%)</i>	1.5	3.1	4.6	2.3	1.6
EE (%)	75.9	81.3	91.7	90.0	96.4
<i>St Dev</i>	3.5	2.5	1.6	2.1	2.0
<i>RSD (%)</i>	4.6	3.1	1.7	2.3	2.1

Table 3.2b – DL and EE of the alginate/sodium silicate beads

3.3.4 Drug release from the polymer beads

The polymer beads were subject to in-vitro release in PBS where the percentage drug release is illustrated over an 8 hour period (Figure 3.3). From the release studies, the polymer beads showed no sign of controlled release where the entire drug was released within the first hour. Particulate drug delivery systems produced from hydrogels are known to display rapid release rates due to their high porosity, fast swelling and degradation. Also, due to their water loving characteristics, production of drug delivery systems for hydrophilic compounds that are capable of controlled release is known to be a challenging concept. Drug delivery systems produced from these porous materials are often subject to the burst effect, where a formulation releases a large proportion of its cargo upon contact with the release media. Some studies such as the investigation by Mahesh *et al* (2007) have investigated methods to overcome this pitfall of hydrogel drug delivery systems by introducing stronger functional groups that have stronger interactions with the drug in an attempt to prolong the release rate. In this study, sulfonate groups were introduced to alginate nanoparticles to allow stronger

interactions with several positively charged drugs and release sustained over several weeks was achieved. It was expected that the carrageenan beads would allow sustained release to be achieved since the molecules contain sulfonate groups in their backbones, however, although higher drug loadings were obtained, controlled release was not obtainable.

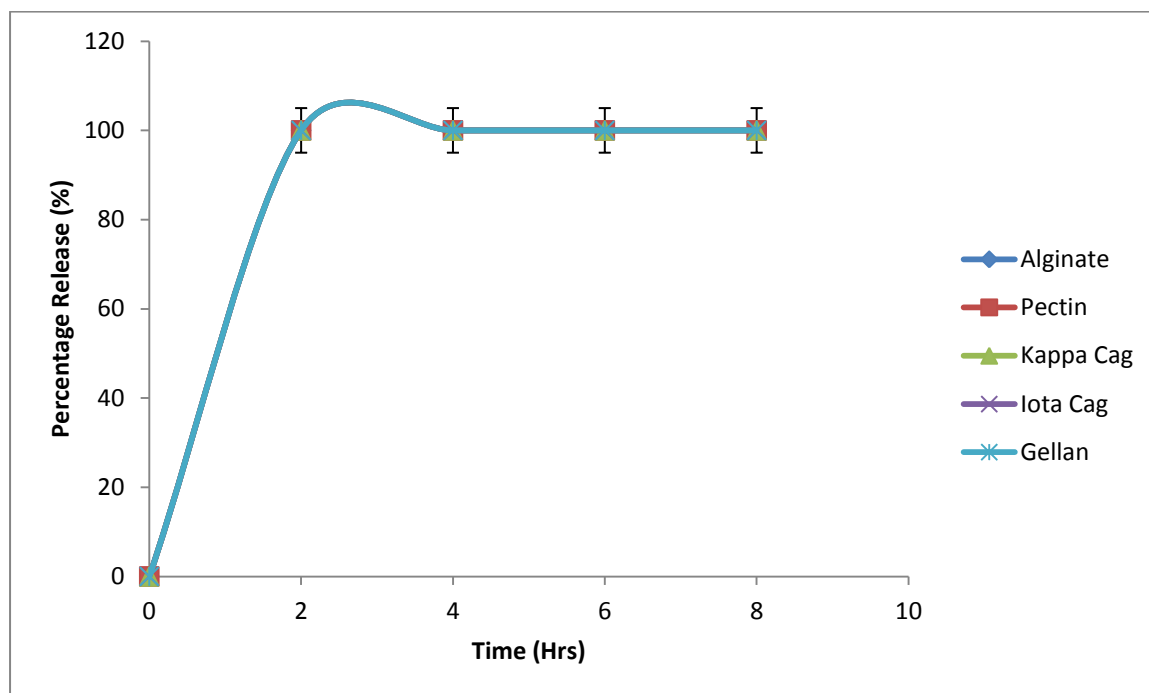


Figure 3.3 – Drug release profile of the polymer beads in PBS illustrating percentage drug release. Each point shows the mean average value taken from three independent studies \pm SD.

The alginate-sodium silicate blend saw an interesting trend in drug release rates compared to the single polymer counterpart where the percentage drug release over the first 12 hours and following 8 week period are illustrated (Figures 3.4a and Figure 3.4b). By varying the concentration of sodium silicate from 1 % - 5 % w/v in 3 % w/v alginate the drug release rate was significantly decreased. After 1 week of the release study, the 1 % w/v formulation released 100 % $\langle p \text{ } 0.98 \rangle$ of the drug whereas 90 % $\langle p \text{ } 0.36 \rangle$, 43 % $\langle p \text{ } 0.03 \rangle$, 28 % $\langle p \text{ } 0.02 \rangle$ and 25 % $\langle p \text{ } 0.02 \rangle$ for concentrations of 2 %, 3 %, 4 % and 5 % respectively, were released at the 1 week time point. Over the first 12 hour period, the release rates vary for beads

containing 2 – 5 % sodium silicate opposed to the decreasing trend with increasing silicate content that is seen over the majority of the study. This is believed to be due to varying masses of surface drug on the exterior of the beads resulting in the initial varied release patterns for the increasing sodium silicate concentrations, which can be a common observation in microencapsulation.

The decrease in drug release rate is believed to be due to several factors. Firstly, drug release of a hydrophilic drug is known to be mainly controlled by diffusion and addition of the sodium silicate into the hydrogel changes the gels microstructure reducing the beads porosity and increases the crosslinking density, making drug diffusion more challenging, thereby decreasing the drug release rate. Also, both alginate and sodium silicate have negative charges allowing them to electrostatically interact with the positive charge of the drug, where the interaction is also believed to aid the decreased release rate. Finally, inorganic materials are known to have slower swelling and degradation rates than organic polymers which are also believed to aid the decreased release rate. By combining the polymer drug interaction with high crosslinking density and reduced porosity the alginate-sodium silicate blend provided an efficient material for the controlled release of the hydrophilic drug, which will be taken forward in the next chapter to be processed into a small microparticle carrier. The idea of this material blend came from the work by Birdi *et al* (2012) where the alginate-sodium silicate beads were produced with the aim to reduce degradation rate of alginate hydrogels. With the addition of silicate, the beads were able to retain their shapes over a period of weeks where pure alginate beads degraded at a faster rate. However, the blend has not been invested or produced into a microparticle based drug delivery system for controlled release applications.

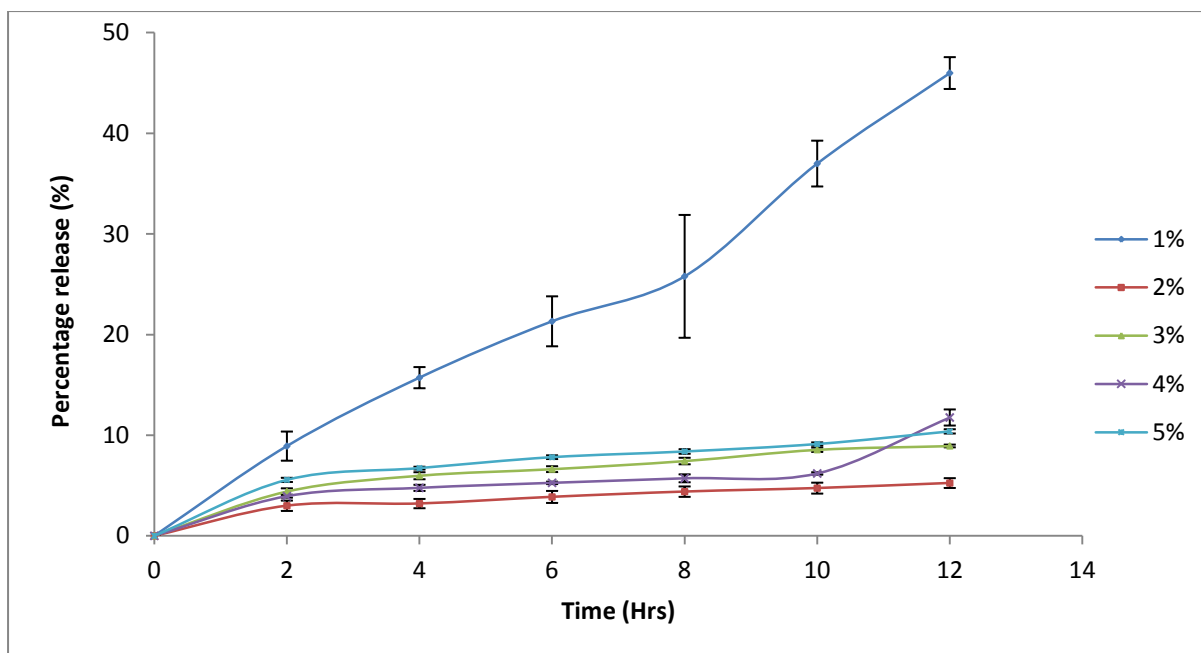


Figure 3.4a – Percentage drug release profile of the alginate sodium silicate beads over the first 12 hours of the release study. Sodium silicate concentrations of 1 – 5 % in 3 % alginate were investigated. Each point shows the mean average value taken from three independent studies \pm SD.

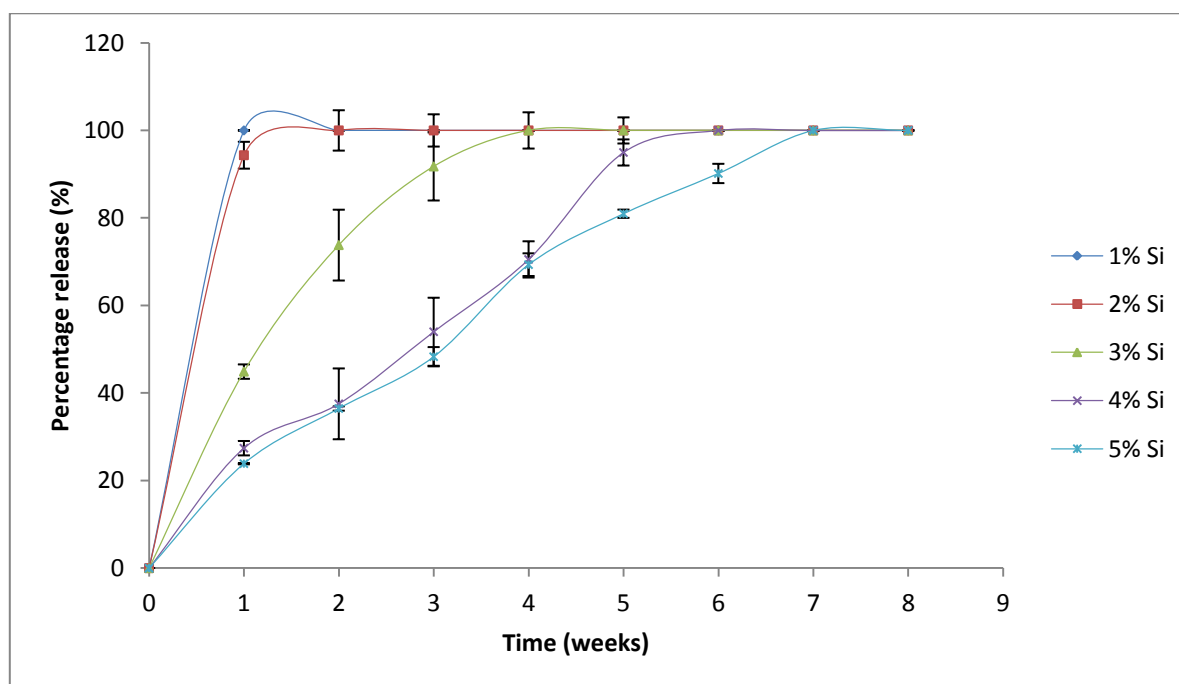


Figure 3.4b – Percentage drug release profile of the alginate sodium silicate beads over the 8 week release period. Each point shows the mean average value taken from three independent studies \pm SD.

3.4 Conclusions

This chapter reviewed various polymers that have seen extensive use in drug delivery where anionic polymers were investigated to encapsulate a small molecular weight hydrophilic drug. Despite their frequent use as drug delivery matrices, the polymers were unable to offer any kind of controlled release characteristics. Sulfonated polymers saw high drug loadings due to the stronger interactions between drug and polymer however these were not sufficient enough to give a sustained release rate. A hybrid of the organic polymer alginate and inorganic sodium silicate was investigated. This combination not only was able to yield high loadings and high entrapment efficiencies, but also allow the drug release rate to be varied from days to weeks by variation of the silica concentration. The presence of the silicate allowed strong gel beads with reduced degradation, porosity and permeability resulting in controlled release of the small molecular weight hydrophilic drug. This material was therefore carried forward to produce into a microparticle delivery system to act as the drug delivery component of the PIP system for TACE. Controlled release of hydrophilic compounds is an area that has seen limited success; therefore this organic-inorganic blend shows great potential for both this work and other drug delivery applications.

CHAPTER 4

MICROPARTICLES FOR DRUG DELIVERY APPLICATIONS

4.1 Introduction to Microparticle Drug Delivery Systems

Following the advances in drug delivery technology, controlled delivery systems have seen extensive research to overcome pitfalls in traditional drug delivery methods. Of such controlled release technologies, particulate based drug delivery systems offer an attractive administration method due to their spherical geometries and ability to tailor the drug release rate to a desired timeframe (Madhav *et al* 2011). Particles also allow protection of drugs from environments such as those along the gastro intestinal tract, a concept that is vital in some oral dosage forms, where drugs can be rapidly degraded in the stomach acid or rapidly absorbed while in transit inside the small intestine. They can also allow taste masking of foul tasting drugs, increasing patient compliance. Controlled release also reduced the dosage of the drug which can result in a reduction of the number of side effects and reduce the frequency of treatments compared to traditional delivery.

These drug delivery particles can range from tens of nanometres to large millimetre sized beads (Padalkar *et al* 2011) and are commonly in the form of solid spheres or capsules (Figure 4.1). Spheres consist of a solid matrix type delivery system such as a crosslinked hydrogel network where drugs are distributed within the matrix core. Capsules are systems composed of a liquid substance entrapped within a solid shell. Oil soluble drugs are entrapped within a water soluble polymer shell and water based drugs are encapsulated within a hydrophobic polymer shell (Vauthier *et al* 2009).



Figure 4.1 – Commonly used particle systems in drug delivery. Microspheres (left) which consist of a solid matrix and capsules (right) consisting of a liquid core encapsulated within a solid shell (Vauthier *et al* 2009).

Spheres on the nano and microscale have seen extensive research in controlled release applications due to their solid structures allowing desirable release profiles of a variety of drugs to be achieved. Cho *et al* (2014) encapsulated resveratrol, a poorly water soluble drug, into chitosan particles crosslinked with tripolyphosphate by a nozzle vibrating method. Particles produced were in the size range of 150 – 200 μm and controlled the release rate of the drug over 5 hours with encapsulation efficiencies up to 97%. Soni *et al* (2010) encapsulated theophylline, a slightly water soluble drug into alginate particles by the water in oil external crosslinking method. Depending on the formulation parameters, particles ranging from 10 – 20 μm were produced where the drug release was controlled over an 8 hour period with encapsulation efficiencies ranging from 70 – 90 %. Dahtat *et al* (2013) produced insulin loaded alginate/chitosan beads crosslinked with calcium chloride followed by glutaraldehyde by the ionotropic gelation method where large beads, approximately 1.2 mm in diameter delivered insulin over an 8 hour period.

Each drug has a minimum level where an effective therapeutic effect can be achieved along with a minimum toxicity point where unwanted side effects can arise (Figure 4.2). The range in-between is known as the therapeutic window which can be narrow or wide depending on the drug (Padalkar *et al* 2011). Pharmaceutical companies have taken to improve upon existing products by producing controlled release systems where the key aim is to control the

release of the drug within the therapeutic window for a desired period of time. This is a region where the best effective therapeutic effect can be achieved. Regions below this point (minimum therapeutic point) are non-effective where the region above this point (minimum toxic point) can result in toxic effects. This method of drug delivery avoids overdosing, reduces the frequency of treatments, reduces the dose of drug required and avoids peaks in toxicity which can result in unwanted side effects. This is particularly important for anti-cancer drugs which can have high toxicities and narrow therapeutic windows.

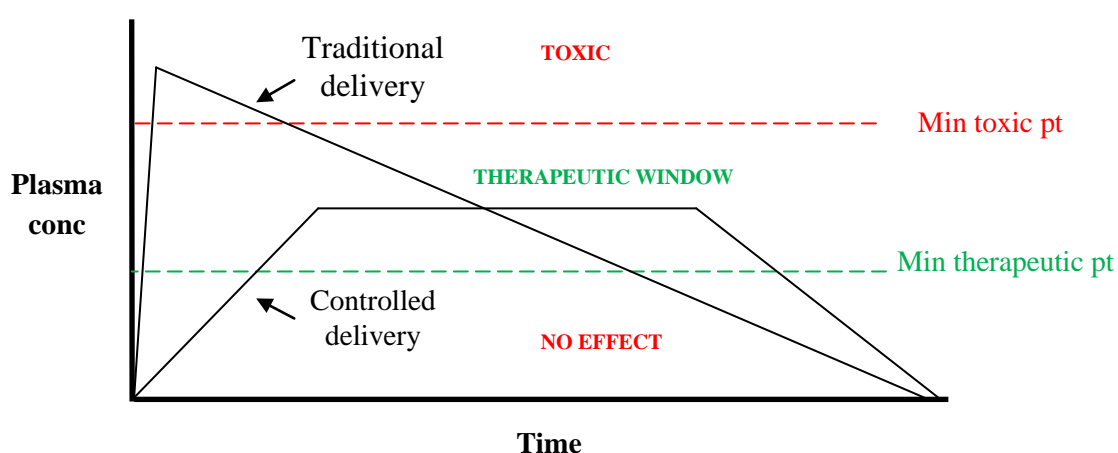


Figure 4.2 – The idealised controlled release profile. In conventional methods, drugs can reach high toxicity levels resulting in unwanted side effects and has no control over release rate. In controlled release formulations, the drug concentration can be controlled within the therapeutic window for a desired time period.

Advantages of particulate based drug delivery include; tailoring size and surface characteristics, controlled release to increase efficiency and decrease side effects, site specific delivery, taste masking and drug protection and also increased patient compliance (Padalkar *et al* 2011). Disadvantages include difficulty in producing uniform sized particles which can lead to irregular results in drug release. Also, microparticles below 100 μm in diameter tend to display poor flow properties which can affect the dosage uniformity when producing a capsule or tablet. Also small microparticles below 100 μm can be highly cohesive making

them liable to agglomeration and their high surface areas can result in rapid release rates of the encapsulated drug (Padalkar *et al* 2011).

4.2 Particle production methods

The choice of production method for micro/nanoparticles is highly dependent on the materials being processed and more importantly, the drug to be encapsulated. For example, producing particles for water soluble drugs by the oil in water emulsion, a method that consists of a large volume of water can result in low entrapment efficiencies due to migration of the drug from the oil droplets to the continuous water phase. Therefore the process method used requires some consideration. Several methods that are suitable for encapsulation of hydrophilic compounds are discussed.

4.2.1 Emulsions

Emulsions have not only been used as an administration method for drugs but also as a particle production method (Figure 4.3). Emulsions consist of three main ingredients, the dispersed phase, the continuous phase plus a surfactant/emulsifier. The dispersed phase forms small droplets that are dispersed throughout a continuous phase when the emulsion is agitated by methods such as mixing or sonication. Surfactants are dissolved within the continuous phase and stabilize the dispersion of droplets, allowing them to remain in a uniform state (Billany). Depending on the ingredients used within the emulsion, several types can be produced. Water-in-oil (w/o) emulsions consist of water droplets dispersed throughout an oil continuous phase while oil-in-water (o/w) emulsions are oil droplets dispersed throughout a water phase. Multiple emulsions consist of primary emulsions within secondary emulsions and are classed as water-in-oil-in-water (w/o/w) or oil-in water-in oil (o/w/o). For the former, a w/o is emulsified in a secondary water phase and for the latter, a

o/w emulsion is emulsified in a secondary oil phase. For water soluble drugs, w/o and w/o/w emulsions have proven to produce particles with high drug loadings due to the drugs poor solubility in the continuous phase (Billany). When using w/o/w emulsions to manufacture particle systems for hydrophilic drugs, the mixing speed is an important factor since if set to high, the high shear can force the water droplets in the primary w/o emulsion to the external water phase, resulting in low entrapment efficiencies.

The general process of particle formation by the emulsion process involves dispersion of a polymer solution into to an appropriate continuous phase containing the surfactant under mixing or sonication. Hydrophobic polymers such as PLGA are dissolved in dichloromethane and are commonly emulsified in a continuous phase of water containing PVA as a surfactant while hydrophilic polymers such as alginate are commonly emulsified in isooctane containing span 80 as the emulsifier. The polymer is mixed at a set speed to obtain particles of a desired size where faster mixing speeds result in droplets of a smaller size. The droplets are then formed into solid particles by a hardening process where for polymers such as PLGA, solid particles are formed by evaporation of the dichloromethane and for polymers such as alginate, the relevant chemical crosslinking agent is added to the emulsion inducing crosslinking. The obtained solid particles are then separated from the emulsion by filtration or centrifugation followed by washing in an appropriate solvent. The obtained slurry is then dried under atmospheric conditions, by freeze drying or under vacuum.

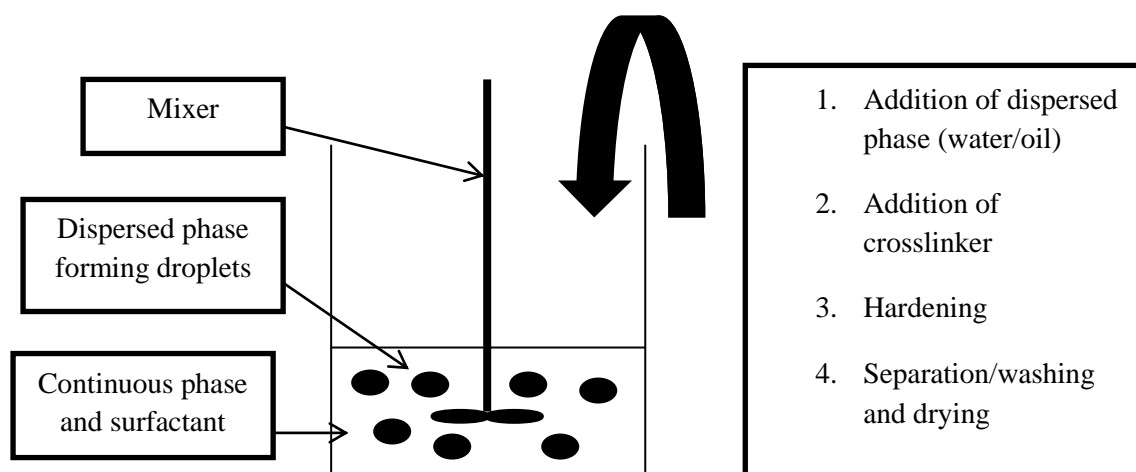


Figure 4.3 - Formation of particles by the emulsion method. Firstly, the polymer is dispersed into the continuous phase containing surfactant under mixing followed by addition of crosslinker (for polymers requiring crosslinking). Then, droplets are left to harden followed by separation, washing and finally drying.

As mentioned above, emulsions require addition of surfactants to stabilize the water and oil phases. Without presence of surfactants, droplets would be attracted to one and other forming aggregates, a process known as coalescence (Billany 2007). The primary job of surfactants is to avoid this by the application of a protective layer around the surface of the droplets that will cause approaching droplets to repel and therefore, remain uniformly distributed within the continuous phase (Billany 2007). This also decreases the surface tension between the water and oil phases allows the breakdown of the dispersed phase into droplets to be an easier process, which can also result in the formation of smaller particles. A wide variety of surfactants are available where the best choice can generally come from practical experience with emulsion science however, the type of emulsion used can eliminate many surfactants since they will not be soluble in the continuous phase. The choice can be further narrowed by use of the hydrophilic lipophilic balance (HLB) (Figure 4.4). The HLB is a measure of the hydrophilic and lipophilic groups in the surfactant and assigns each group a number where a lower numbers are oil soluble and higher numbers are water soluble (Billany 2007).

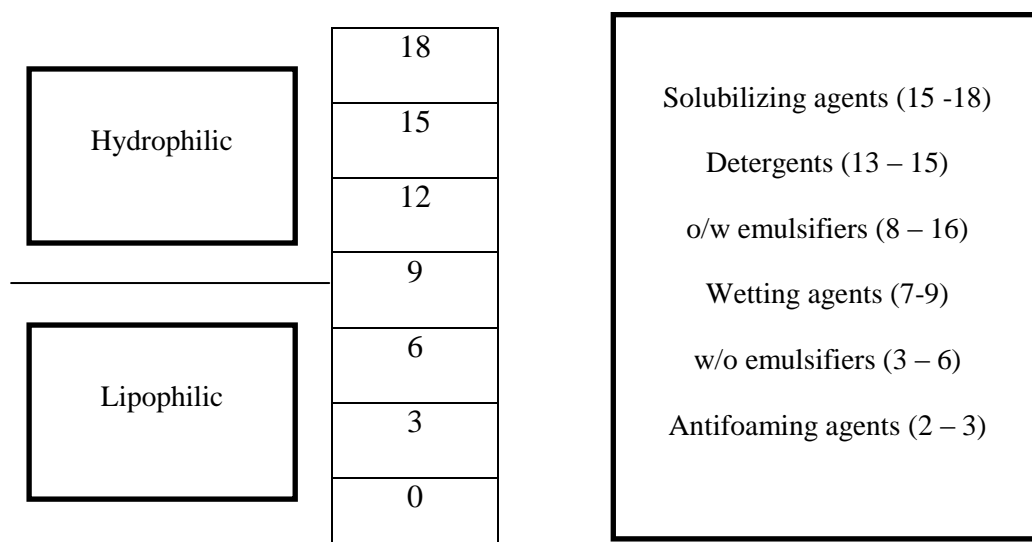


Figure 4.4 – HLB values for various emulsifying agents

The formulation process of particles through emulsions has various processing parameters including polymer concentration, surfactant concentration, mixing speed, crosslinker concentration, crosslinking time and ratio of dispersed phase to continuous phase. The general effect of these on particle size and formation is shown in Table 4.1.

Parameter	Effect on size	Effect on morphology
Polymer concentration	Increasing increases particle size due to higher viscosity	At high conc, clumpy particles can be formed
Surfactant concentration	Increasing decreases particle size due to reduced surface tension	When inefficient agglomerated particles are formed
Mixing speed	Increasing decreases particle size due to increased shear	Irregular sizes can be formed at low speeds
Crosslinking concentration	Increases slightly decreases particle size due to denser crosslinking	When inefficient particles can lose their structure during separation process
Crosslinking / hardening time	As with crosslinking concentration	As with crosslinking concentration
Dispersed: Continuous	Increasing increases particle size due to increased dispersion concentration	When in too high agglomerated forms can be produced

Table 4.1 – General effect of emulsion processing parameters on particle size and formation

The effect of the above parameters has seen extensive research in particle production. Soni *et al* (2013) investigated the effects of polymer concentration on the formation of alginate microspheres by the w-o emulsion. Increasing polymer concentrations from 2 %, 4 % and 8 % saw an increase in particle size from 7.6, 8.2 and 12.5 μm . A study by Jose *et al* (2011) investigated the effects of drug concentration, mixing speed and emulsifier concentration of the production of chitosan particles by the emulsion method. Increasing the mixing speed from 1000, 1500 and 2000 rpm decreased the particle size from 12.7, 8.6 and 5.2 μm . Also increasing the emulsifier (Span 80) concentration from 0.5 %, 1 % and 1.5 % w/v decreased particle size from 10.3, 8.6 and 7.2 μm . The choice of oil used as the continuous phase can have a large effect on the size of particles produced even when identical parameters such as mixing speeds are used. Particles produced using mineral oil as the continuous phase can give larger particles than those produced in isooctane due to the higher viscosity of the oil phase.

4.2.2 Ionic gelation/polyelectrolyte formation

One pitfall of the emulsion method is the requirement of organic solvents and high energy inputs making them undesirable for some drugs. Ionic gelation, also known as polyelectrolyte formation is a mild particle formulation process where microparticles are formed in an aqueous environment with mild processing methods (Vauthier *et al* 2009). A polymer is added to its corresponding gelling agent in dilute solutions under mixing. This forms a pre-gel phase where the polymer chains react with the gelling agent forming small clusters. By addition of a second polysaccharide of opposite charge to the initial polymer, the clusters are stabilised by formation of a complexation between the two oppositely charged polysaccharides (Vauthier *et al* 2009). In the production of alginate particles, alginate is added to solutions of calcium chloride in dilute solutions forming the pre gel phase which is

then stabilised by addition of a cationic polymer such as chitosan (De *et al* 2003). It is possible to form particles by simply mixing the two oppositely charged polymers in dilute solutions however, use of the pre gel phase is known to allow more compact gels to be obtained (Rajaonarivony *et al* 1993). Although mild processing conditions can allow sensitive drugs to be encapsulated, particle size is difficult to control. Also, the method is limited to dilute polymer solutions, which can give gels with limited crosslinking densities, therefore giving limitations to their controlled release applications. Key process parameters are the concentrations of the oppositely charged polymers and if used, the crosslinking agent in the pre gel phase.

This approach has also been used as a coating technique known as the layer-by-layer approach. Particles can be coated with alternating layers of oppositely charged polymers through electrostatic interactions with the goal of prolonging release rate and reducing the burst effect. Several formulations consisting of coating particles with an oppositely charged polymer have known to reduce drug release rate. Lui *et al* (2013) investigated this method to coat liposomes with alternating layers of alginate and chitosan that was attracted to the oppositely charged surfaces, where the drug release of vitamin E was sustained compared to un-coated liposomes.

4.2.3 Spray Drying

Spray drying (Figure 4.5), despite being a drying technology has been used for the encapsulation of drugs into polymeric microparticles. The general process allows the formation of a liquids, emulsions, dispersions and gels into dry powders in a single step which is easier to scale up than emulsions and ionic gelation methods (Richardson *et al* 2002).



Figure 4.5 – The Buchi B-290 mini spray dryer. Particles are formed by pumping a solution to a nozzle where it is atomized into small droplets. The droplets are then rapidly dried in a drying chamber where fine particle masses are removed by a cyclone and the product is collected. Compressed nitrogen is frequently used as the drying gas (Buchi UK)

The spray drying process involves three main stages. Firstly the material to be spray dried is fed through to the spray drying unit to a nozzle of a desired size where the liquid is atomized. The atomization process is an important one since it determines the size of droplets produced and therefore the particle size. Atomization occurs when a gas under high pressure travels through a tube with a reduced diameter causing the gas to increase in momentum. This increase in momentum creates a pressure drop causing the feed to exit the atomizer as a spray of droplets which are rapidly dried in a drying chamber at a desired temperature where solid

particles are formed (Richardson *et al* 2002). Fine particle masses are separated in a cyclone and the product is collected in a collection vessel at the end of the process.

Several types of atomizers are available which are based on being a single fluid, twin flow or rotary disc atomizers (Figure 4.6). Single fluid atomizers force the liquid out under high pressure through an orifice creating the fine spray. They are the most energy efficient but can block easily due to the fast evaporation rate of the liquid (Billany 2007, Richardson *et al* 2002). Twin fluid nozzles involve flow of two fluids, the polymer to be spray dried in an interior nozzle and the drying gas through an exterior section where compressed air or nitrogen is frequently used (Billany 2007, Richardson *et al* 2002). Rotary disk atomizers involve the liquid being fed to rotating discs under high speeds of 10,000 to 30,000 rpm. The feed is fed from the disc to the exterior of the atomizer where it becomes thinner and is eventually ejected from the atomizer as a fine spray of droplets. Rotary disks are commonly used on the industrial scale but require drying tanks with relatively large diameters (Billany 2007 and Richardson *et al* 2002).

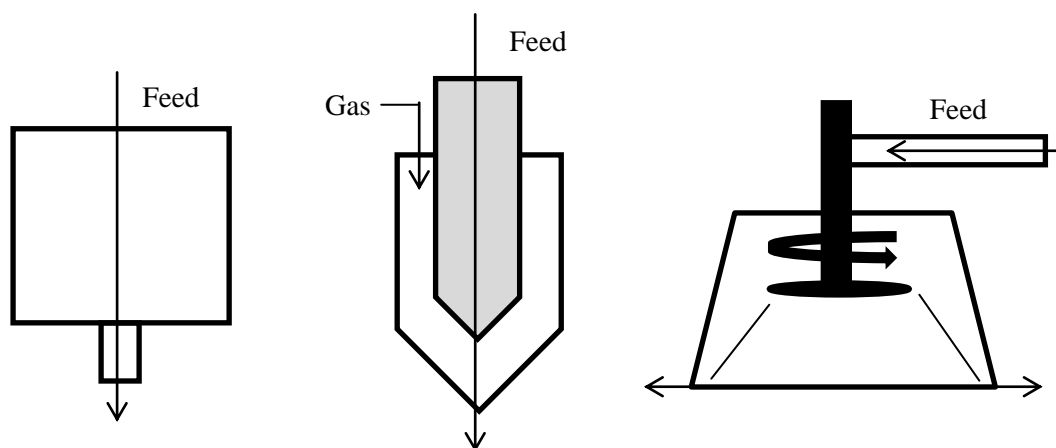


Figure 4.6 – Atomizers used in spray drying. Single flow (left), Twin flow (middle) and rotating disk (right)

Once atomized, the droplets are sprayed into a drying chamber where solid particles are formed by evaporation of the solvent which can take several to tens of seconds depending on the volatility of the solvent used to dissolve the material (Richardson *et al* 2002). Initially the droplets velocity and direction of flow are that which is provided by the atomizer. It is necessary for the gas to be well mixed with the droplets allowing evaporation to initiate and influence the movement of droplets in the drying process and preventing material sticking to the sides of the drying chamber (Richardson *et al* 2002). The air flow within the drying chamber can operate in a co-current or counter-current flow pattern. In co-current flow, the air flows in the same regime as the atomized liquid. This flow regime has the benefit of low product temperatures which is useful for heat sensitive materials however they have relatively low efficiencies. In counter-current flow regimes, the spray from the atomizer initially flows in the opposite direction to the flow of gas which then falls due to gravitational force causing the material to resume flow in the direction of the gas. Co-current flow regimes have higher efficiencies however are limited due to degradation of heat sensitive products (Richardson *et al* 2002).

Advantages of spray drying include a rapid production process in one step, ease to scale up, the process is less dependent on the hydrophilicity or hydrophobicity of the raw materials, high encapsulation efficiencies can be achieved, less residual solvent is left in the dried product and the process can operate under sterile conditions. The main drawback of spray drying is the equipment is bulky and expensive and the process can be difficult for heat sensitive drugs such as proteins.

Several of the critical processing parameters in spray drying that effect particle size and morphology are the polymer concentration, flow rate and inlet temperature (Estevinho *et al* 2013). Generally increasing each parameter increases the size of the microparticles produced (Bowey 2009). For water soluble polymers concentrations are typically 2 – 3 % w/v. On

increasing the concentration, the increase in polymer viscosity makes atomization a more challenging process resulting in larger particles of broader size distributions being produced (Lorenzo-Lamosa *et al* 1998). Concentrations higher than 3 % can be too viscous to be fed and atomize resulting in inefficient production rates and uniform particle size and geometries. Also increasing polymer concentration is known to increase the overall production yield since larger particles are formed resulting in less product being lost to the cyclone. Feed rates for water soluble polymers are dependent on the concentration to be spray dried where for alginate at 2 % w/v flow rates approximately 5 - 10 mL/min have been reported. Like with increased polymer concentrations, increasing feed rate increases particle size. However, when the feed rate is too high, atomization is an inefficient process resulting in large amounts of material sticking to the drying chamber where clumpy products are obtained in the collection vessel (Estevinho *et al* 2013). Operating temperatures are dependent on the material and also, the drug to be spray dried. For natural polymers, inlet temperatures of 150 °C have been a frequently reported within the literature. Despite high inlet temperatures being required, outlet temperatures (the temperature of the drying chamber) are lower than that of the inlet temperature. Also, the air-water interface is only exposed to this temperature for a fraction of a second since evaporation begins the instant the droplets are atomized which is a rapid process, resulting in fast cooling of the droplet. Therefore, drugs at the interior of the droplets are not exposed to the high temperatures (Desai *et al* 2005).

A study by Roberto *et al* (2013) investigated the encapsulation of mangiferin into pectin and chitosan particles using the Buchi B-290 mini spray dryer. Polymer concentrations of 1 % w/v, an inlet temperature of 160 °C and flow rate of 6 mL/min were the operating conditions used to produce the particles. Bowey (2009) investigated encapsulation of insulin into alginate particles with the Buchi B-290 mini spray dryer. Polymer concentrations of 1 – 2 % w/v, inlet temperature of 150 °C and a flow rate of 5 mL/min were the investigated

parameters. Particle sizes of 1.2 and 1.6 μm were found for 1 and 2 % alginate respectively and yields of 15 and 30 % were obtained for 1 and 2 % respectively. Another study by Mobus *et al* (2012) produced alginate particles at 1 % w/v with several other polymers blended in at operating conditions of 145 °C and flow rate of 7 mL/min using a Buchi B-190 mini spray dryer. Spherical particles were formed ranging from 2.9 – 5 μm depending on the polymers blended with the 1 % alginate.

4.3 Particle Characterization methods

4.3.1 Imaging

Imaging methods provide information about a particulate systems size and morphology. Light microscopy is a quick effective imaging method that allows a population of microparticles from several microns in size to be viewed. In the case of hydrogel based microparticles, the dry particles are best viewed when suspended in water where they swell allowing a clear image to be viewed. Detailed characteristics such as the size and shape of particles from 5 – 10 μm in diameter can be easily viewed and images can be captured with an attached digital camera. Fluorescent microscopes are useful tools in analysing particles containing dyes such as coated particles. Also, when formulating emulsion systems light microscopes can be useful in overcoming issues in stability such as insufficient surfactant concentrations.

When formulating sub-micron sized particles, light microscopy is not sufficient enough to provide a detailed image. SEM produces images by a source of electrons being accelerated down a column through a number of lenses and apertures to produce a focused beam that is used to scan a specimen. As the electrons scan the specimen, secondary electrons are produced which are collected by a detector to produce an image of the sample at a higher resolution than that of light microscopes. Care must be taken when imaging with SEM as

some polymers used to fabricate microparticles can be ruptured by the electron source during imaging. SEM is particularly useful for sub-micron size particles and allows a detailed view of the particles microstructure. However they are large and costly to operate and samples must be placed on adhesive discs and coated with gold or platinum prior to viewing.

4.3.2 Particle sizing

Particle size is an important physical characteristic of a microparticle system. Size is a factor that governs the drug release rate where small particles release drugs faster than larger particles due to their increased surface area. Many applications will require a particular size with narrow size distributions. Drugs for pulmonary delivery require particles of 1 - 5 μm in diameter to allow drugs to be delivered deep to the alveoli region of the lung which contains a high surface area for the drugs to enter the system circulation. Also, in the case of this work microparticles of a size calibrated to a patient's blood vessels are needed to effectively target and embolize the tumour.

One common method of obtaining this information is through laser diffraction. This technique measures how a particle scatters light as a laser beam is passed through a particulate dispersion. Large particles will scatter the light at small angles and smaller particles will scatter light at larger ones. Data is then collected where the average size and size distribution of the particles are determined by Mie's theory of scattering light. Optical properties such as refractive index are required in this theory in order to produce accurate data. Other theories such as the Fraunhofer approximation assume particles to be completely opaque and allow a simpler method that does not require optical properties. It can give accurate size data on large particles that are opaque however can lead to inaccurate results for particles below 10 μm or that are transparent. Particle size by laser diffraction is commonly reported as a volume distribution by a plot of particle size and % volume that details the

distribution of a particulate population. Particle sizes typically reported are the mean particle size (D50), the size below 10 % of the population (D10) and the size greater than 90 % of the population (D90) (Figure 4.7).

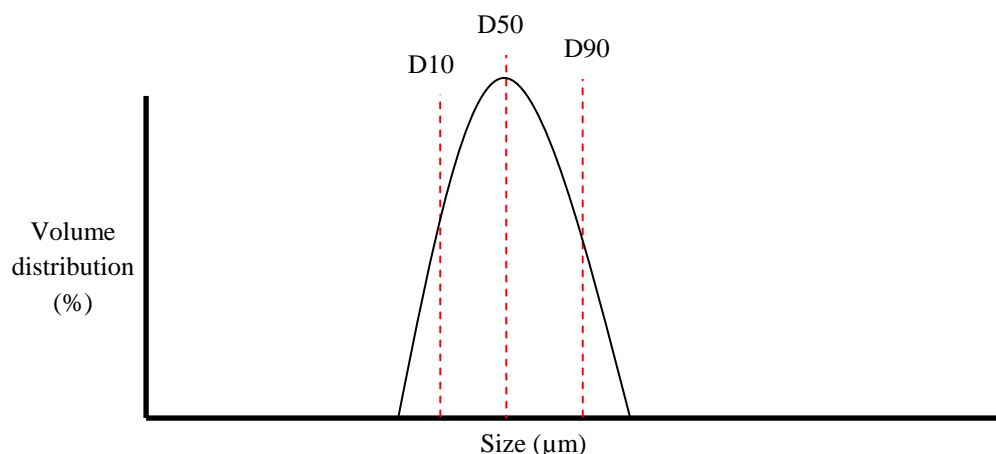


Figure 4.7 – A typical laser diffraction particle size plot showing the volume distribution of a particle population. The positions of the D10, 50 and 90 are illustrated.

4.3.3 Drug loading, Encapsulation and Drug release

DL and EE are determined by treating a known mass of particles suspended in water or an appropriate solvent through methods such as sonication to remove the encapsulated drug contents. The solution is analysed with methods such as UV spectroscopy to determine the mass of drug within the particles by use of a calibration curve of the encapsulated compound. DL is the ratio of drug released from a unit mass of particles, for example if 100 mg of particle release 10 mg of drug, the DL is 10 %. EE is the amount of drug encapsulated into a unit of particles over the initial loading of drug, for example if 100 mg of drug is used to produce a batch of particles and 50 mg is encapsulated, the EE is 50 %. Ideally DL and EE are required to be as high as possible to lower the mass of material used in a dosage form, and to reduce loss of drug during the production process. Drug release is termed as being in-vitro or in-vivo where the former is performed in chemicals simulating a particular environment and the latter in a live specimen. Samples are taken on a regular basis to monitor the rate at

which a drug diffuses out of a polymer matrix allowing a release profile to be plotted showing how the drug is released. Spectroscopy techniques such as UV spectroscopy are useful tools for analysing the absorbance of a drug solution where a mass of drug can be determined from a calibration curve prepared by serial dilution.

4.3.4 Swelling

Swelling of polymer materials, particularly hydrogels is an important factor which contributes to the drug release rate. This can be a measurement of change in diameter or mass of the particles. Swelling is determined by a known mass of dry particles being added to water for a set period of time to induce swelling. The gels are then removed where excess water is removed and the hydrated masses are then recorded from which a swelling ratio, or intake of water can be determined. Swelling rates can vary from hydrogels of varying density caused by variations in process conditions such as polymer concentration, crosslinking concentration, molecular weight and crosslinking time.

4.3.5 Zeta potential

When a particle system is dispersed in a liquid medium, two layers of ions can exist surrounding the solid particles. These are made up of an inner layer (stern layer) and an outer layer (diffuse layer). Ions in the stern layer are held tightly by the solid particle whereas the ions in the outer layer are less associated with the particle. The potential at the boundary of these layers is known as the zeta potential which can have a large effect on how a particulate system behaves and is frequently used to assess the stability of a particulate system. A typical zeta potential value for microparticle drug carriers can range from - 100 mV to + 100 mV where zeta potential values below - 30 mV and above + 30 mV will generally display a stable dispersed particle system where the particles will give a uniformly dispersed population. When a particulate dispersion has a low zeta potential, there will be less charges

to repel adjacent particles causing the particles to aggregate forming large clusters. The pH of a solution will have a large effect of the zeta potential of a particle suspension. Particles that display a strong negative charge suspended in a solution with a high alkali content can acquire a higher negative charge, likewise for particles with a positive charge in a highly acidic medium the system will display a higher positive charge. An unstable aggregated particle system is undesirable in drug delivery applications since the irregular sized clusters will have various drug release properties due to the variance in cluster/particle size and surface area.

CHAPTER 5

PRODUCTION OF THE DRUG DELIVERY PARTICLES

5.1 Introduction

In this chapter, the alginate-sodium silicate blend previously investigated was developed into a microparticulate drug delivery system where verapamil hydrochloride was encapsulated. Microparticles offer an attractive method of delivering drugs to the body due to their small spherical geometries, allowing uniform and reproducible release patterns to be achieved. Their small size also allows administration by the parental route, allowing controlled release of an encapsulated drug. Particles can also allow protection of encapsulated compounds along with controlled release by diffusion of the drug through a polymer matrix. Two production methods were investigated, the water in oil emulsion and spray drying. Critical process parameters for each method were investigated where the parameter's effects on particle size and form were analysed with light microscopy, Scanning Electron Microscopy (SEM) and laser diffraction. Along with the morphologies of the particles, the DL, EE and drug release characteristics were analysed by UV spectroscopy. More specifically, the objectives of this section were to;

- Investigate production processes for the development of crosslinked alginate particles suitable for the encapsulation of hydrophilic drugs.
- Explore the effects of the critical processing parameters on particle formation for the chosen methods.
- Characterize the developed particle systems for their size, shape, DL/EE and drug release properties.

5.2 Materials

Alginate sodium salt (ID # 180947, MW 120,000 – 190,000 g/mol, viscosity (1 %) 15-20 cP, M/G 1.56), sodium silicate, Span 85 and Tween 85 were supplied by Sigma Aldrich UK. Calcium chloride dihydrate, isooctane, hexane and phosphate buffered saline (PBS) was supplied by Fisher Scientific UK. Verapamil hydrochloride was supplied by Cambridge Bioscience. All aqueous solutions were produced with distilled water.

5.3 Methods

5.3.1 Water in oil emulsion method

Alginate particles were produced by the w-o emulsion method similar to the method investigated by Soni *et al* (2010). The formulations produced are listed in Table 5.1 where effects of alginate concentration (formulations A1 – A3), mixing speed (formulations M1 – M3), calcium chloride concentration (formulations C1 – C3), surfactant concentration (formulations S1 – S3) and sodium silicate concentration (formulations Si1 – Si3) were investigated.

The dispersed phase was prepared by producing various alginate concentrations by dissolving the polymer in distilled water over night. A continuous phase was produced by mixing various concentrations of Span 85 and Tween 85 in a ratio of 0.8: 0.2 into 100 mL isooctane in a 200 mL beaker. 10 mL of the alginate solution was added to the continuous phase under homogenization (IKAT25 Fisher Scientific) at various speeds and mixed for 30 seconds where the speed was then reduced to 3000 rpm. 2 mL calcium chloride at various concentrations were then added and mixed for an additional 5 minutes. The emulsions were left at 4 °C for 20 minutes to allow the particles time to crosslink. Emulsions were then spun in a centrifuge at 10,000 rpm for 5 minutes, washed with hexane and re-spun twice. Finally,

a third washing was performed using distilled water and the particles were collected by suction filtration then dried in an oven and stored for analyses.

For the alginate-sodium silicate particles, equal volumes 6 % w/v alginate and various sodium silicate concentrations were mixed then processed as above.

	Alginate (% w/w)	Mixing speed (rpm)	CaCl₂ (M)	Surfactants (% w/w)	Na Silicate (% w/w)
A1	1	15000	1	5	-
A2	2	15000	1	5	-
A3	3	15000	1	5	-
M1	2	5000	1	5	-
M2	2	15000	1	5	-
M3	2	25000	1	5	-
C1	2	15000	0.25	5	-
C2	2	15000	0.5	5	-
C3	2	15000	1	5	-
S1	2	15000	1	1	-
S2	2	15000	1	3	-
S3	2	15000	1	5	-
Si1	2	15000	1	5	1
Si2	2	15000	1	5	2
Si3	2	15000	1	5	3

Table 5.1 – Investigated processing parameters in the w-o emulsion for microparticle formation.

5.3.2 Spray Drying

A spray drying method was also investigated for production of alginate particles using a Buchi B-290 mini spray dryer fitted with a twin fluid nozzle operating with a co-current flow. A method was produced based on the training provided by the equipment supplier (Buchi UK). The processing parameters investigated in the study are listed in Table 5.2. The effects of alginate concentration (A1 – A3), inlet temperature (T1 – T3), flow rate (F1 – F3), sodium silicate concentration (Si1 – Si3), verapamil hydrochloride concentration in alginate (V1 – V3) and verapamil hydrochloride concentration in alginate-sodium silicate (VS_{Si1} – VS_{Si3}) on particle formation were investigated.

Various alginate solutions were prepared by dissolving the polymer in distilled water. The desired inlet temperature and flow rate was set and the aspirator was set at 100 % for all runs. Compressed nitrogen was used as the drying gas and was supplied at 5 bar for all runs. The gas supply was activated followed by activation of the aspirator. The inlet temperature was activated and allowed to reach the set temperature. Once the temperature was reached, the alginate solution was fed to the dryer unit at the set flow rate initiating particle production. Once all the processing material had been spray dried, the tubing and nozzle was cleaned by pumping distilled water for 10 seconds. The pump was switched off followed by deactivation of the inlet temperature, then the compressed nitrogen gas and finally the aspirator. The equipment was allowed to cool until an inlet temperature setting gave a reading of 90 °C before being dismantled for particle collection, since some particle of the equipment would be too hot to handle immediately after drying. The spray dried particles were then crosslinked by mixing a 10 % w/v mass of particles in 1 M calcium chloride for 10 seconds and leaving to crosslink at 4 °C for 20 minutes. The resulting particles were then collected by suction filtration and washed with distilled water. The alginate-sodium silicate particles were produced by mixing equal volumes of 6 % alginate with various silicate concentrations and processing as above.

Drug loaded alginate particles were produced by mixing equal volumes of alginate and verapamil hydrochloride which was processed as above. As for the alginate-sodium silicate particles, alginate and verapamil hydrochloride were well mixed with mild heating in a ratio of 1: 0.5 which was then followed by addition of the sodium silicate in a ratio of 1: 0.5 to the volume of alginate used. The mixture was well mixed and processed as above.

	Alginate (% w/w)	Inlet Temp (°C)	Flow rate (mL/min)	Na silicate (%/w/w)	VHCL (% w/w)
A1	2	150	10	-	-
A2	3	150	10	-	-
A3	4	150	10	-	-
T1	3	120	10	-	-
T2	3	150	10	-	-
T3	3	180	10	-	-
F1	3	150	5	-	-
F2	3	150	10	-	-
F3	3	150	20	-	-
Si3	3	150	10	1.5	-
Si1	3	150	10	3	-
Si2	3	150	10	4.5	-
VA1	3	150	10	-	0.5
VA2	3	150	10	-	1
VA3	3	150	10	-	2
VSi1	3	150	10	1.5	0.5
VSi2	3	150	10	1.5	1
VSi3	3	150	10	1.5	2

Table 5.2 – Parameters investigated for the spray dried particles.

5.3.3 Particle Characterization

5.3.3.1 Light microscopy

Particles characterised by light microscopy (Olympus BH2) were suspended in water then several drops of the dispersion were placed on a microscope slide then covered with a cover slip. The particles were viewed at X 20 magnification where images were taken with an attached digital camera.

5.3.3.2 SEM

Particles analysed with SEM (JEOL 6060) were mounted on an aluminium SEM stub and subsequently coated with platinum using a sputter coater. The samples were coated for 2 minutes with a deposition pressure of 20 bar depositing a layer of platinum equivalent to 150 Angstrom.

5.3.3.3 Particle sizing

The particle size and size distribution were analysed by laser diffraction using wet dispersion on the Malvern Mastersizer 2000. A solution of 0.1 % Tween 85 was used as the dispensing media with a particle concentration of 10 % w/v which was added to the sample dispersion unit under mixing at 2000 rpm using a plastic pipette. Five measurements were performed per formulation where each measurement was subject to a run time of 10 seconds. The $D_{10, 50}$ and $_{90}$ particle sizes along with the particle size distribution curves were reported.

5.3.3.4 Drug loading and Encapsulation efficiency

To determine the drug loading and encapsulation efficiencies, 50 mg of particles were suspended in 50 mL PBS and sonicated for 4 hours. 1 mL was removed and analysed as detailed in chapter 3.

5.3.3.5 Drug release

The particles were subject to in-vitro release. 100 mg of particles were suspended in 100 mL PBS in 250 mL conical flasks plugged with polystyrene foam plugs and mixed at 100 rpm at 37 °C in an orbital shaker. Samples were taken as in discussed in the chapter 3.

5.4 Results and Discussion

5.4.1 Water in oil emulsion method

The w-o emulsion was investigated as a microparticle production method for the alginate-sodium silicate blend. Critical processing parameters of alginate concentration, mixing speed, crosslinking concentration, surfactant concentration and the ratio of alginate: sodium silicate were investigated and analysed by light microscopy, laser diffraction along with the DL/EE and drug release by UV spectroscopy.

5.4.1.1 Effect of alginate concentration on particle size and formation

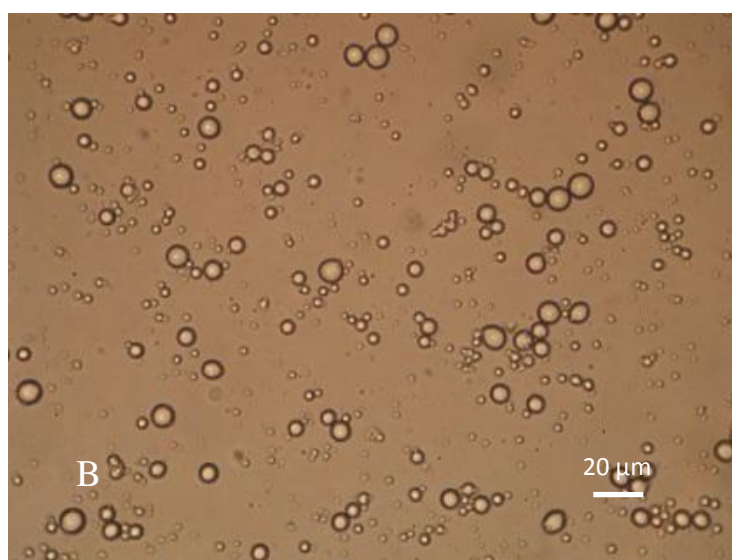
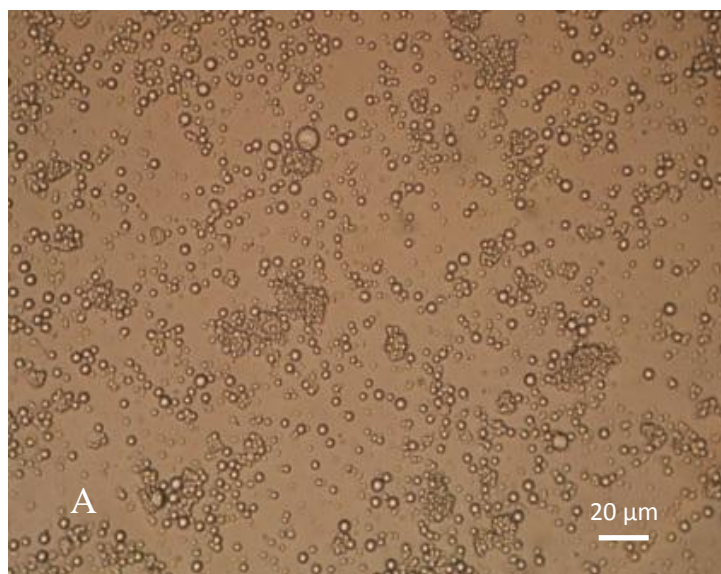
The effect of alginate concentration on the particle size and form was investigated and analysed with light microscopy and laser diffraction where concentrations of 1 %, 3 % and 5 % w/v were explored. Increasing the polymer concentration from 1 % to 5 % had several effects on the particle's size and morphology as illustrated in the light microscopy images (Figure 5.1) and particle sizing data (Figure 5.2 and Table 5.3). Firstly, upon increasing polymer concentration, larger particles with increased size distributions were obtained where average sizes of 4.5, 9.7 and 55.8 μm were determined from 1 %, 3 % and 5 % alginate respectively. Also, particles produced with 1 % alginate appeared to be in a clustered order compared to those prepared with 3 % and 5 % alginate solution.

During the emulsification process, the dispersed phase is broken down into droplets which form the templates for the produced particles. Increasing polymer concentration results in a larger particle size due to the increase in polymer viscosity. This is due to the increased viscosities of the dispersed phase being a more challenging process to be broken down into the droplets that form the solid microparticles. In some cases, increases in mixing speed will be required to provide adequate shear to form spherical particles of a desired size. This was particularly true for particles produced with 5 % alginate where the average size and size distribution was much larger than particles produced with 1 % and 3 % alginate solutions due to the higher viscosity. To allow a more uniform size range to be produced with 5 % alginate, the homogenization speed or time could be increased to allow further breakdown the droplets, although the homogenization time was deliberately kept short in order to minimise drug loss. As for the clustered particles produced with 1 % alginate, reduction in polymer concentration results in smaller particles being produced due since the polymer is easier to break down during the mixing process. Small particles are known to aggregate, as seen with

the 1 % alginate particles. It would have been worth assessing the zeta potential of the particles produced with the varying alginate concentrations to assess effect of alginate concentration on particle stability. The alginate particles are likely to display a negative charge which could increase with increasing alginate concentration. This increased charge could attract more ions lowering the zeta potential (below -30mV) producing a system with greater stability, where the 1 % alginate particles could possibly not be attracting a sufficient concentration of ions to allow the particles to stay uniformly distributed. Since imaging was conducted in distilled water, effects in acidic and alkali conditions would need to be addressed to assess the effect of pH on the stability of the system.

Very few studies tend to investigate production of small microparticles using water soluble polymers by the emulsion method with concentrations greater than 2 % w/v due to the high viscosity resulting in large particle formation. A study by Varma *et al* (2014) investigated production of chitosan particles by the w-o emulsion. Increasing the polymer concentration from 1 – 2 % w/v gave a small increase in particle size of 10.2 – 11.6 μm . The study by Soni *et al* (2010) investigated production of alginate particles by the w-o emulsion method investigating concentrations from 2 – 8 % w/v. Increasing the polymer concentration saw a general increase in particle size from 7.6 – 22.5 μm , however mixing speeds were also increased for increased polymer concentrations. All formulations gave spherical morphologies apart from 8 % alginate which gave irregular geometries (Soni *et al* 2010). Alnaief *et al* (2011) also investigated effects of alginate concentration on particle formation. Varying the concentration from 1.5 – 3 % w/v resulted in a particle size increase from 318 – 608 μm . These particles were relatively large compared to others reported in the literature and in this work which was possibly due to vegetable oil being used as the continuous phase which has a relatively high viscosity compared to isooctane, the continuous phase used in this emulsion. Also, the surfactants and mixing speed used was 1 % and 400 rpm respectively

while in this system 3 % and 15,000 rpm were used which gave lower surface tensions and higher shear rates, resulting in generation of smaller microparticles. As well as polymer concentration, the mixing speed and surfactant concentration can have significant effects on particle size which are discussed below.



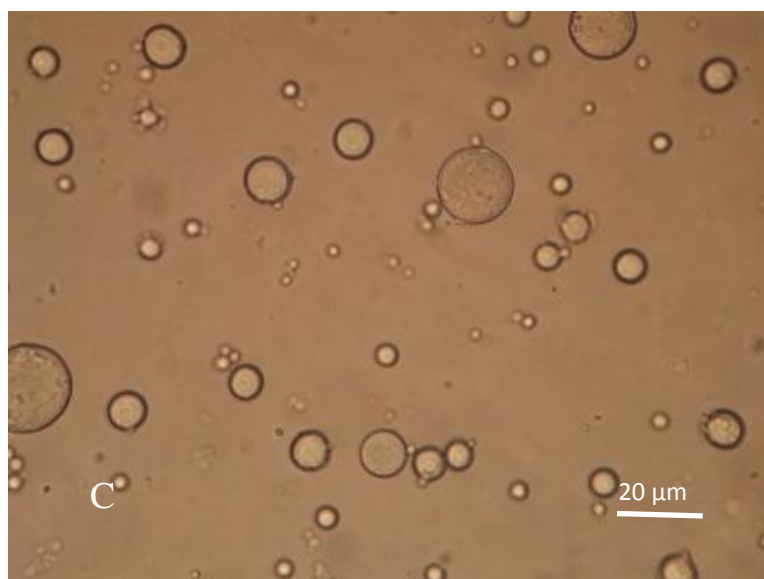


Figure 5.1 – Light microscope images of the alginate microparticles produced with (A) 1 %, (B) 3 % and (C) 5 % w/v alginate. The effect on particle form is illustrated. The surfactant concentration, mixing speed and calcium chloride concentration used in all alginate formulations were 5 %, 15000 rpm and 1M respectively.

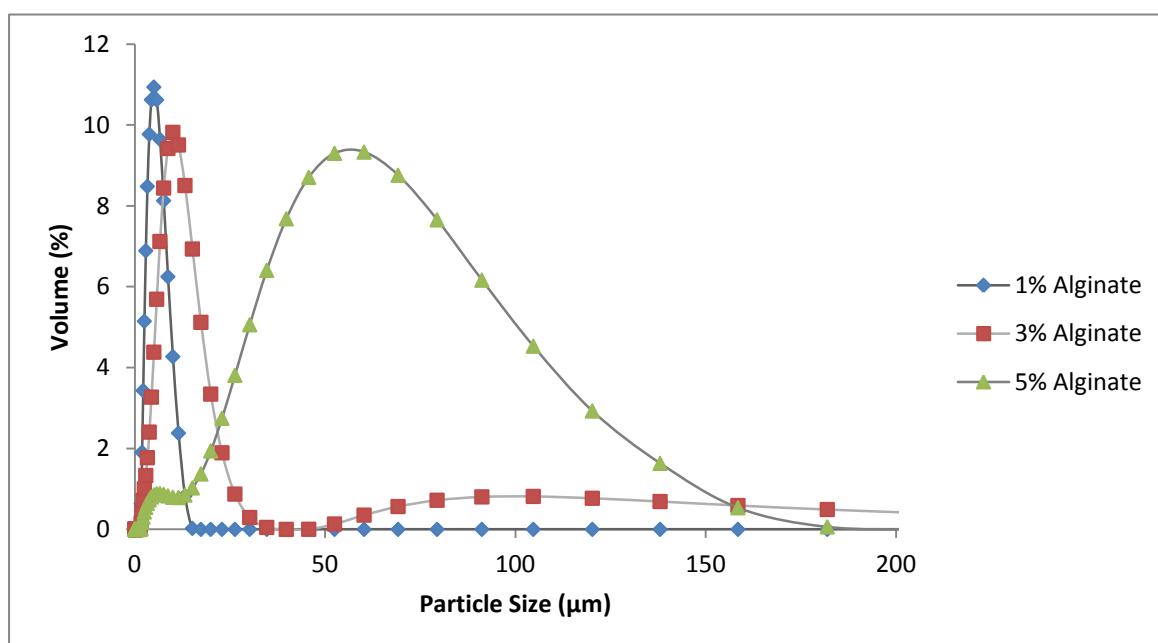


Figure 5.2 – Size distribution of the alginate microparticles produced with 1 %, 3 % and 5 % alginate. The effect of alginate concentration on the particle size and size distribution is illustrated. The surfactant concentration, mixing speed and calcium chloride concentration were 5 %, 15000 rpm and 1M respectively.

	D₁₀ (µm)	D₅₀ (µm)	D₉₀ (µm)
1% Alginate	2.4	4.5	8.9
<i>ST Dev</i>	0.4	0.6	0.8
<i>RSD (%)</i>	16.7	13.3	89
3% Alginate	4.5	9.7	20.3
<i>ST Dev</i>	0.8	0.6	1.3
<i>RSD (%)</i>	17.8	6.2	6.4
5% Alginate	13.5	55.8	135.1
<i>ST Dev</i>	1.7	3.6	11.7
<i>RSD (%)</i>	12.6	6.5	8.7

Table 5.3 – Sizing data for the alginate particles produced with 1 %, 3 % and 5 % alginate showing the D₁₀, D₅₀ and D₉₀ sizes. Each value shows the mean average of three independent studies ± SD

5.4.1.2 Effect of mixing speed on particle production

The effect of the emulsion mixing speed on particle size and form was investigated by light microscopy (Figure 5.3) and laser diffraction (Figure 5.4 and Table 5.4). Agitation methods used in emulsions are dependent on the desired size of the particles where for this process, a high speed homogenizer was used since the high shear was capable of breaking the polymer down into small droplets allowing particles 1 – 5 µm to be produced. Mixing speeds of 5000, 15000 and 25000 rpm were investigated that was shown to strongly influence particle diameter. Firstly, by increasing the mixing speed, smaller particles with narrower size distributions were obtained. Also, like in the case with decreasing polymer concentration the higher mixing speeds produced particles that displayed signs of aggregation. Small particles are known to aggregate due to an increase in adhesive and cohesive forces caused between adjacent particles and surfaces that are known to give them poor flow properties.

The mixing process creates shearing within the emulsion resulting in breakdown of the dispersed droplets. Increasing the mixing speed increases the shear created in the emulsion easing droplet breakup allowing smaller droplets to be produced. For polymers that require chemical crosslinking, a sufficient level of shearing to produce turbulent flow of the continuous phase is required to allow the polymer and crosslinker droplets to collide, in order

for the polymer droplets to form solid particles. Also, emulsions can tend to result in large size distributions due to the shear variation within the mixing vessel. Forces around the agitator will be high while those at the outskirts of the vessel will be low. Due to the decreased levels of shear at the outskirts of the vessel, droplets in this region are liable to agglomeration resulting in an increase in the average size and size distribution. This was particularly true for particles produced at 5000 rpm since this speed gave the lowest level of agitation. This can be resolved by increasing the mixing time however as discussed, the mixing time was kept short to avoid high levels of drug loss.

The effects of mixing speed have been detailed in various studies in the literature. A study by Alnaief *et al* (2011) investigated mixing speeds of 200 – 1400 rpm in the w-o emulsion to produce alginate particles where increasing the mixing speed decreased particle size from 547 – 75 μm . Alnaief also discuss that effects of viscosity of the continuous phase can also affect particle size. Since vegetable oil which has a higher viscosity than isooctane was used as the continuous phase, their particles were considerably larger than the particles produced in this chapter. Vaidya *et al* (2009) produced pectin particles using isooctane as the continuous phase with mixing speeds of 500 – 2000 rpm, where the same decreasing trend was seen where the size decreased from 13.9 to 9.8 μm . The slowest mixing speed investigated in this work was 5000 rpm which produced large particles of 34.5 μm . Vaidya's fastest investigated mixing speed was 2000 rpm which produced smaller particles (2.9 μm) than the 5000 rpm mixing speed investigated in this work, where the general trend for increasing mixing speeds has shown to decrease particle size, which was the opposite in this case. The type of mixing equipment (magnetic/overhead etc) can have a large influence on the particle size even when operating at the same speed since different shear intensities and flow patterns can be produced with various types of impellers/flees etc. Also, particle size can be greatly affected by the ingredients used in the emulsion such as polymer

concentration, polymer molecular weight and surfactant concentration, which all vary from different studies.

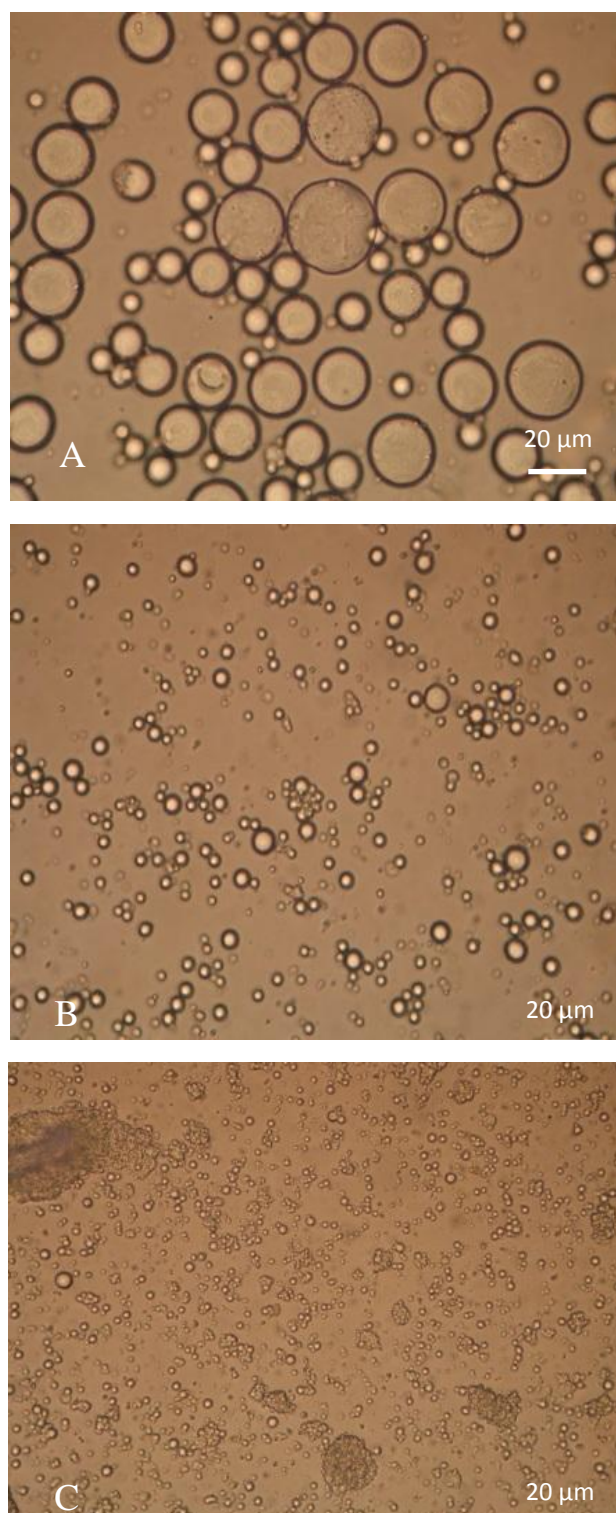


Figure 5.3 – Light microscope images of the alginate microparticles produced at (A) 5000, (B) 15000 and (C) 25000 rpm. The effect on particle size and form is illustrated. The alginate concentration, calcium chloride concentration and surfactant concentrations were 3 %, 1M and 5 % respectively.

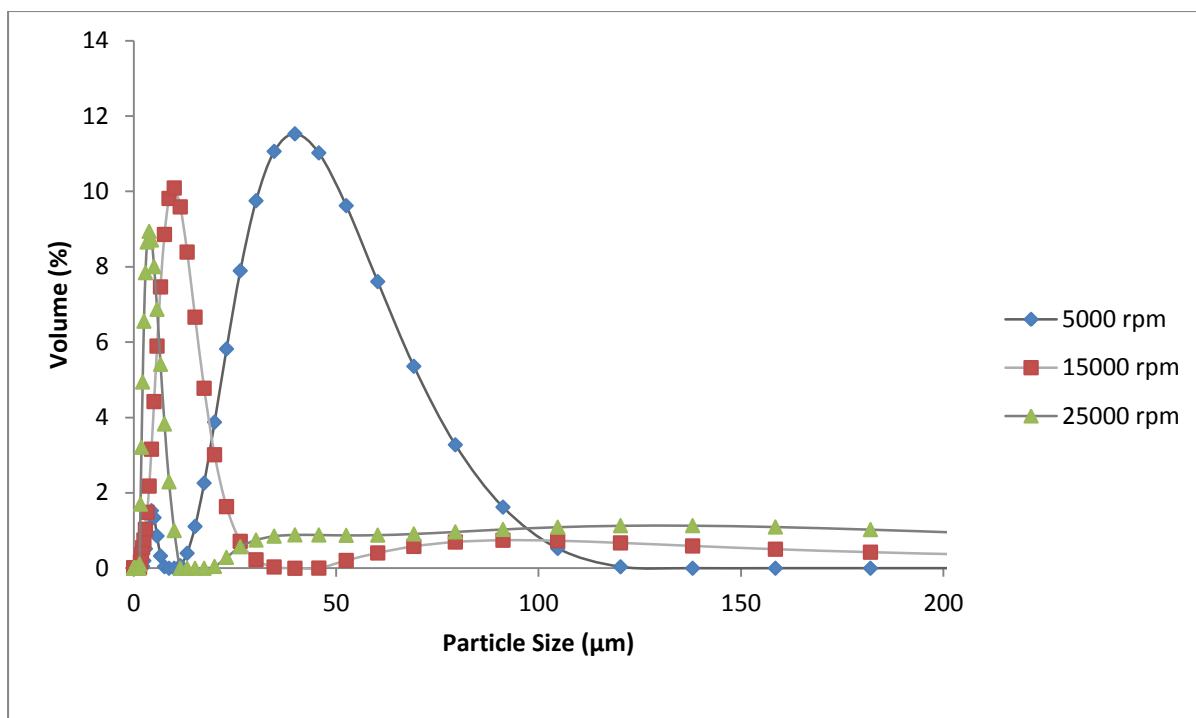


Figure 5.4 – Particle size distribution curves for alginate microparticles produced at 5000, 15000 and 25000 rpm. The effect on the size distribution is shown. The alginate concentration, calcium chloride concentration and surfactant concentrations were 3 %, 1M and 5 % respectively.

	D₁₀ (μm)	D₅₀ (μm)	D₉₀ (μm)
5000 rpm	16.3	34.5	61.6
<i>St Dev</i>	2.4	5.8	14.7
<i>RSD (%)</i>	14.7	16.8	23.8
15000 rpm	4.7	9.5	22.9
<i>St Dev</i>	0.3	2.4	9.3
<i>RSD (%)</i>	6.3	25.6	40.6
25000 rpm	2.8 μ	4.3	80.8
<i>St Dev</i>	0.7	0.2	19.9
<i>RSD (%)</i>	25	4.6	24.6

Table 5.4 – Sizing data for the alginate particles produces at 5000, 15000 and 25000 rpm showing the effect of mixing speed on the D₁₀, D₅₀ and D₉₀. Each size is the mean average of three independent studies ± SD.

5.4.1.3 Effect of surfactant concentration on particle production

The effect of surfactant concentration on the particle size and form was investigated. Span 85 and Tween 85 in a ratio of 0.8: 0.2 at concentrations of 1 %, 3 % and 5 % v/v were explored.

By varying the surfactant concentrations, two key characteristics were found. Firstly, upon increasing the surfactant concentration, the particle size decreases where average sizes of 24.5, 12.3 and 7.3 μm were determined for 1 %, 3 % and 5 % respectively as shown in the sizing data (Table 5.5). Also, upon increasing the surfactant concentration, particles produced were less aggregated and more uniformly dispersed with narrower size distributions as illustrated in the light microscopy images and particle size graphs (Figure 5.5 and 5.6).

Emulsions require the addition of surfactants in order to increase the stability of the system allowing droplets to stay dispersed. Without stabilisation, the two phases will aggregate until the water and oil phases revert back to their separate individual states. Emulsion stability is based on the interfacial film theory. Addition of surfactants to an emulsion system adds an interfacial layer around the dispersed droplets. Since surfactants are amphiphilic materials, the hydrophilic and hydrophobic portions will arrange into the relevant areas of the emulsions (i.e. hydrophilic portions at the water droplets surface and hydrophobic portions in the continuous phase). With the surfactants covering the surface of the water droplets, adjacent droplets will repel preventing coalescence and allowing them to stay uniformly dispersed allowing fine particulate powders to be formed. The concentration of surfactants in the emulsion must be sufficient enough to give an effective level of stabilization keeping the droplets dispersed. When low levels are present, agglomerated products are formed as with particles produced with 1 % surfactants. Another effect of surfactant concentration is their effect on particle size. As well as increasing stability, they also reduce the surface tension between the water and oil interface and therefore, ease the process of droplet breakdown producing smaller particles as shown in the sizing data. Combination of surfactants with different Hydrophilic Lipophilic Balance (HLB) values (i.e. one hydrophilic and one hydrophobic) has been reported to give increased stability by introducing more hydrophilic/lipophilic groups into the emulsion system. Span 85 is a commonly used

lipophilic surfactant in w-o emulsions where several reviews have also used it along with Tween 85 (a hydrophilic surfactant) to increase stability, such as a study by Wong *et al* (2002) who used the two surfactants to produced pectin microspheres. When developing emulsions containing various surfactants with different HLB values, the HLB provides a good idea of the ratios of surfactants required to produce a stable emulsion however experimentation is recommended to ensure the best stability can be obtained.

The pectin particles produced by Vaidya *et al* (2009) investigated various surfactant (Span 80) concentrations ranging from 0.75 – 1.5 % where particle size decreased from 10.8 – 8.7 μm . Like the study by Vaidya, many other reviews discuss use of surfactant concentrations below 2 % and where spherical particles with a uniform size and size distribution are obtained however, with this study, surfactant concentrations at 1 % were not sufficient enough to stabilise the emulsion. It is unknown why surfactant concentrations required to stabilise the emulsion in this work had to be significantly higher than those recorded within the literature. If experimental conditions such as reducing the dispersed phase were to be investigated, the reduction of water surfaces in need of stabilisation could overcome the stabilization issue.

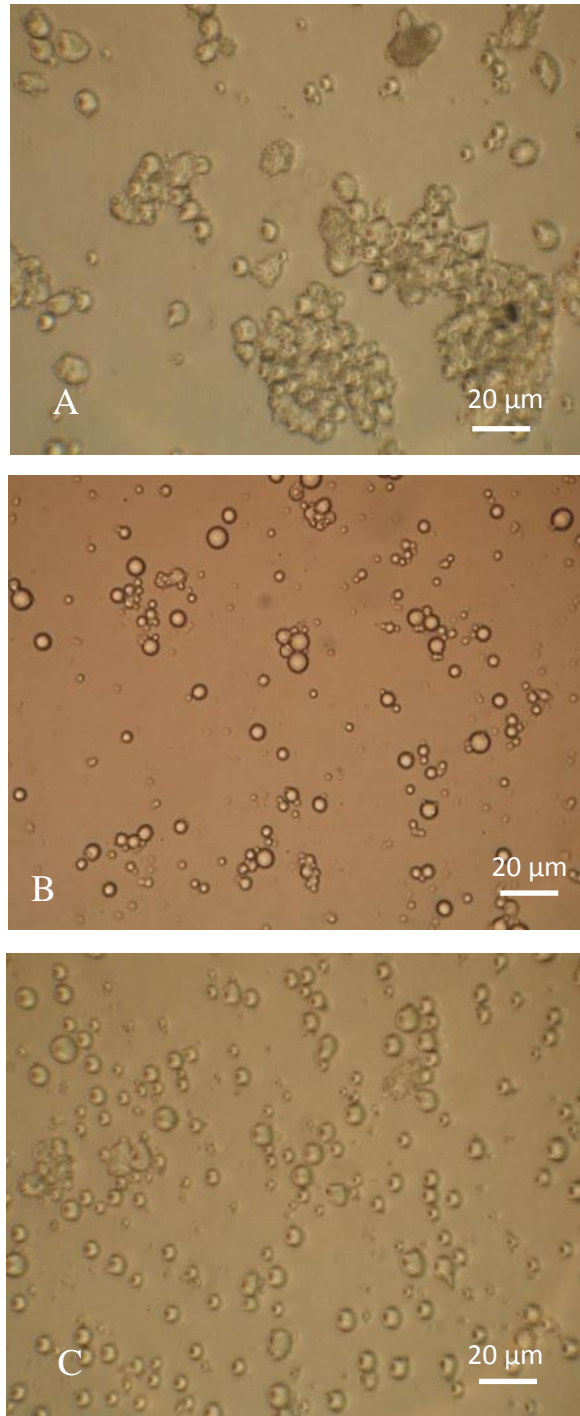


Figure 5.5 – Light microscope images of the alginate microparticles produced with (A) 1%, (B) 3% and (C) 5% surfactants. The effect of surfactant concentration on particle size and form is illustrated. The alginate concentration, mixing speed and calcium chloride concentration was 3%, 15000 rpm and 1M respectively.

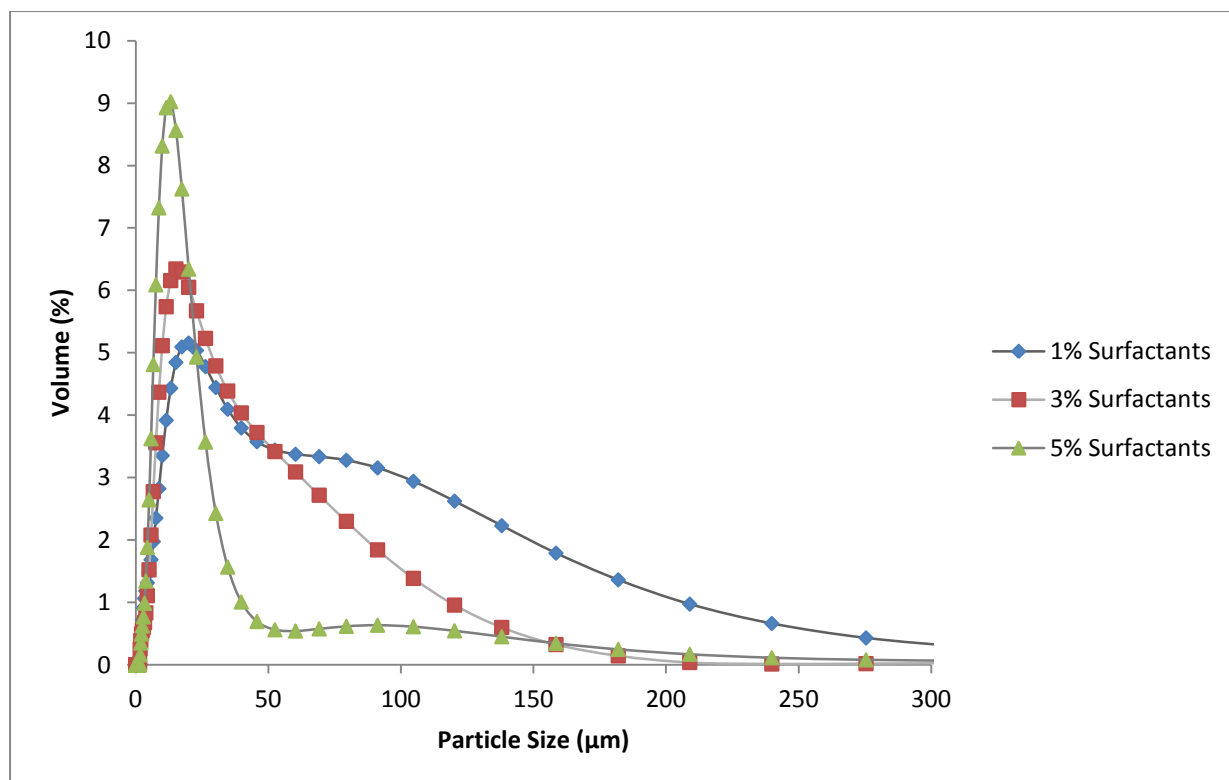


Figure 5.6 – Size distribution curves for the alginate microspheres produce with 1%, 3% and 5% surfactants.

The size distribution and average particle size is illustrated. The alginate concentration, mixing speed and calcium chloride concentration was 3%, 15000 rpm and 1M respectively.

	D₁₀ (μm)	D₅₀(μm)	D₉₀ (μm)
1% surfactants	6.3	24.5	114.9
<i>St Dev</i>	1.3	6.9	24.6
<i>RSD (%)</i>	20.6	28.2	21.5
3% surfactants	6.7	12.3	52.5
<i>St Dev</i>	1.7	4.6	18.3
<i>RSD (%)</i>	25.4	36.5	34.8
5% surfactants	3.2	7.3	28.1
<i>St Dev</i>	0.8	3.6	6.2
<i>RSD (%)</i>	25	4.9	22.1

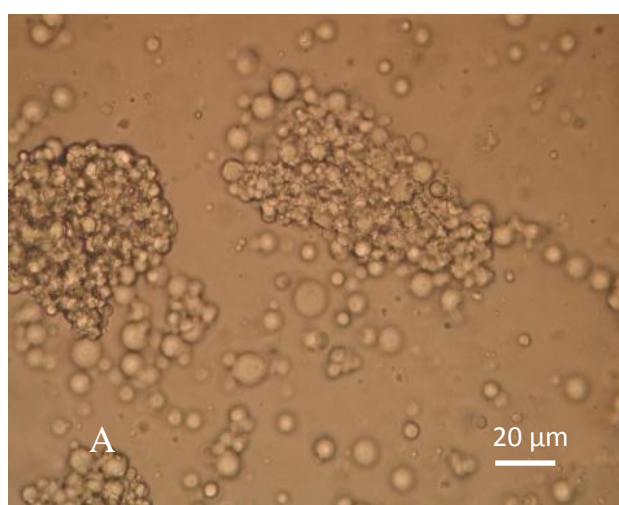
Table 5.5 – Sizing data for the alginate particles produced with 1 %, 3 % and 5 % surfactants showing their effects on the D₁₀, D₅₀ and D₉₀ sizes. Each size is the mean average of three independent studies ± SD.

5.4.1.4 Effect of calcium chloride concentration on particle production

The effect of calcium chloride concentration as the chemical crosslinking agent was explored where concentrations of 0.25, 0.5 and 1 M were investigated. The light microscopy images

illustrate the effects of varying concentration on particle formation (5.7). Particles produced with 0.25 M calcium chloride gave agglomerated forms that were in a poor lumpy formation while those produced with 1 M gave spherical spheres where the particulate product was in a fine powdered form.

Increasing the crosslinking concentration provides a higher concentration of calcium ions to interact with the alginates carboxyl groups. When insufficient concentrations are available, weak gels are formed producing the poor clumpy products. The exterior of the spheres are hardened however, the interiors remain weak which causes them to deform during the separation process such as filtration and centrifugal force. This could be overcome by increasing crosslinking time however, long periods would be required which could lead to high drug loss in the production process. Since these particles would have to undergo a secondary encapsulation process to produce the Particle-in-Particle system, drug loss at this stage must be kept to a minimum. Also, increasing crosslinking concentrations is known to decrease particle size due to tighter, denser gels being produced however, the particles produced with 0.25 and 0.5 M calcium chloride concentrations failed to produce a uniform population of spherical particles.



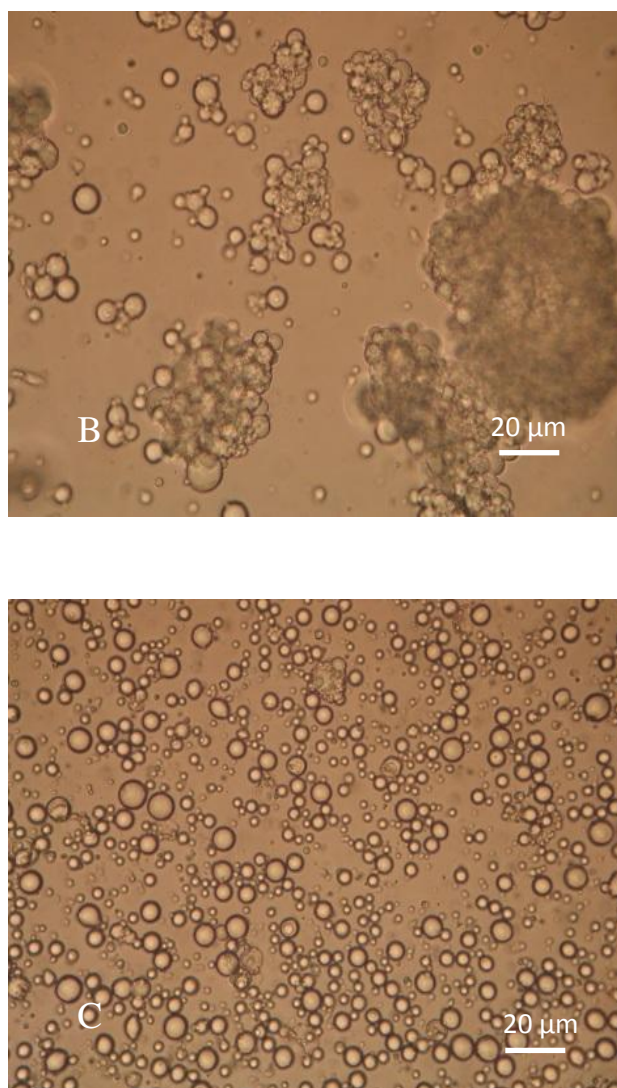


Figure 5.7 – Light microscope images of the alginate microspheres produced with (A) 0.25M, (B) 0.5M and (C) 1M calcium chloride solution showing its effect on particle formation. Alginate concentration, mixing speed and surfactant concentration was 3%, 15000 rpm and 5% respectively.

5.4.1.5 Effect of sodium silicate concentration on particle production

Sodium silicate concentrations of 0.75 %, 1.5 % and 3 % was incorporated into 3 % alginate yielding a 0.5: 1, 1: 1 and 1: 1.5 ratio of alginate: silicate and the particles were analysed with light microscopy and laser diffraction (Figures 5.8 and 5.9 and Table 5.6). Compared to the pure alginate particles, the organic-inorganic hybrid was highly aggregated with irregular morphologies and large size distributions. 0.75 % silicate produced the most uniform

particles however, 1.5 % and 3 % produced highly aggregated forms with no uniform particulate products.

Since this combination of materials has not been explored within the literature, it is believed that crosslinking the droplets with calcium chloride cause them to rupture since they displayed spherical geometries prior to the crosslinker addition. After crosslinking, they take on the aggregated forms as shown in the microscopy images. As previously discussed, it is known that the sodium silicate interacts with the crosslinking mechanism of the alginate and calcium ions. When the sodium silicate to alginate ratio is high (1:1.5), it is believed that the strong interaction between the sodium silicate and calcium ions causes the organic-inorganic droplets to rupture into aggregated masses of material preventing spherical particles from being produced as shown in the light microscopy images. Perhaps by varying the process conditions by reducing the ratio of dispersed phase could allow more uniform products to be formed.



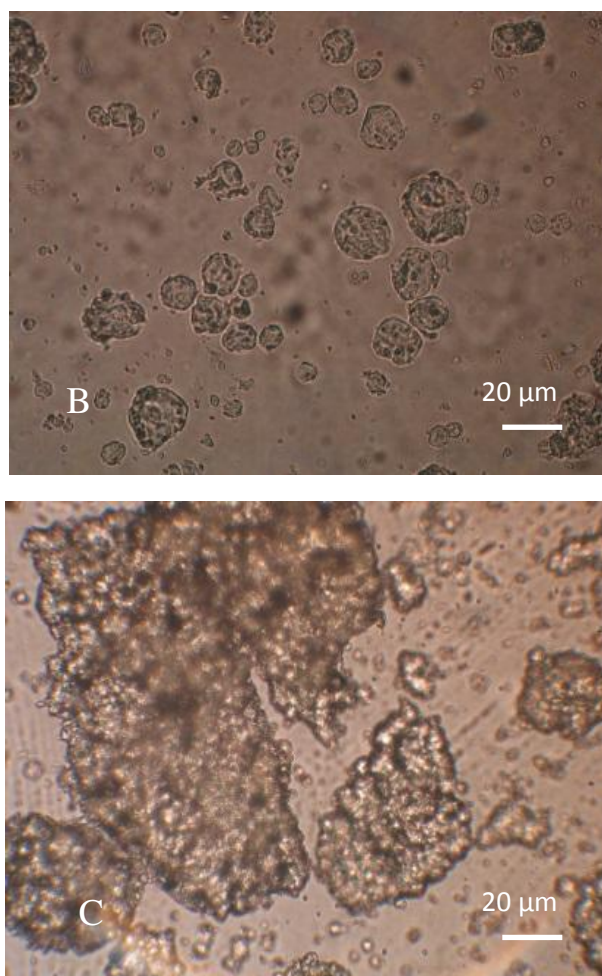


Figure 5.8– Light microscope images of the Alginate/Sodium silicate particles produced with 3 % alginate and (A) 0.75 %, (B) 1.5 % and (C) 3 % sodium silicate showing the effect of sodium silicate on particle formation.

The mixing speed, surfactant concentration and calcium chloride concentration was 15000, 5 % and 1M respectively.

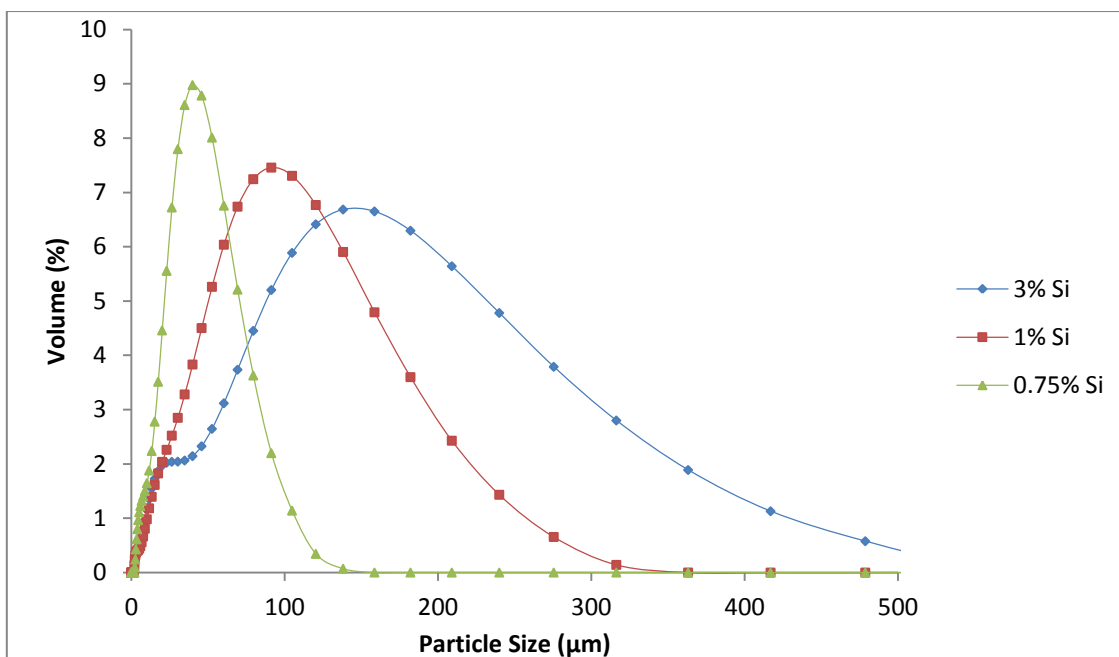


Figure 5.9 – Particle size distribution curves for the alginate sodium silicate particles produced with 3% alginate and 0.75 %, 1.5 % and 3 % sodium silicate showing its effect on particle size and size distribution. The mixing speed, surfactant concentration and calcium chloride concentration was 15000, 5% and 1M respectively.

	D₁₀ (μm)	D₅₀ (μm)	D₉₀ (μm)
0.75 % Si	8.5	32.1	64.8
<i>St Dev</i>	3.5	11.4	24.1
<i>RSD (%)</i>	41.2	35.5	37.2
1.5 % Si	14.3	67.6	143.1
<i>St Dev</i>	7.3	21.4	49.4
<i>RSD (%)</i>	51	31.7	34.5
3 % Si	13.4	97.5	243.1
<i>St Dev</i>	4.6	22.3	53.6
<i>RSD (%)</i>	34.3	22.9	22.1

Table 5.6 – sizing data for the alginate sodium silicate particles produced with 0.75%. 1% and 3% sodium silicate showing their effects on the D₁₀, D₅₀ and D₉₀ particle sizes. Each size is the mean average of three independent studies ± SD.

5.4.1.6 Drug loading

Despite fine particles being produced by the w-o emulsion method, it was not possible to obtain any drug loaded particles. Polymer: Drug ratios up to 1: 2 were investigated however a 0 % drug loading was obtained in all cases. Other parameters known to increase

encapsulation such as increased dispersed phase, shorter mixing times, increased surfactant concentrations, high polymer concentration and no washing stages were investigated however, these also failed to produce any drug loaded particles.

The w-o emulsion required high speed homogenization resulting in high shearing on the alginate droplets. Also, extensive washing stages are required in order to remove the excess oil from the particles resulting in increased drug loss. Encapsulation of hydrophilic drugs by the emulsion method is known to be a challenging process since the drug can migrate from the droplets to the continuous phase, resulting in low encapsulation efficiencies. Despite the drug being a hydrophilic one, with low solubility in the isooctane used as the continuous phase, it is believed that the porous nature of the alginate along with the high energy created by the high speed homogenization resulted in the drug migrating into the oil phase. A sample of the oil was analysed by UV spectroscopy for verapamil hydrochloride content however, a reading could not be obtained where the UV absorbance reading rapidly fluctuated.

5.4.2 Spray drying method

Spray drying was a second method investigated for the production of the microparticles. The method is known to be ideal as a particle production process due to its one step process, ease to scale up and has potential to achieve high drug loading and encapsulation efficiencies. The critical process parameters investigated were polymer concentration, flow rate, inlet temperature, flow rate, polymer: silicate ratio and polymer: drug ratio. Nozzle size also effects particle size however, as only one was available this parameter was not explored.

5.4.2.1 Effect of alginate concentration on particle production

The effect of alginate concentration on the particle size and morphology was investigated and analysed with SEM (Figure 5.10) and laser diffraction (Figure 5.11 and Table 5.7) where

concentrations of 1 %, 2 % and 4 % w/v were investigated. With increasing polymer concentration the particle size increased as illustrated in the SEM images and sizing data. Average sizes of 2.9, 4.7 and 5.3 μm were produced with 1 %, 2 % and 4 % respectively. Also upon increasing the alginate concentration, the particle size distribution increased as shown in the size distribution curves.

During the spray drying process, a spray of droplets are produced by atomization of the polymer solution fed to the nozzle. Increases in polymer viscosity make it more difficult for the polymer mass to pass through the nozzle, making atomization a difficult process that will result in larger particles with wider size distributions being produced. Microparticles produced with water soluble polymers by spray drying are rarely used with solutions greater than 2 – 3 % w/v due to the high viscosity of the solution. However, 4 % alginate was explored since the increased density could potentially prolong the release rate.

Various polymer concentrations have been investigated for the production of microparticles by spray drying using natural polymers. 2 % w/v alginate is a common concentration investigated where Benchabane *et al* (2007) produced BSA loaded alginate particles with a uniform size distribution that displayed an average size of approximately 2.5 μm . The alginate particles produced by Benchabane displayed a similar particle size to the particles produced in this work where Benchabane used a flow rate of 7 mL/min and inlet temperature of 150 °C as the operating conditions to produce their microparticles. Mladenovska *et al* (2007) produced alginate microspheres where a concentration of 3.5 % alginate produced particles with an average size of 6.2 μm . No size distribution curves were reported however the SEM gave an image of a single particle showing a spherical geometry.

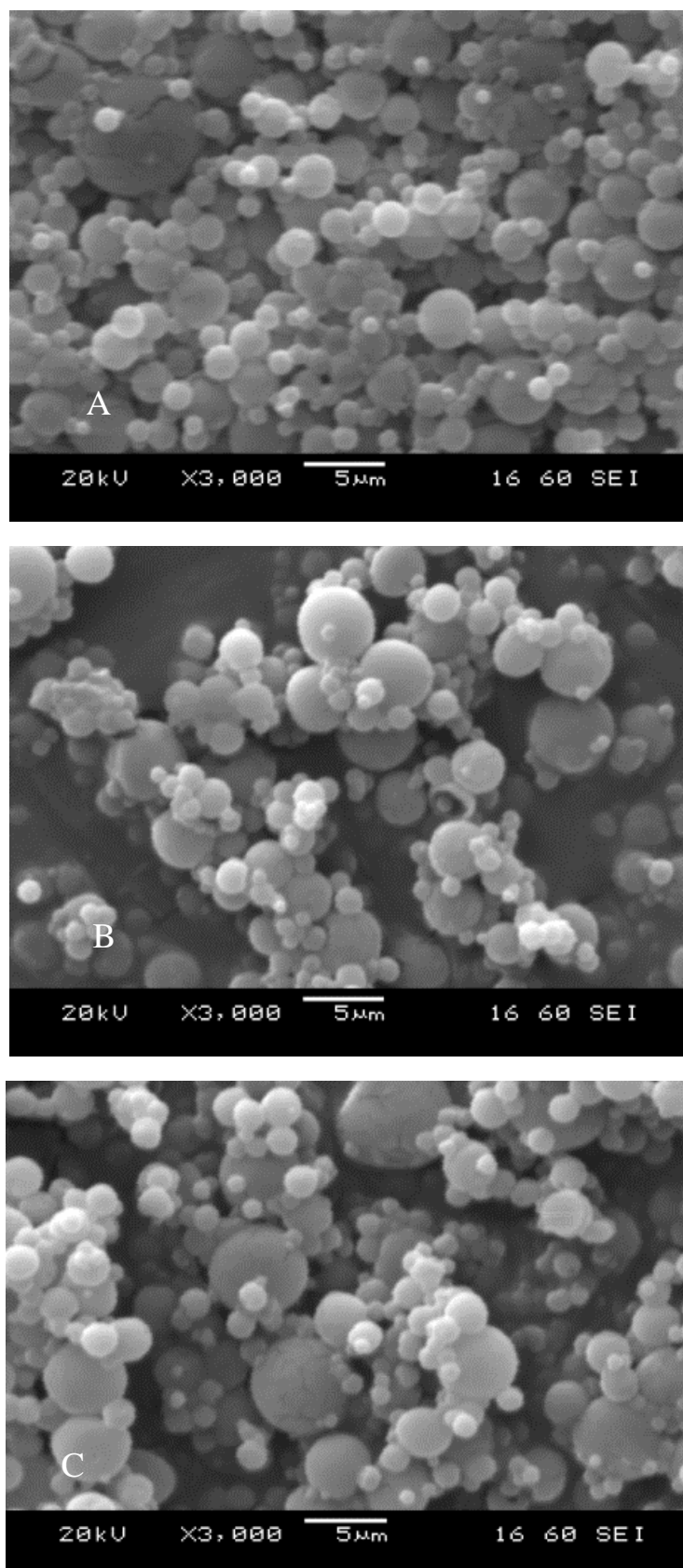


Figure 5.10 – SEM images of the alginate particles produced with (A) 2 %, (B) 3 % and (C) 4 % alginate showing its effect on particle size and form. The inlet temperature and pumping rate was 150 °C and 10 mL/min respectively.

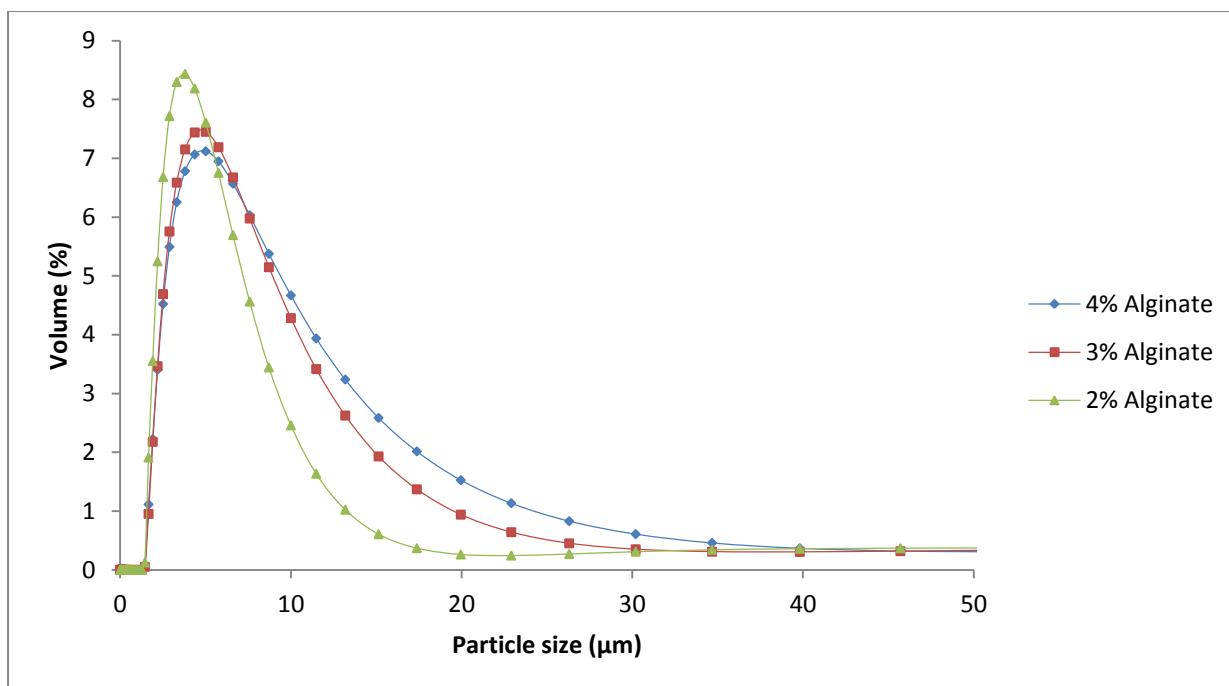


Figure 5.11 – Particle size distribution curves of the alginate particles produced with 2 %, 3 % and 4 % alginate showing its effect on the average size and size distribution. The inlet temperature and pumping rate was 150 °C and 10 mL/min respectively.

	D₁₀ (μm)	D₅₀ (μm)	D₉₀ (μm)
2% Alginate	1.8	2.9	122.5
<i>St Dev</i>	0.2	0.4	27.3
<i>RSD (%)</i>	11.1	13.7	22.3
3% Alginate	2.4	4.7	110.1
<i>St Dev</i>	0.4	0.2	32.4
<i>RSD (%)</i>	16.7	4.3	29.1
4% Alginate	2.3	5.3	35.8
<i>St Dev</i>	0.2	0.6	4.7
<i>RSD (%)</i>	8.9	11.3	13.1

Table 5.7 – Particle sizing data of the alginate particles showing the D₁₀, D₅₀ and D₉₀ particle sizes. Each value is the mean average of three independent studies ± SD.

One of the benefits that make spray drying attractive is its one step process, where methods such as emulsions require additional washing and drying stages. However the microparticles produced in this spray drying method were not crosslinked. Without chemical crosslinking, the particles would dissolve resulting in rapid release of the drug which is not ideal since controlled release of the active is required. Therefore, the particles were crosslinked post-

production where some degrees of aggregation occurred. When crosslinked, it is believed that the high surface area of the particles causes the particles to highly aggregate since the uncrosslinked particles were more uniformly dispersed when viewed by SEM (Figure 5.11). The zeta potential of the particles in the calcium chloride solution would also be worth investigating as the pH of the solution could be reducing the stability of the particle system causing the particles to aggregate to a higher degree where particles are then crosslinked to adjacent particles forming the larger aggregates. Performing the crosslinking in calcium chloride solutions with modified pH levels could possibly allow a more uniform distribution of particles to be produced, however this method would have to ensure the calcium ions do not interact with the added pH modifiers allowing them to crosslink the alginate chains.

Various methods have produced particles that are crosslinked in the drying process, allowing particles to be produced in the one step procedure. Erdinc *et al* (2011) produced a polyelectrolyte complex composed of alginate and chitosan where the lightly crosslinked gel was spray dried into microparticles. Alginate concentrations of 0.2 – 2 % w/v were investigated where particles became highly clustered at higher concentrations. The average size also increased from 2.2 to 4.9 μm with increasing polymer concentration. Also, Mobus *et al* (2012) added a solution of $\text{Zn}(\text{NH}_3)\text{SO}_4$ to alginate solutions where during the drying process, water and ammonia are expelled from the alginate droplets, leaving zinc to crosslink the polymer chains producing the crosslinked particles.

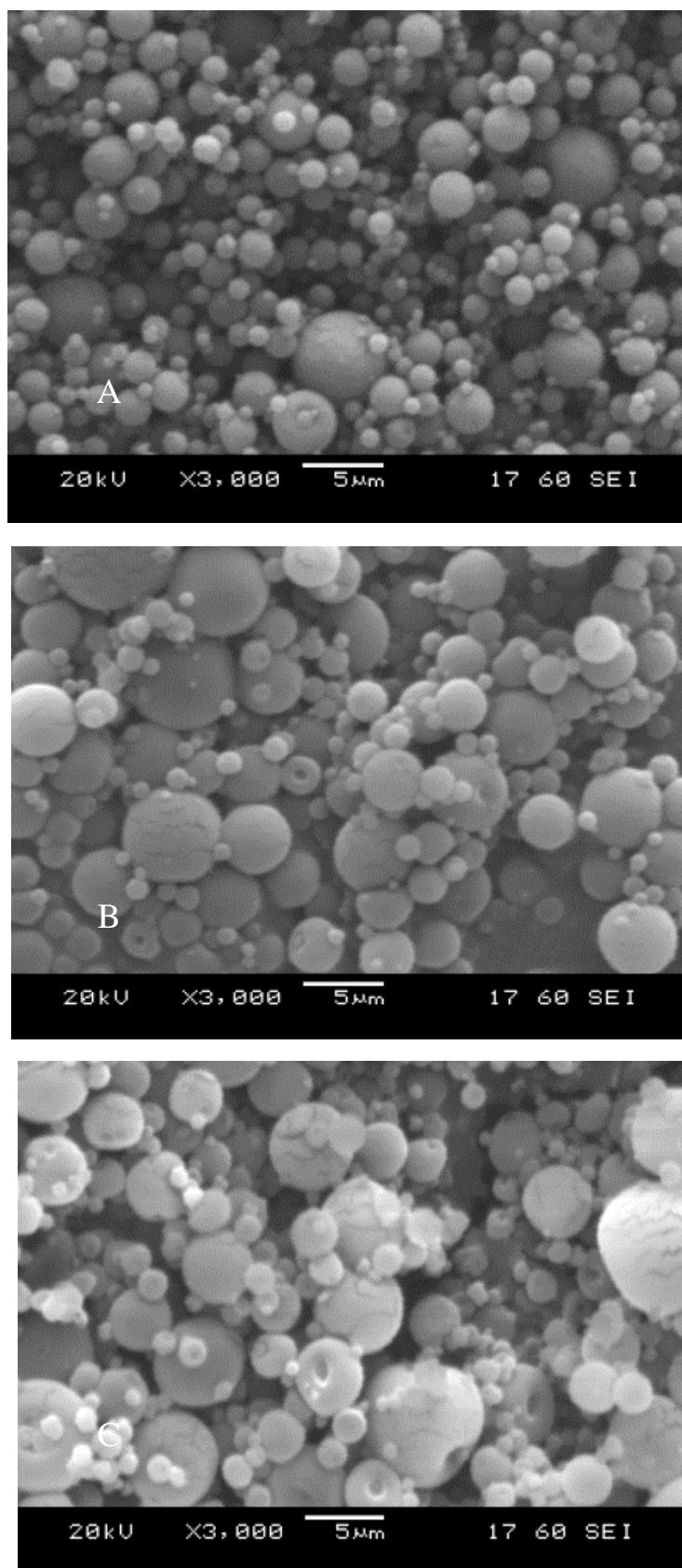


Figure 5.12 – SEM of the un-crosslinked alginate particles produced with (A) 2 %, (B) 3 % and (C) 4 % alginate particles showing the effect on particle size and form. The inlet temperature and pumping rate was 150 °C and 10 mL/min respectively.

5.4.2.2 Effect of inlet temperature on particle production

The effect of the inlet temperature on particle size and form were analysed with SEM (Figure 5.12) and particle sizing (Figure 5.13 and Table 5.8). Upon increasing the inlet temperature, no noticeable changes in particle size was seen where the average sizes produced were 5.7, 5.4 and 5.8 μm for inlet temperatures of 120, 150 and 180 $^{\circ}\text{C}$ respectively. However, particles produced at 120 $^{\circ}\text{C}$ saw a slightly more aggregated product compared to the higher inlet temperatures.

Upon atomization of a polymer solution, the liquid spray is rapidly dried which can take several seconds to approximately 10 seconds depending on volatility the material being spray dried. When drying temperatures are not sufficient, water can be retained in the collected particles leading to aggregated formations being produced. Particles produced at 120 $^{\circ}\text{C}$ are believed to retain water after drying resulting in these aggregated particles being formed. This can be overcome by increasing the inlet temperature or by use of a different flow pattern that gives the droplets a longer drying time in the drying chamber which would be better suited to drugs that are heat sensitive.

The effect of varying inlet temperatures are not often reviewed in spray drying where temperatures of 150 $^{\circ}\text{C} \pm 10^{\circ}\text{C}$ are often used for water soluble polymers. Results vary within the literature where increasing inlet temperatures have seen the change in particle size increase, decrease or show no effect. Benchabane *et al* (2007) varied inlet temperatures from 150 – 200 $^{\circ}\text{C}$ and no variation in particle size was seen whereas Marshall (1954) commented on an increase in particle size with increasing inlet temperature. This could also be down to the sizing method used and the chemical properties of the materials being used (molecular weight/concentration etc). Particles produced from polymers on high concentration and molecular weight will have a reduced swellability, and when sizing methods such as laser

diffraction are used, the particles can swell in while suspended in the dispersant, where these varying concentrations and molecular weights can result in different particle sizes being measured.

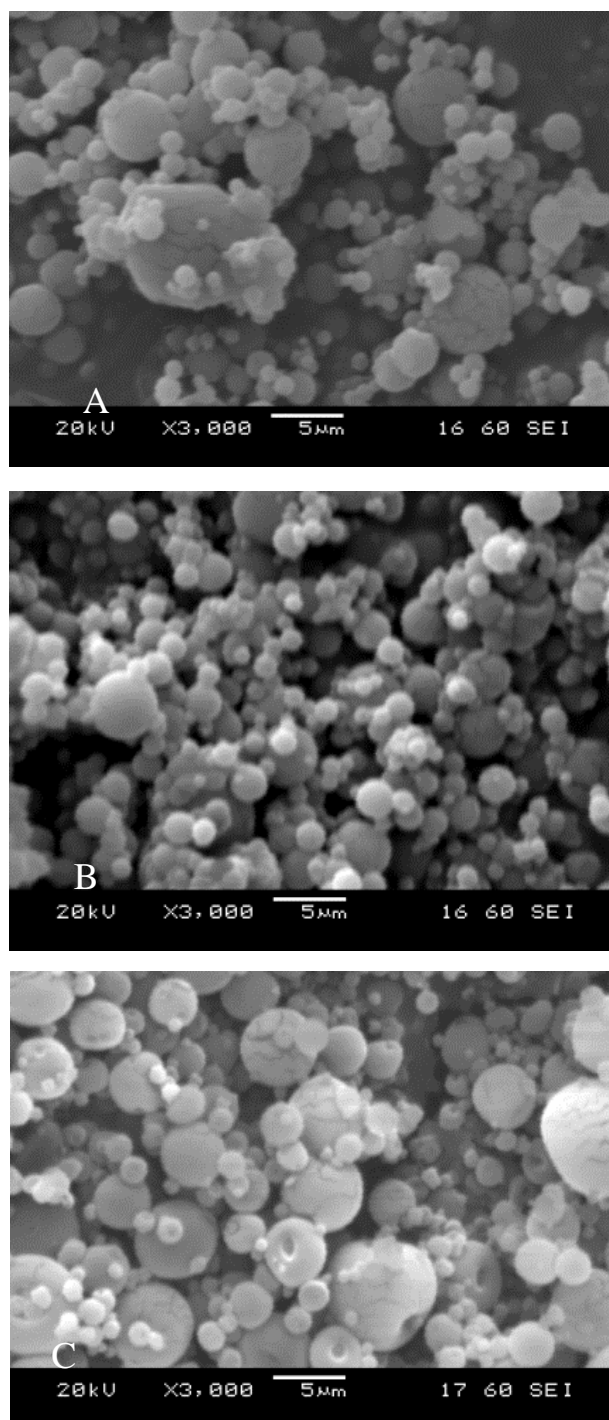


Figure 5.13 – SEM images of the alginate particles produced at temperatures of (A) 120 (B) 150 and (C) 180 °C showing their effects on particle size and form. The alginate concentration and pumping rate was 3 % and 10 mL/min respectively.

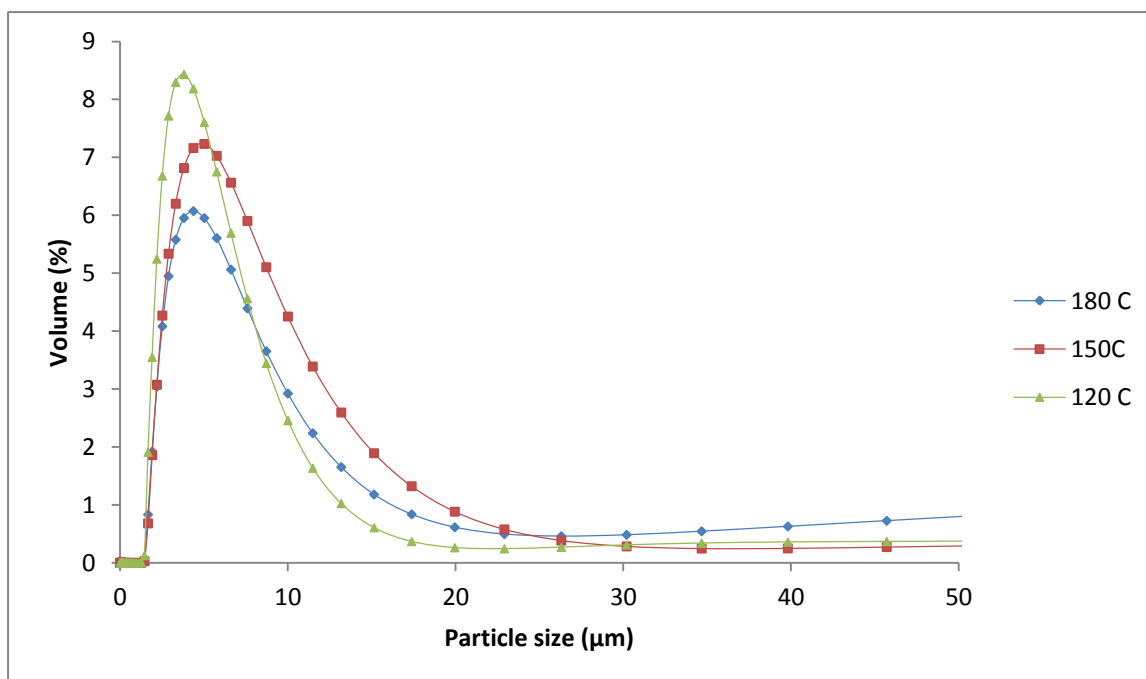


Figure 5.14 – Particle size curves of the alginate particles produced at temperatures of 120 150 and 180 °C showing its effect on the average particle size and size distribution. The alginate concentration and pumping rate was 3 % and 10 mL/min respectively.

	D₁₀ (μm)	D₅₀ (μm)	D₉₀ (μm)
120 °C	1.8	5.7	201
<i>St Dev</i>	0.3	1.4	52.7
<i>RSD (%)</i>	16.7	24.6	26.2
150 °C	2.5	5.4	236
<i>St Dev</i>	1.2	2.4	93.6
<i>RSD (%)</i>	48	44.4	39.7
180 °C	2.7	5.8	221
<i>St Dev</i>	0.9	1.7	74.7
<i>RSD (%)</i>	33.3	29.3	33.8

Table 5.8 – Sizing data of the alginate particles produced at 120, 150 and 180 °C showing its effect on the D₁₀, D₅₀ and D₉₀ particle sizes. Each value is the mean average of three independent studies ± SD.

5.4.2.3 Effect of alginate flow rate on microparticle production

The effect of polymer flow rate on particle size and form was investigated and analysed with SEM (Figure 5.14) and laser diffraction (Figure 5.15 and Table 5.9). By increasing the flow rate from 5, 10 and 20 mL/min, average particle sizes of 3.9, 5.7 and 8.9 μm were determined

for the increasing flow rates. Flow rates of 20 mL/min were too fast for the atomization process resulting in highly aggregated particles being formed.

Like with increasing polymer concentration, increasing the polymer flow rates makes the atomization process more difficult resulting in increased particle size and increased size distribution. At exceptionally high flow rates (greater than 20 mL/min), large amounts of material can be deposited on the sides of the drying chamber which increases when larger volumes of material are spray dried. This can result in low production yields since a large proportion of the material is lost in the drying chamber and the particles that are collected show signs of aggregation perhaps due to inadequate drying like in the case with insufficient inlet temperatures. This effect could possibly be overcome by use of higher drying temperatures or use of counter current flow patterns to dry the droplets faster and allow longer contact times during drying. Also, increasing the nozzle size can allow increased flow rates (and also polymer concentrations) to be used allowing higher production rates, which would then also increase particle size.

Benchabane *et al* (2007) processed alginate solutions at 12 and 24 mL/min and saw the same increasing trend in particle size increase from 2.7 to 3.2 μm . Coppi *et al* (2001) produced alginate particles at a flow rate of 5 mL/min where an average size of 2.1 μm was produced, similar to those produced in this work.

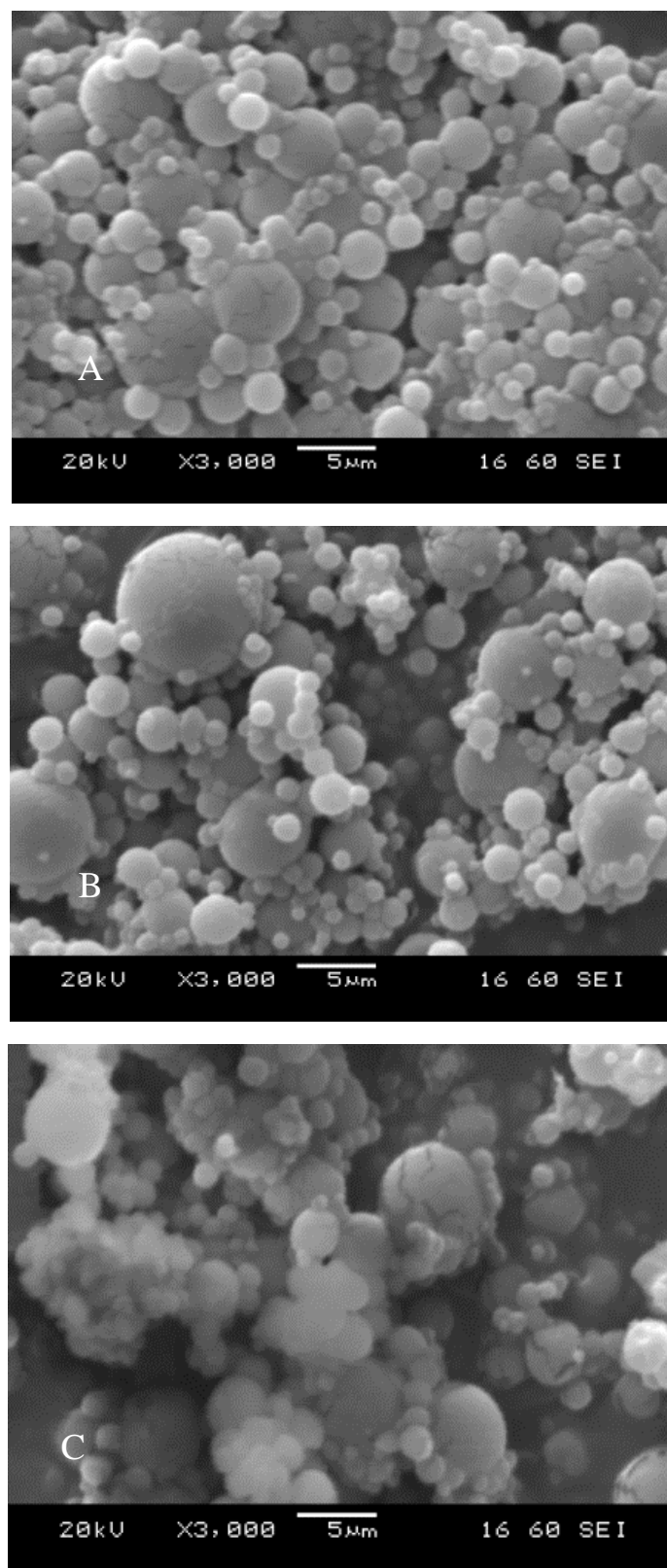


Figure 5.15 – SEM images of the alginate particles produced at flow rates of (A) 5, (B) 10 and (C) 20 mL/min where the effect on particle size and form are shown. The alginate concentration and in let temperature were 3 % and 150 °C.

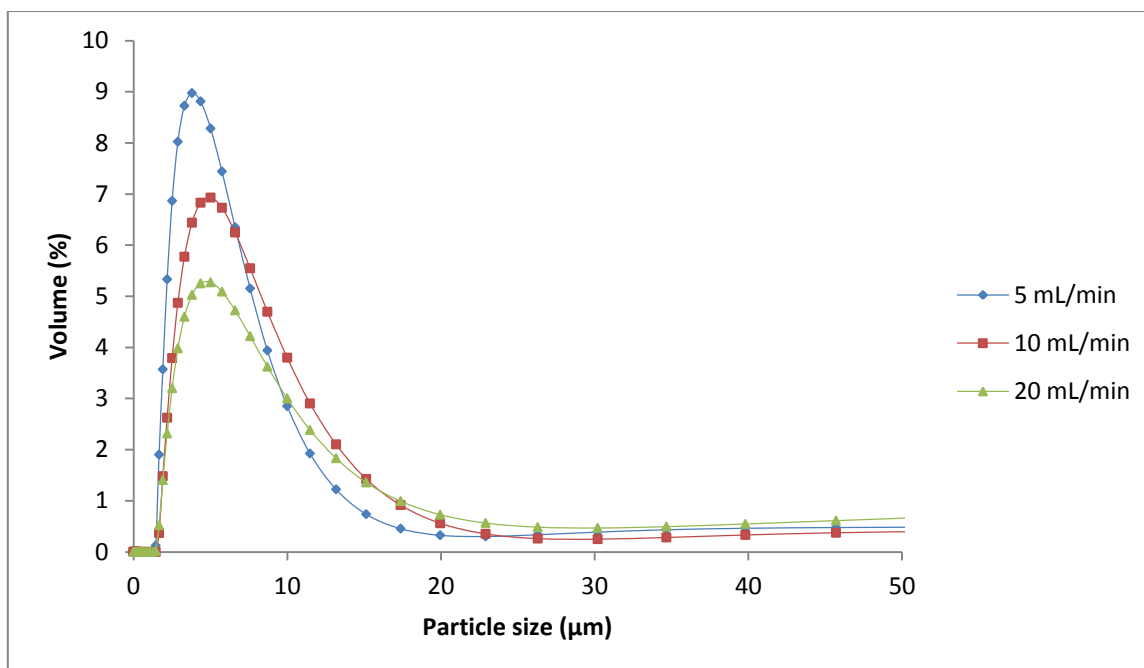


Figure 5.16 – Particle size curves for the particles produced at flow rates of 5, 10 and 20 mL/min showing the effect on the average particle size and size distribution. The alginate concentration and inlet temperature were 3 % and 150 °C respectively.

	D₁₀	D₅₀	D₉₀
5 mL/min	2.1	3.9	183
<i>St Dev</i>	0.3	0.3	28.8
<i>RSD (%)</i>	14.2	7.7	15.7
10 mL/min	2.5	5.7	273
<i>St Dev</i>	0.3	0.6	89.9
<i>RSD (%)</i>	12	10.5	32.9
20 mL/min	2.9	8.9	417
<i>St Dev</i>	0.2	1.3	101.4
<i>RSD (%)</i>	6.9	14.6	24.3

Table 5.9 - Particle sizing data for the alginate particles produced at 5, 10 and 20 mL/min showing the effect on the D₁₀, D₅₀ and D₉₀ particle sizes. Each value shows the mean average of three independent studies ± SD.

5.4.2.4 Drug loading and encapsulation efficiency of the alginate microparticles

The alginate particles were loaded with 1 % w/v verapamil hydrochloride and the effects of alginate concentration on DL and EE were investigated (Table 5.10). On increasing polymer concentration from 2 % - 4 % w/v the DL decreased from 18.7 % to 12.2 % and EE increased from 37.4 % to 48.8 %.

The particles were produced with constant drug concentrations while the mass of polymer was increased. Since DL is a measure of the ratio of polymer to drug, keeping the mass of drug constant is likely to see a general decrease in DL as the polymer concentration increases. EE will tend to increase with increased polymer concentration since higher crosslinking densities are capable of retaining higher masses of drug due to the decrease in particle porosity.

Mobus *et al* (2012) produced alginate particles with 1 % alginate by the spray drying method encapsulating the protein bovine serum albumin (BSA) with encapsulation efficiencies as high as 96.5 %. BSA is a large molecular weight protein and the particles were crosslinked in the drying chamber, whereas particles in this process were crosslinked post production, where some drug was lost to the crosslinking solution. Drugs with larger molecular weights can also result in higher EE since the increase in the size of the molecule makes it more difficult to diffuse out of the microparticle. As previously discussed reviews for alginate particles encapsulating hydrophilic drugs are limited, where many spray drying methods have been emphasized towards proteins and large molecular weight compounds.

	2% Alginate	3% Alginate	4% Alginate
DL (%)	18.7	15.3	12.2
<i>St Dev</i>	1.2	0.9	1.3
<i>RSD (%)</i>	6.4	5.9	10.7
EE (%)	37.4	46.2	48.8
<i>St Dev</i>	2.5	3.5	5.2
<i>RSD (%)</i>	6.7	7.6	10.7

Table 5.10 – Drug loading and encapsulation efficiency of the alginate particles produced with 2%, 3% and 4% alginate loaded with 1% verapamil hydrochloride. Each value shows the mean average of three independent studies \pm SD.

5.4.2.5 Drug release from the alginate microparticles

The alginate particles produced with varying alginate concentrations of 1 %, 2 % and 4 % were subject to in-vitro release in PBS (Figure 5.16). Like with the alginate beads discussed in the previous chapter, all formulations released the entire mass of drug within the first hour. It was hypothesized that increased polymer concentrations could potentially result in controlled release due to increased crosslinking density however, all formulations resulted in rapid release rates due to the high porosity of the alginate and rapid diffusion of the small molecular weight hydrophilic drug into the PBS release media.

The majority of alginate microparticle based drug delivery systems have been applied to the encapsulation of large molecular weight compounds, where the larger size of the molecule can potentially allow the diffusion process to be reduced resulting in slower release rates. The alginate particles produced by Mobus *et al* (2012) allowed sustained release of BSA from alginate particles within 48 hours with an initial burst release of 60 % within the first 8 hours.

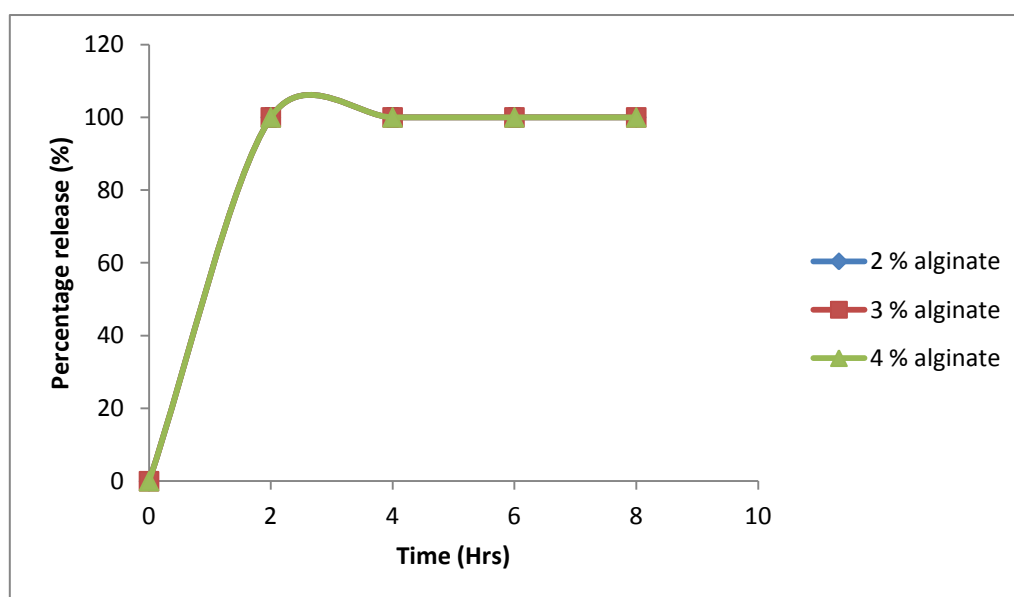


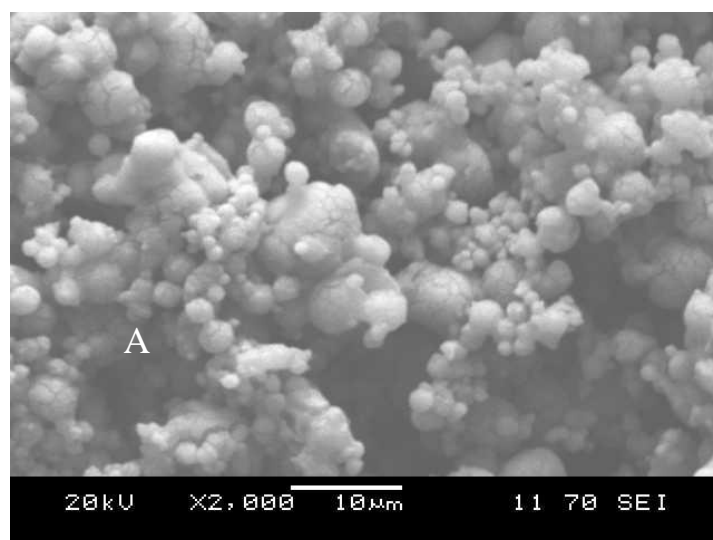
Figure 5.17 – Drug release profile for the verapamil hydrochloride loaded alginate particles produced with 2 %, 3 % and 4 % alginate. Each point shows the mean average of three independent studies.

5.4.2.6 Effect of alginate: sodium silicate ratio on particle production

The effect of alginate: sodium silicate ratio on microparticle formation was analysed with SEM and laser sizing where concentrations of 1.5 %, 3 % and 4.5 % in 3 % alginate were investigated (Figures 5.17 and 5.18 and Table 5.11). By increasing the sodium silicate ratio, the aggregation of the particles greatly increased resulting in large particle clusters displaying wide size distributions.

Like with the investigated polymer concentrations in pure alginate particles, the aggregation was mainly believed to be due to the particles high surface area. With increasing the silicate concentration, alginate becomes the less dominant material within the particle which can possibly result in the silicate dissolving out of the smaller mass of alginate resulting in a aggregated irregular structure being formed.

This formation could possibly be overcome by crosslinking the particles during the drying process by the release of the crosslinker ions as to the method by Mobus *et al* (2012) to allow alginate particles with higher degrees of sphericity and containing higher silicate masses to be produced.



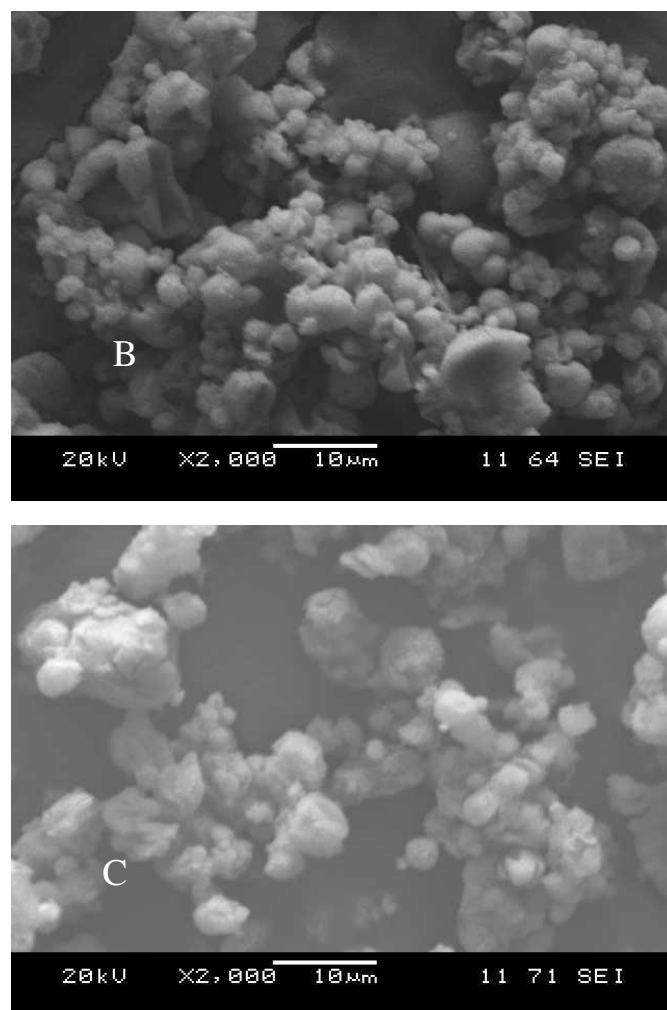


Figure 5.18 – SEM of the alginate/sodium silicate particles produced with sodium silicate concentrations of 1.5 %, 3 % and 4.5 %. The effect on particle form is shown. The alginate concentration, inlet temperature and pumping rate were 3%, 150 °C and 10 mL/min respectively.

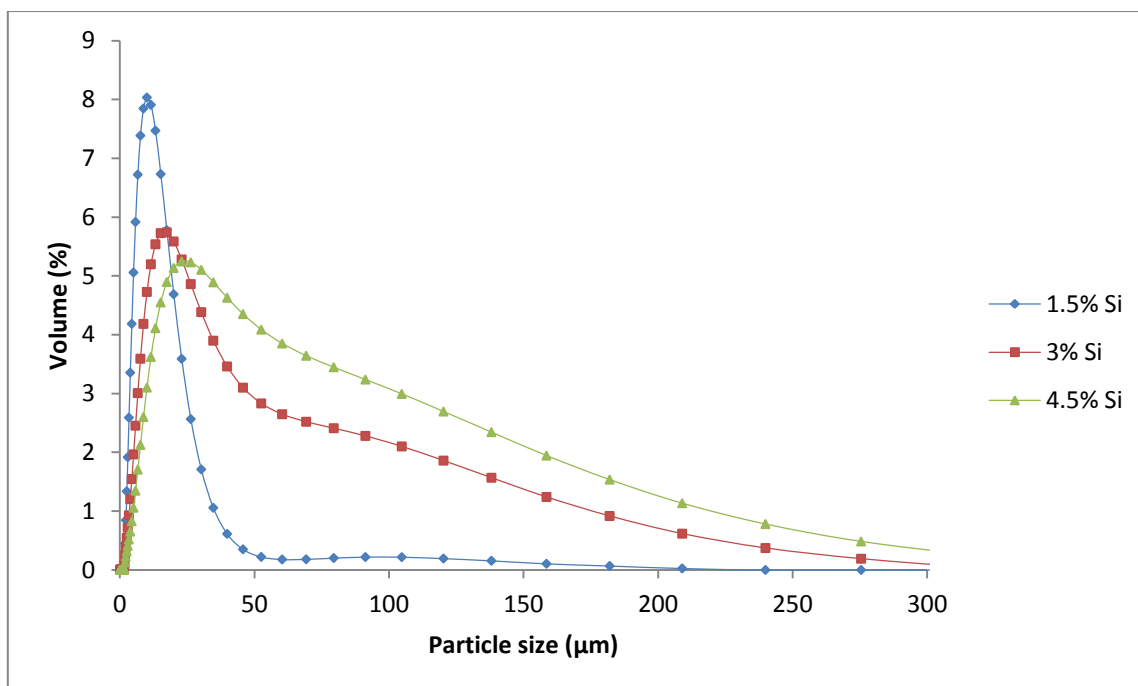


Figure 5.19 – Particle size distributions of the alginate sodium silicate particles produced with sodium silicate concentrations of 1.5 %, 3 % and 4.5 % sodium silicate. The effect of silicate concentration on the size distribution is shown.

	D₁₀	D₅₀	D₉₀
1.5% Si	3.7	9.3	21.1
<i>St Dev</i>	0.7	2.7	4.9
<i>RSD (%)</i>	18.9	29	23.2
3% Si	12.5	18.4	83.5
<i>St Dev</i>	4.1	3.7	22.2
<i>RSD (%)</i>	32.8	20.1	26.6
4.5% Si	17.4	27.7	115.5
<i>St Dev</i>	4.6	6.2	44.8
<i>RSD (%)</i>	26.4	22.4	38.8

Table 5.11 – Particle size data of the alginate particle produced with sodium silicate concentrations of 1.5 %, 3 % and 4.5 %. Each value is the mean average of three independent studies \pm SD.

Like with the alginate particles, un-crosslinked alginate sodium silicate particles were also analysed with SEM (Figure 5.19). The particles were more spherically uniform compared to the crosslinked product indicating that the aggregated formation occurs during the crosslinking process. Like with the other aggregated particle issues, this could also be down

to particle instability in the calcium chloride solution which could be addressed by determination of the zeta potential.

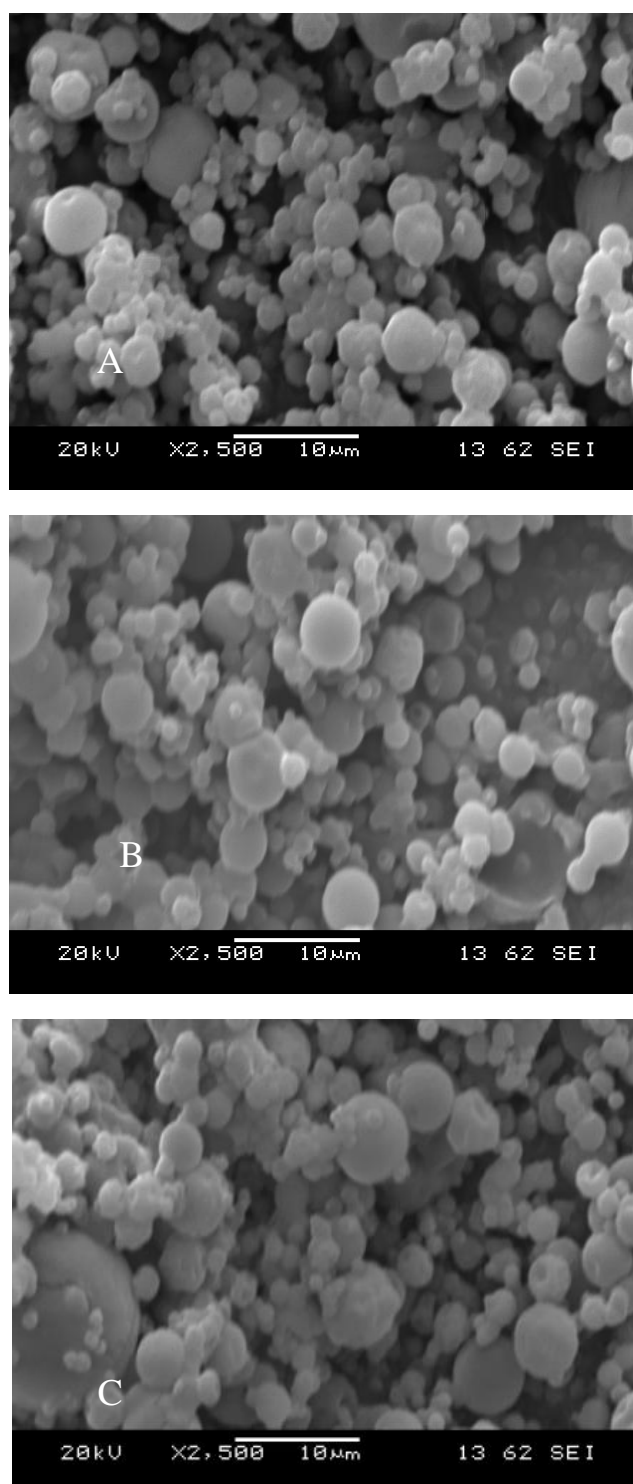


Figure 5.20 – SEM images of the un-crosslinked alginate sodium silicate particles produced with 1.5, 3 and 4.5 % sodium silicate. The alginate concentration used was 3 % w/v.

5.4.2.7 Drug loading and encapsulation efficiency of the alginate sodium silicate microparticles

The effect of alginate concentration on the DL and EE of the alginate sodium silicate particles was investigated where a 1 : 1.5 ratio of alginate and silicate was investigated (Table 5.12). With increasing alginate concentration, the drug loadings decreased from 15.2 % to 9.3 % in 2 % to 4 % alginate due to the concentration of drug staying constant while the material mass increases. As for the EE, with increasing polymer concentration, the EE increases from 60.8 % to 75 % due to the increased gel density.

	2% alginate	3% alginate	4% alginate
DL (%)	15.2	10.7	9.3
<i>St Dev</i>	1.6	1.5	1.3
<i>RSD (%)</i>	10.5	23.3	14
EE (%)	60.8	65.1	75
<i>St Dev</i>	6.6	9.7	9.6
<i>RSD (%)</i>	10.9	14.9	12.8

Table 5.12 – Effect of alginate concentration on drug loading and encapsulation efficiency of the alginate sodium silicate microparticles. Concentrations of 2 %, 3 % and 4 % were investigated. Each value is the mean average of three independent studies \pm SD.

The effect of sodium silicate concentration on DL and EE were also investigated (Table 5.13). By increasing the silicate concentration from 1.5 to 4.5 % w/v in the 3 % alginate particles, DL again decreased from 11.1 % to 8.5 % when EE increased from 49.9 % to 64.3 % due to the increased gel density retaining higher masses of drug.

	1.5 % Na silicate	3 % Na silicate	4.5 % Na silicate
DL (%)	11.1	9.6	8.5
<i>St Dev</i>	1.6	1.5	1.2
<i>RSD (%)</i>	14.4	15.6	14.1
EE (%)	49.9	58.2	64.3
<i>St Dev</i>	6.6	9.7	8.9
<i>RSD (%)</i>	13.2	16.7	13.8

Table 5.13 – Effect of alginate: sodium silicate ratio on drug loading and encapsulation efficiency of the alginate sodium silicate microparticles. Concentrations of 1.5, 3 and 4.5 % w/v in 3 % alginate were investigated. Each value is the mean average of three independent studies \pm SD.

The effect of drug concentration was also investigated (Table 5.14). By increasing the drug concentration from 0.5 % to 2 %, the DL increases from 5.5 to 20.1 %. As expected, by increasing the initial loading of drug, higher DL can be obtained. Particles produced with 2 % verapamil hydrochloride were however highly aggregated. When the polymer and drug are mixed the interaction between the drug and polymer can potentially increase the viscosity of the solution making the atomization process more challenging resulting in the aggregated particles. The EE however decreased with increasing drug concentration. This is believed to be due to the limited number of carboxyl groups available for interaction with the drug resulting in a decrease in EE. A similar effect was observed by Maesh *et al* (2007) where methylene blue was encapsulated within alginate nanospheres where the methylene blue concentration ranged from 5 – 15 mg per mL of alginate (1%). The EE saw a decrease from 99.8% to 74.1 % by increasing the drug concentration from 5 – 15 mg/mL where they concluded the decrease was due to limited carboxyl groups available to interact with the drug.

	0.5% VHCl	1% VHCl	2% VHCl
DL (%)	5.5	10.7	20.1
<i>St Dev</i>	0.6	1.5	1.6
<i>RSD (%)</i>	10.9	14	8
EE (%)	67	64.6	60.4
<i>St Dev</i>	10.9	9	4.8
<i>RSD (%)</i>	16.3	13.9	7.9

Table 5.14 – Effect of verapamil hydrochloride concentration on drug loading and encapsulation efficiency of the alginate sodium silicate microparticles. Concentrations of 0.5%, 1% and 2% were investigated. Each value is the mean average of three independent studies \pm SD.

5.4.2.8 Drug release from the alginate sodium silicate microparticles

The alginate sodium silicate particles were subject to in-vitro release in PBS where effects of alginate concentration, silicate concentration and drug concentration were investigated (Figures 5.20, 5.21 and 5.22 respectively). By increasing the alginate and silicate concentrations slight decreases in drug release were observed as shown by the cumulative release and percentage release profiles. However, due to the short release period of 4 hours and when experimental error is taken into account, these variations of the process parameters could be having no real effect on drug release rate since the particles high surface area along with the water loving nature of the drug result in fast release rates. The particles do however see an improvement on the single alginate microparticle systems where the drug is instantly released due to the reduced porosity/increased material interaction and reduced degradation as discussed in the previous chapter.

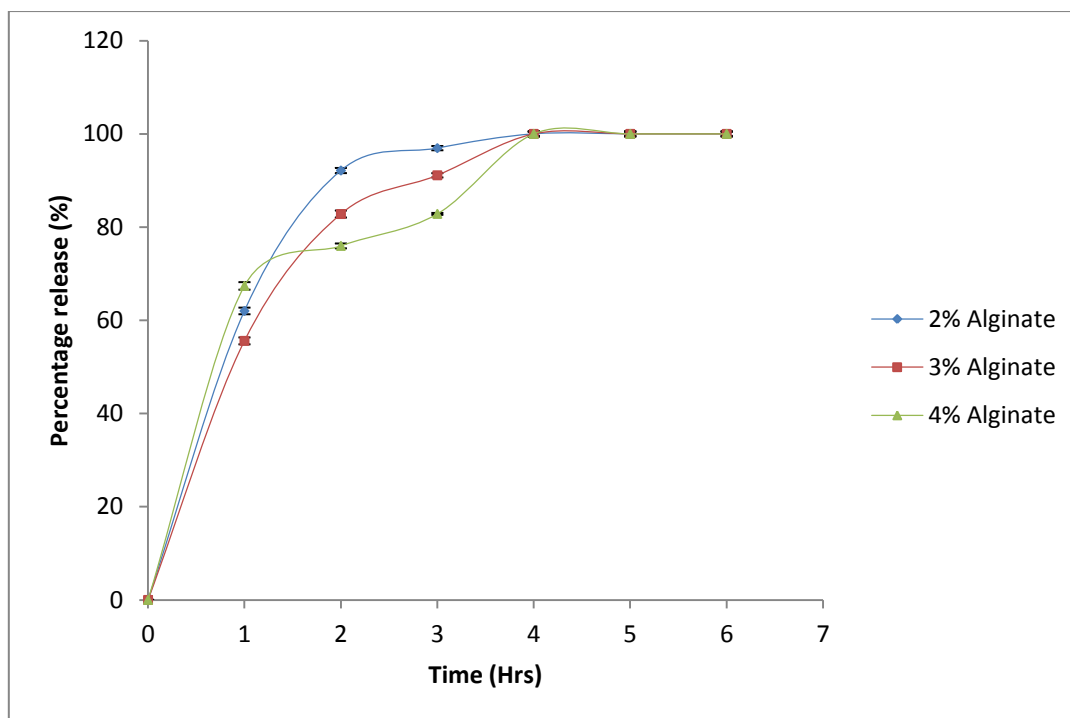


Figure 5.21 – Percentage drug release of the alginate sodium silicate particles illustrating the effect of alginate concentration on drug release rate. Concentrations of 2%, 3% and 4% were investigated. Each point is the mean average of three independent studies \pm SD.

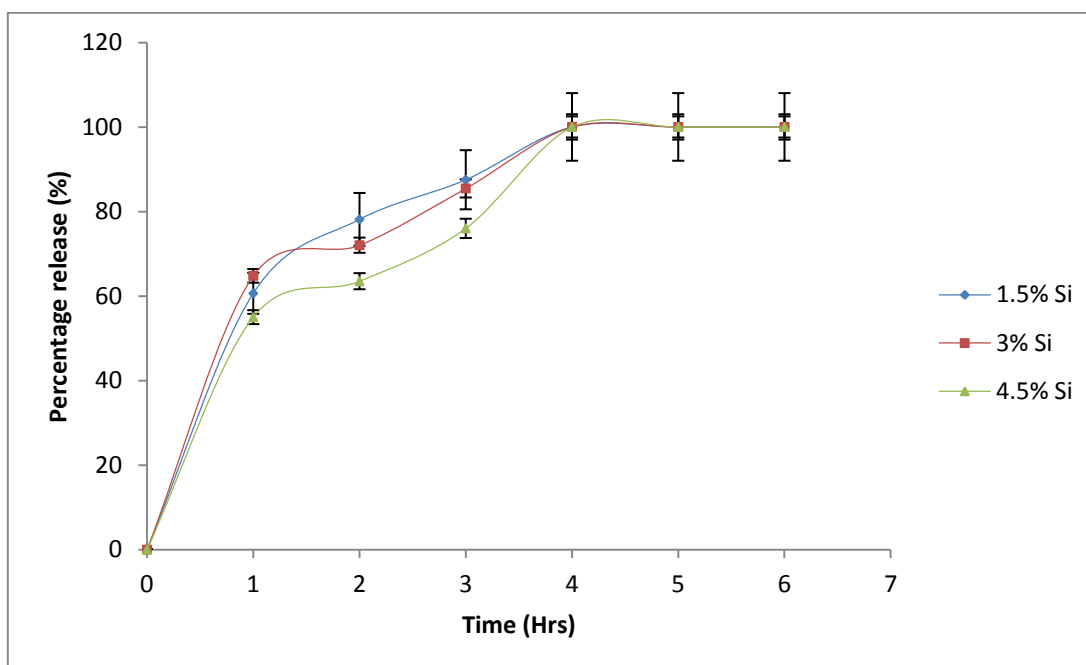


Figure 5.22 – Percentage drug release of the alginate sodium silicate particles illustrating the effect of silicate concentration on drug release rate. Concentrations of 1.5%, 3% and 4.5% were investigated. Each point is the mean average of three independent studies \pm SD.

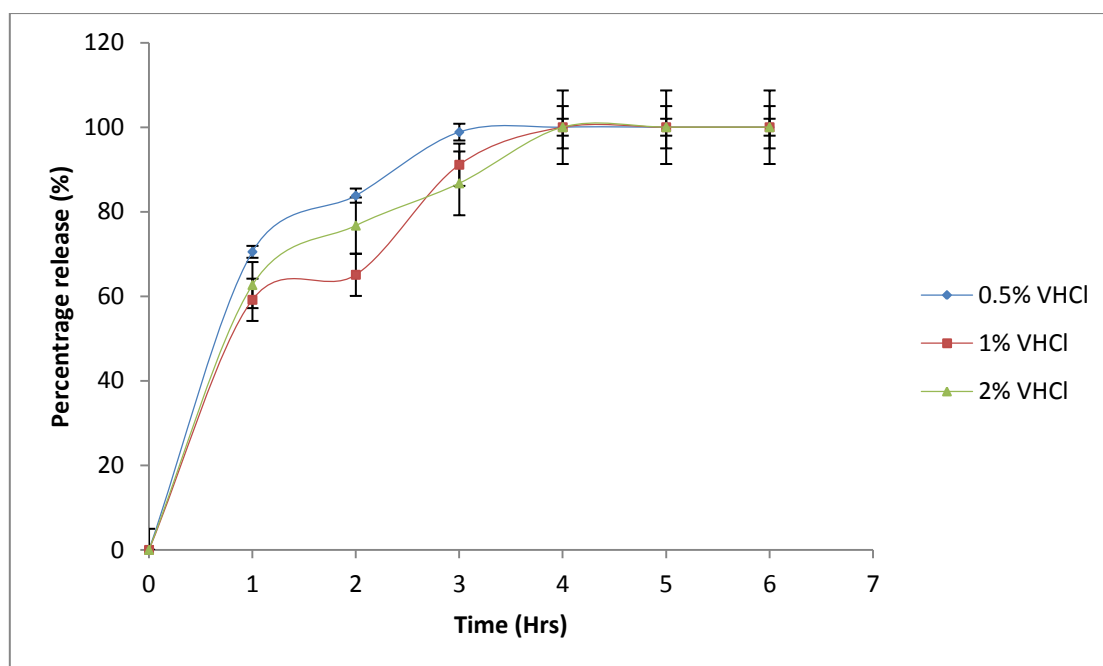


Figure 5.23 – Percentage drug release of the alginate sodium silicate particles illustrating the effect of drug concentration on drug release rate. Concentrations of 0.5%, 1% and 2% were investigated. Each point is the mean average of three independent studies \pm SD.

5.5 Conclusion

In this section, microparticle production methods for the alginate sodium silicate blend were investigated. The w-o emulsion and spray drying methods were chosen due to their ability to produce particles as carriers for hydrophilic drugs. In the w-o emulsion, effects of polymer concentration, mixing speed, crosslinking concentration and surfactant concentration were explored illustrating their effects on particle formation. Successful formation of the particles was highly dependent on sufficient stabilization in the emulsion along with adequate crosslinking concentrations. Also, the desired size of particles was found to be highly dependent on choice of the appropriate polymer concentration and mixing speeds. Although uniformly distributed spherical particles were produced, the method failed to allow drug loaded particles to be produced which was believed to be due to the transfer of the drug into the oil phase. Spray drying was investigated since it is known to produce particles with high

EE in a single step. Parameters investigated where the polymer/silicate concentration, inlet temperature, polymer flow rate and drug concentration where the effects on the particle formation were analysed. Again, choice of the appropriate processing parameters allowed various particle sizes to be obtained. The particles produced displayed spherical geometries that were uniformly distributed and displayed high loadings and controlled release of the encapsulated compound. These microparticles did not significantly increase the release rate compared to the alginate counterpart since was over a 5 hour period with a burst of approximately 60 % within the first hour. However it offered an improvement over the alginate particles where the drug was instantly released. The 3 % alginate / 1.5 % sodium silicate containing 1 % verapamil hydrochloride is the formulation to be carried forward for encapsulation into the larger embolic particles producing the PIP system for TACE. This formulation displayed the highest uniformity with high drug loadings where other investigated parameters failed to display significant variations in drug release rate.

CHAPTER 6

PRODUCTION OF THE EMBOLIC PARTICLES AND ENCAPSULATION OF THE DRUG DELIVERY PARTICLES

6.1 Introduction

In this chapter, microspheres were produced as embolizing particles where the 3 % alginate / 1.5 % sodium silicate / 1 % verapamil hydrochloride formulation produced in chapter 5 was encapsulated into the optimized embolic particles, producing the PIP system. Two methods for production of the embolic particles were investigated, the w-o emulsion and the nozzle vibrating method. Parameters effecting particle size and form were investigated. Once optimum production procedures were obtained, the drug delivery particles were encapsulated yielding the PIP system. The morphology of the embolic particles were analysed with microscopy and laser diffraction along with the DL/EE and drug release rates which were determined by in-vitro analysis with UV spectroscopy. The aims of this chapter were to;

- Investigate methods for producing large microparticles in the TACE size range (100 – 1000 μm) with narrow size distributions.
- Investigate the effects of processing parameters on embolic particle size and form for the chosen methods.
- Investigate drug delivery particle loading, ensuring the drug delivery particles are uniformly dispersed within the embolizing particles.
- Ensure the microstructure of the embolizing particles allow the effect of particle size on drug release rate to be decoupled.

6.2 Particle-in-Particle systems for drug delivery applications

The concept of a PIP system is one that has been explored to overcome several obstacles within drug delivery. Such obstacles include; protection of oral dosage forms along the gastrointestinal tract, prolonged drug release rates and delivery by the pulmonary route. Production methods for PIP systems are similar to those used to produce single particle systems where the particles to be encapsulated are dispersed into the matrix material where methods such as spray drying, emulsions and ionotropic gelation have been frequently explored. It is to the best of this author's knowledge that no other researcher has attempted to develop a PIP system that decouples drug release rate from particle size while also allowing encapsulation of a range of drugs not only for TACE, but for drug delivery in general. Therefore, this concept is one that has potential for a variety of drug delivery applications.

Firstly, for TACE specifically, only one other PIP system has been found within the literature. The work of Pouponneau *et al* (2011) investigated the production of a doxorubicin loaded particle system where the anti-cancer drug was loaded into PLGA microparticles along with iron cobalt nanoparticles (Figure 6.1). The PLGA particles controlled the release of the drug over several days and the magnetic iron cobalt nanoparticles acted as a steering mechanism so that when magnetic fields were introduced, the PLGA particles could be directed to the tumour site. A similar PIP system was used as a delivery system for inhalation in the treatment of lung cancer. Here, McBride *et al* (2013) produced a system composed of spray dried lactose microparticles loaded with doxorubicin and iron oxide nanoparticles where once again, the magnetic field could guide the particles to the relevant site of the lung tumour.

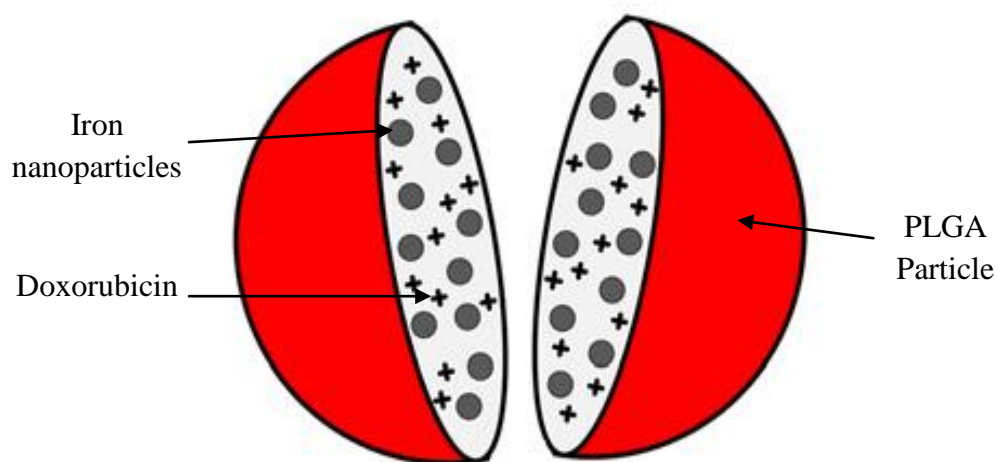


Figure 6.1 – The only other known PIP system used for TACE. The system is composed of magnetic nanoparticles and doxorubicin encapsulated within PLGA microparticles (Pouponneau *et al* 2011).

When alteration of release rates have been an aim, PIP systems reported within the literature have aimed to extend the release rate rather than decouple it from the particle size. Hassan *et al* (2009) composed a system of ibuprofen loaded PCL nanoparticles entrapped within PLGA microparticles with the intent to reduce the burst effect and sustain release rate. The PCL nanoparticles released the majority of the drug instantly, whereas the PIP system displayed an initial burst release of 21 % in the first 15 minutes followed by a sustained release rate over an 8 hour period. The work by Lee *et al* (2008) produced a catechin loaded liposome system in calcium pectinate beads by the ionotropic gelation method. Calcium pectinate makes an attractive material for oral delivery however suffers from rapid release of small molecular weight drugs. Liposomes were designed to control release of catechin, where the liposomes were then loaded into calcium pectinate beads, where the system saw a controlled release rate over 4 hours.

Many PIP systems have been developed with the intent of protecting the encapsulated drug loaded particles after oral administration from the conditions of the gastro intestinal tract. The environment in the stomach is highly acidic where fast degradation can occur, particularly for protein based compounds. Also, the small intestine has a high surface area

where high absorption rates occur. The colon makes an attractive site for drug delivery due to its neutral pH and long transit time however, drugs or drug loaded particles require protection whilst traveling along the upper gastro intestinal tract. Alginate makes an attractive material to protect against conditions of the stomach acid since it contracts in acidic media. Garrait *et al* (2014) produced a microparticle system composed of alginate microparticles containing amaranath red loaded chitosan nanoparticles. The alginate particles had an average diameter of 285 μm and the nanoparticles a diameter of 690 nm. In-vitro studies in conditions simulating the stomach saw a release of less than 5 % and conditions simulating the small intestine saw a rapid release of the drug. The work by Barea *et al* (2012) produced 5-ASA loaded chitosan coated liposomes within Eudrajit S100 microspheres for oral delivery to the colon. The Eudragit S100 protected the drug loaded liposomes in the acidic conditions of the stomach and small intestine until the colon site was reached. Once at the colon, the Eudragit S100 degraded and allowed controlled release of the 5-ASA from the liposome system.

PIP systems have seen increasing interest for delivery of proteins and insulin by the pulmonary (lung) route. The work of Kaye *et al* (2009) produced a PIP system where antibodies were encapsulated into PLGA particles. These particles were then formulated into a PIP system by entrapment into lactose microspheres in a one-step spray drying method. The lactose particles were designed so that their size (1-5 μm) would allow deep penetration into the airways and then dissolve upon contact with the aqueous environment. The PLGA particles would then adhere to the lining of the lung, allowing controlled release of the encapsulated compound.

6.3 Production of the embolizing particles by Nozzle Vibrating technology

One method that has seen limited attention for particle production is based upon a theory investigated by Lord Rayleigh in the late 19th century (Figure 6.2). He found that when liquid jets fall under gravity, they will break up into droplets caused by disturbances along the length of the falling liquid jet. When the jet length exceeds its diameter by a factor of 3.13, instability along the jet increases, resulting in rupturing of the falling jet generating droplets (Brandenberger *et al* 1998). Application of a disturbance such as a vibration to a liquid jet flowing in a laminar fashion causes the jet to be broken down into uniformly sized droplets which can be processed into particles of a uniform size range. For optimum droplet formation, Rayleigh defined the optimum wavelength of a falling liquid jet for droplet formation in Equation 6.1 (Brandenberger *et al* 1998).

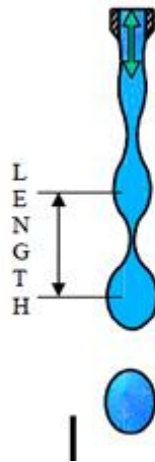


Figure 6.2 – Break-up of a falling liquid jet caused by growing disturbances along the jet length. As the length increases, disturbances also increase generating droplets.

$$\lambda_{\text{OPT}} = \pi \times \sqrt{(2d)}$$

Equation 6.1 – The optimum wavelength defined by Rayleigh

Rayleigh's theory applied to Newtonian fluids such as water however, the work by Weber extended this principle for Non-Newtonian fluids such as alginate by adding the effects of viscosity, density and surface tension to Rayleigh's theory. Weber's optimum wave length definition is given in Equation 6.2 (Brandenberger *et al* 1998).

$$\lambda_{OPT} = \pi \sqrt{(2d) \times \sqrt{1 + [(3\eta) / \sqrt{(\rho\sigma d)}]}}$$

Equation 6.2 – The optimum wavelength taking effects of density, viscosity and surface tension into account defined by Weber.

By knowing the optimum wavelength, an approximate vibrating frequency for optimum droplet formation can be determined by Equation 6.3. The diameter of the droplet can also be determined by Equation 6.4 (Brandenberger *et al* 1998).

$$f = v / \lambda$$

Equation 6.3 – Optimum operating frequency for droplet formation.

$$d = \sqrt[3]{(1.5 \times d^2 \times \lambda_{OPT})}$$

Equation 6.4 – Diameter of the produced droplets.

Where;

- λ – wavelength (m)
- d – nozzle diameter (m)
- η – viscosity (Pa s)
- σ – surface tension (N m⁻¹)
- ρ – density (Kg m³)
- v – velocity (m s⁻¹)
- f – frequency (Hz)

Several pieces of apparatus have been developed based on this principle to form microspheres of a uniform size. Gaudio *et al* (2005) used a nozzle vibrating unit to produce large alginate beads whilst investigating the effects of polymer concentration on bead formation using a vibrating frequency of 250 Hz and nozzle of 400 μm . The diameter of the beads ranged from 0.5 – 3.5 mm when increasing the alginate concentration from 0.5 % - 2.5 % w/v. Lee *et al* (1996) used a sound induced vibrating method to produce uniform alginate beads where the size of the beads ranged from 1.5 – 3.5 mm depending on the flow rate, frequency and nozzle size used.

The nozzle vibrating encapsulator used in the work also applies an electrostatic charge to the surface of the falling droplets causing them to repel into a fine spray, which prevents aggregation allowing particles with narrower size ranges and highly spherical geometries to be produced with adjustable sizes. Particle formation by nozzle vibrating technology has been a limited area of study when compared to methods such as emulsions and spray drying. The nozzle vibration method provides a good alternate to the ionotropic gelation method, one that has the benefit of mild preparation but suffers from production of relatively large beads. Benefits of the method are faster production rates and access to a wide range of particle sizes from 150 – 2000 μm , whilst still allowing mild processing conditions. Particles produced with this method also fit the embolizing particle specifications of TACE such as uniform size, calibrated sizes and smooth hydrophilic surface with spherical geometries. The method however is limited to polymer concentrations that are able to flow through the nozzles. When particles less than 300 μm are required, alginate concentrations are limited up to ~ 1.5 % w/v.

6.4 Materials

Alginate (ID # 180947, MW 120,000 – 190,000 g/mol, viscosity (1 %) 15-20 cP, M/G 1.56) kappa carrageenan (ID # 22048, 0.3 % solution viscosity 5 – 25 mPa.s), mineral oil and sodium silicate were supplied by Sigma Aldrich UK. Calcium chloride dihydrate, hexane and phosphate buffered saline (PBS) were supplied by Fisher Scientific UK. Verapamil hydrochloride was supplied by Cambridge Bioscience. Food grade vegetable oil was used. Distilled water was used to produce all aqueous solutions.

6.5 Methods

6.5.1 Production of the embolic particles by the w-o emulsion

The embolizing microparticles were produced by the w-o emulsion method. A solution of 6 % w/v kappa carrageenan was produced by dissolving the polymer in distilled water at 90 °C for 8 hours. The drug loaded particles were dispersed into water at 50 °C where equal volumes of the dispersion and hot carrageenan were mixed, yielding a dispersion of 3 % carrageenan containing 2 % or 5 % w/v drug loaded particles. 5 mL of the dispersion was then added rapidly through a syringe to 50 mL of vegetable oil at 50 °C under mixing at 400, 600 or 800 rpm by use of an overhead stirrer (IKARW 20 Fisher Scientific). Mixing speeds of 400, 600 and 800 rpm would produce small, medium and large micron sized embolic particles in the TACE size range respectively. The emulsion was mixed for 5 minutes with no heating and then left at 4 °C for 10 minutes to allow the carrageenan particles to harden. The particles were then collected through particle sieves (120 µm) and washed in three 50 mL portions of hexane followed by one 50 mL portion of water and then finally oven dried. Blank carrageenan particles were also produced as a control.

6.5.2 Production of embolic particles by nozzle vibrating technology

Alginate microspheres were produced using a Buchi B-395 Pro Microencapsulator unit by a method that was developed based on the standard operating procedure provided by Buchi (Figures 6.3 and 6.4). The effects of alginate flowrate (A1 – A3), vibrating frequency (V1 – V3), electrode strength (E1 – E3) and nozzle size (N1 – N3) were investigated (Table 6.1). 1.5 % alginate and 1M calcium chloride was used to produce and crosslink all formulations. The desired parameters were set and the alginate was added to a 50 mL syringe then fixed to the encapsulation unit. The frequency was activated followed by initiation of the polymer flow rate, where a steady stream of alginate left the nozzle. The electrode was then activated producing the spray of droplets which were collected in a bath of the 1M calcium chloride solution under mixing at 100 rpm. 10 mL of alginate was collected in microsphere formation per 100 mL of calcium chloride solution. The particles were collected by filtration through particle sieves (120 μ m), and stored in air tight vials for analysis.

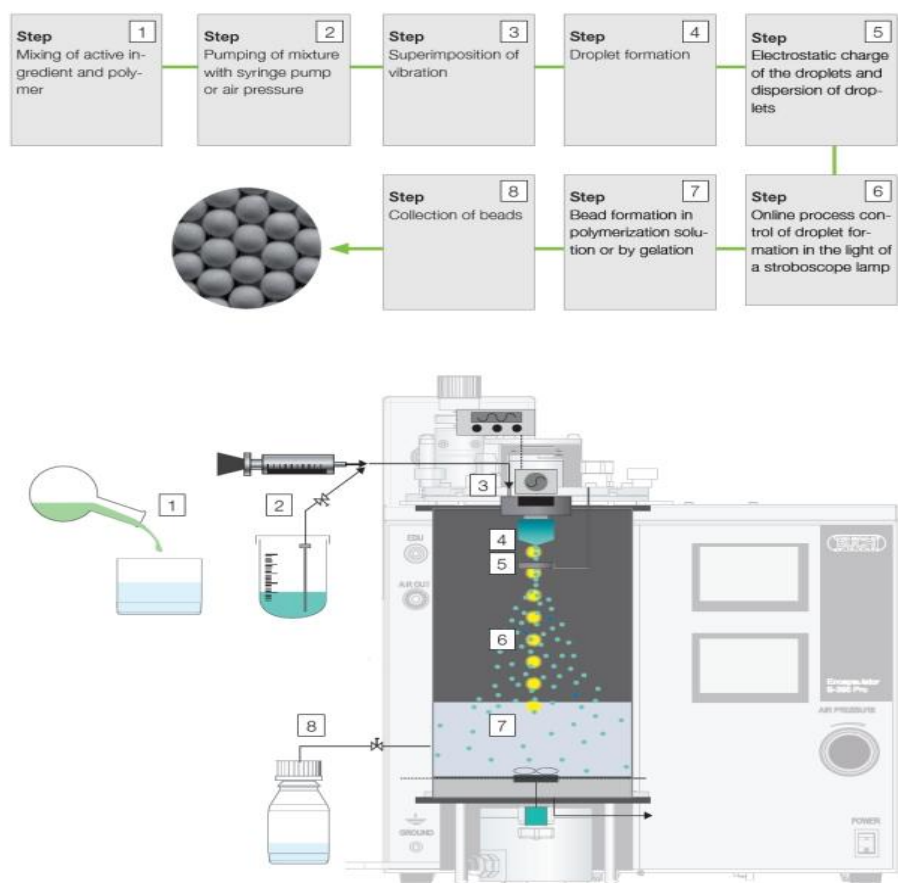


Figure 6.3 – Production of microparticles using the B-395 Microencapsulator (Buchi)

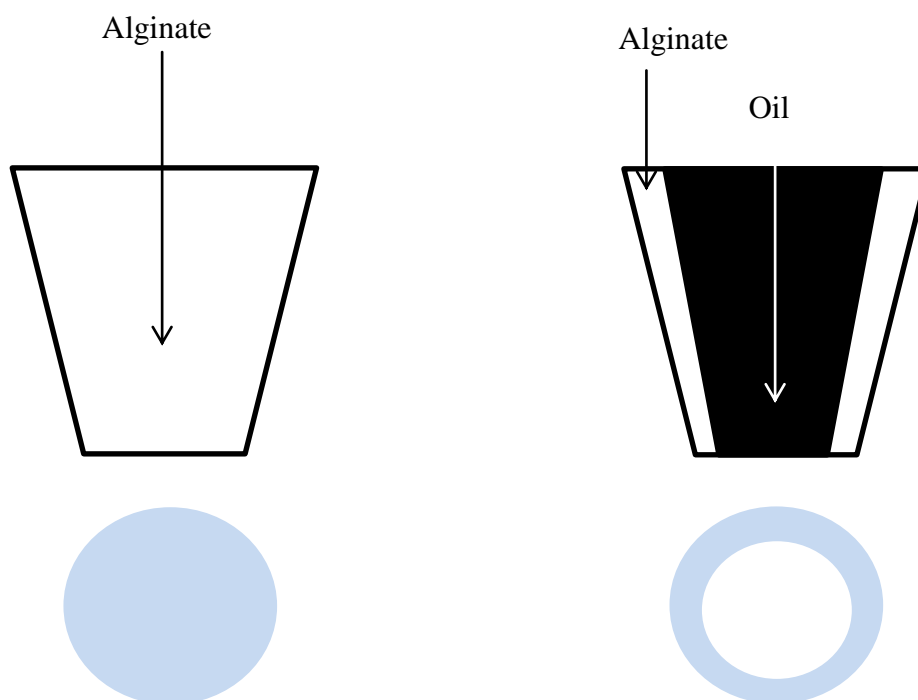


Figure 6.4 – Droplet formation in microspheres (left) and microcapsules (right)

	Alginate flow rate (mL/min)	Vibrating frequency (Hz)	Electrode strength (V)	Nozzle size (μm)
A1	5	1500	2000	300
A2	10	1500	2000	300
A3	15	1500	2000	300
V1	10	1000	2000	300
V2	10	1500	2000	300
V3	10	2000	2000	300
E1	10	1500	1500	300
E2	10	1500	2000	300
E3	10	1500	2500	300
N1	5	2000	1000	150
N2	10	1500	2000	300
N3	20	800	2500	450

Table 6.1 – Process parameters investigated for microsphere formation.

Microcapsules were also produced using the same encapsulation unit where mineral oil was encapsulated into the alginate shells. The nozzle component of the encapsulation has a specific nozzle for microcapsule production where microcapsules of a desired shell and core size can be produced. The smallest core nozzle that allowed the mineral oil to freely flow though was the 200 μm nozzle, therefore this was used in all formulations. Shell nozzles of 300, 400 and 500 μm where the investigated shell nozzles as these fall into the range for TACE.

Again, 1.5 % alginate was crosslinked into 1 M calcium chloride baths in all formulations. The process parameters investigated were the alginate flowrate (A11 – A13), oil flowrate (O1 – O3), and shell nozzle size (Sh1 – Sh3) (Table 6.2). The alginate flowrate was controlled by use of a pressure bottle and the mineral oil flow rate by the microencapsulator's attached syringe pump. The choice of vibration frequency and electrode strength was dependant on the shell nozzle being used for capsule formation, where vibration frequencies of 1500, 800 and 600 Hz and electrode strengths of 1500, 2000 and 2500 V were used for the investigated for the shell nozzles of 300, 400 and 500 μm respectively.

Before capsule production, the desired nozzles were fitted and the vibration and electrode settings were set. The pressure bottle was activated initiating the flow of alginate until the desired pressure (mbar) was reached. This was then followed by activation of the oil flow rate, where a stream of alginate containing the oil was produced. The vibration and electrode were then activated producing the droplet spray where the capsules were collected and crosslinked in the calcium chloride solution under mixing at 100 rpm. Again, 100 mL of calcium chloride was used per 10 mL of alginate processed. At the end of the production all settings were deactivated and the capsules were filtered by use of particle sieves and stored in air tight vials for analysis.

	Alginate flow rate (mbar)	Oil flow rate (mL/min)	Shell nozzle (μm)
Al1	150	10	400
Al2	175	10	400
Al3	200	10	400
O1	175	5	400
O2	175	10	400
O3	175	20	400
Sh1	175	10	300
Sh2	175	10	400
Sh3	175	10	500

Table 6.2 – Process parameters investigated for microcapsule formation. Nozzle vibrations were 1500, 1000 800 Hz for shell nozzles of 300, 400 and 500 μm respectively. Electrode strengths were 2000, 2500 and 2500 V for shell nozzles of 300, 400 and 500 μm respectively.

The microencapsulation unit was also used to produce verapamil hydrochloride loaded alginate-sodium silicate microspheres where 1 % w/v verapamil hydrochloride was loaded into the particles. Investigated parameters were alginate concentration (Alg1 - Alg3), sodium silicate concentration (Si1 – Si3) and nozzle size (No1 – No3) (Table 6.3) which were processed as detailed above.

	Alginate Conc (w/v)	Na Silicate Conc (w/v)	Nozzle size (μm)
Alg1	1	1.5	300
Alg2	2	3	300
Alg3	3	4.5	300
Si1	2	1	300
Si2	2	2	300
Si3	2	3	300
No1	2	3	150
No2	2	3	300
No3	2	3	450

Table 6.3 – Process parameters investigated for verapamil hydrochloride loaded alginate/sodium silicate microspheres. The nozzle vibration used was 1000, 1500 and 2000 Hz for nozzles sizes of 150, 300 and 450 μm respectively. The electrode strength for nozzles of 150, 300 and 450 μm was 1500, 2000 and 2500 V respectively. Alginate flowrates of 5, 10 and 20 mL/min were used for nozzle sizes of 150, 300 and 450 μm respectively.

6.5.3 Particle characterization

Particles were characterised for their size and morphology by light microscopy and laser diffraction along with the DL/EE and drug release rate by UV spectroscopy using the methods previously discussed.

6.6 Results and Discussion

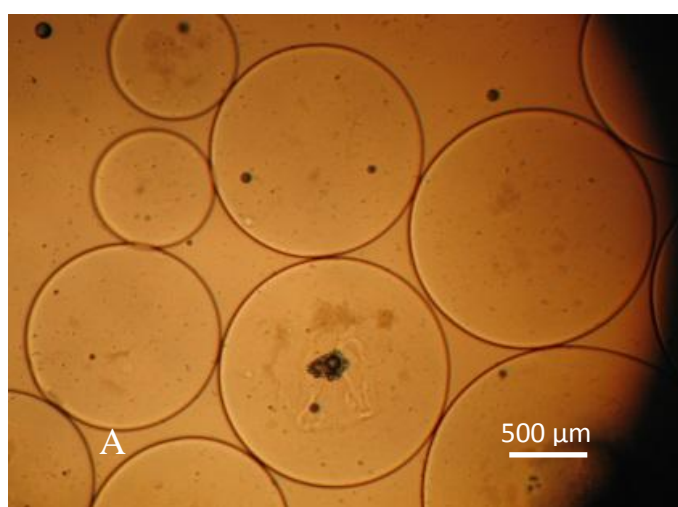
6.6.1 Emulsion method

The w-o emulsion method for production of the PIP system was investigated where the drug delivery particles were encapsulated into kappa carrageenan embolizing particles and the effect of mixing speed and drug particle loading was investigated.

6.6.1.1 Particle production

The embolic particles were produced by the w-o emulsion method where the effect of mixing speed on particle size was investigated by light microscopy and laser diffraction (Figure 6.5

and 6.6 and Table 6.4). By increasing the mixing speed, decreasing particle sizes of 1294, 736 and 378 μm for speeds of 400, 600 and 800 rpm were resulted as a consequence of the increase in shear. Particles are formed by a sol-gel formation as the carrageenan undergoes cooling by formation of double helical junction zones. The temperature of the oil phase was an important factor since if too low, the polymer gels instantly preventing droplet breakdown and resulting in large beads like those produced in the ionotropic gelation method. When the oil is too hot, the polymer is broken down into droplets smaller than 50 μm in diameter even at the slowest mixing speed, which would not allow particles to be produced in the size range suitable for TACE. By heating the oil to 40 $^{\circ}\text{C}$ and rapidly adding the polymer/particle dispersion at 90 $^{\circ}\text{C}$, the exterior of the particles cool rapidly where a specific particle size range can be obtained by adjustment of the mixing speed. The produced microparticles displayed relatively large size distributions however, this could be overcome by passing through a particle sieve to obtain a desired size. This system also did not use a surfactant in the continuous phase since its addition results in formation of droplets too small for the desired TACE size range in this work. Since the polymer droplets harden within seconds of being added to the oil, aggregation of the particles in the emulsion was not an issue.



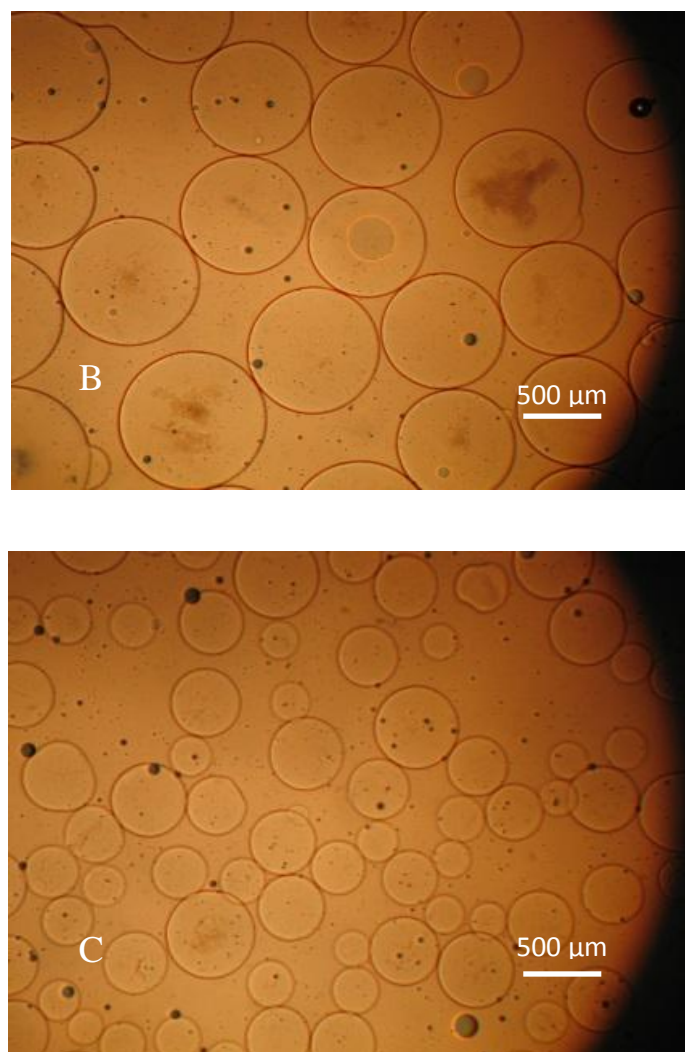


Figure 6.5 – Light microscope images of the 3 % carrageenan microspheres produced at (A) 400, (B) 600 and (C) 800 rpm illustrating the effect of mixing speed on particle size.

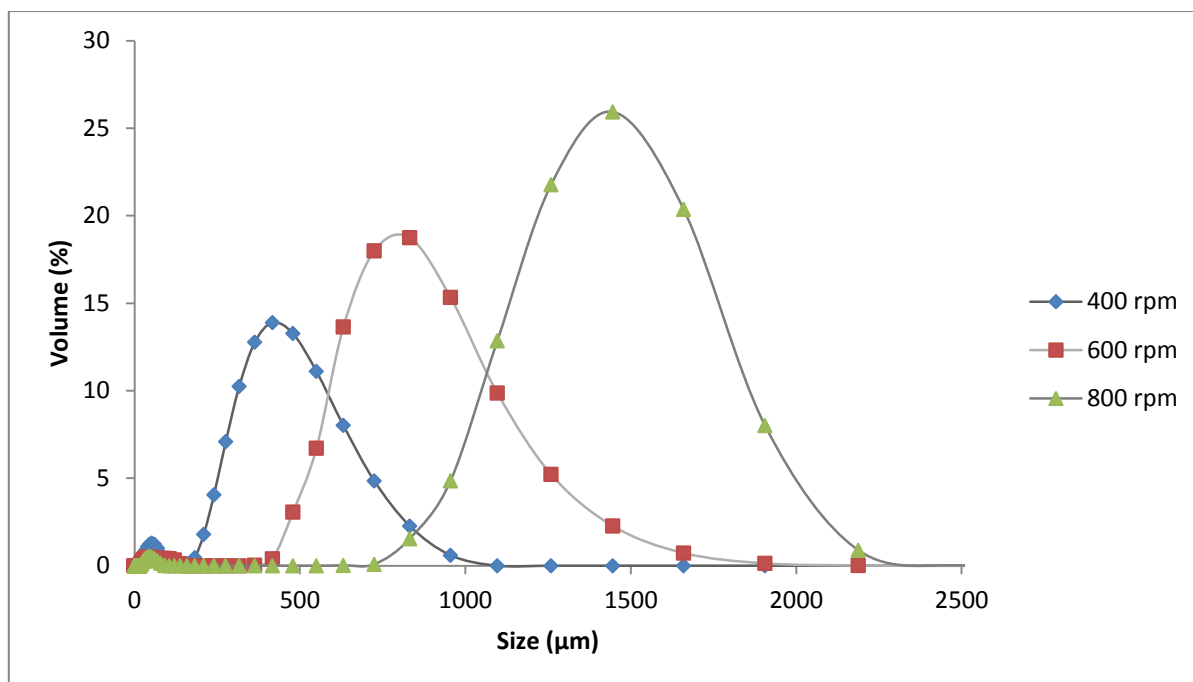


Figure 6.6 – Particle size distribution of the carrageenan particles produced at 400, 600 and 800 rpm illustrating the effect of mixing speed on particle size distribution.

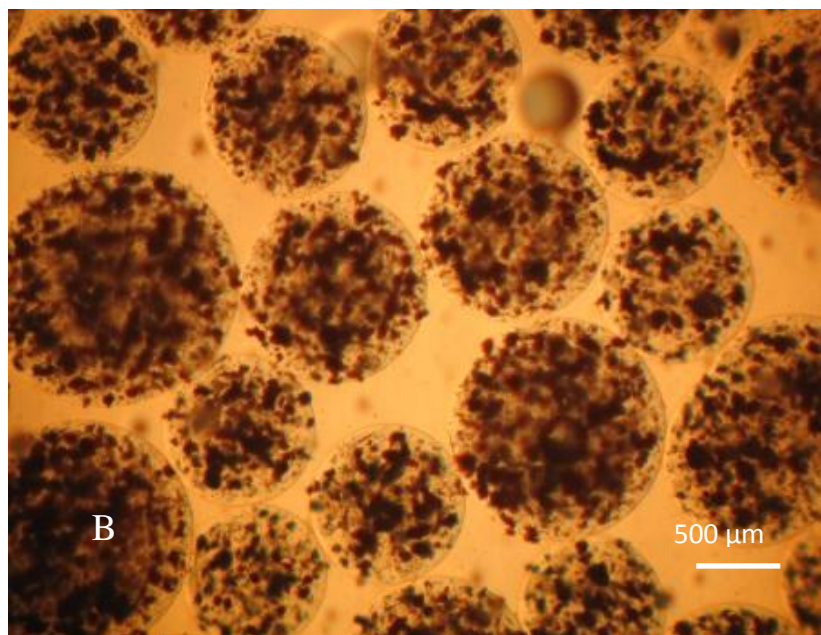
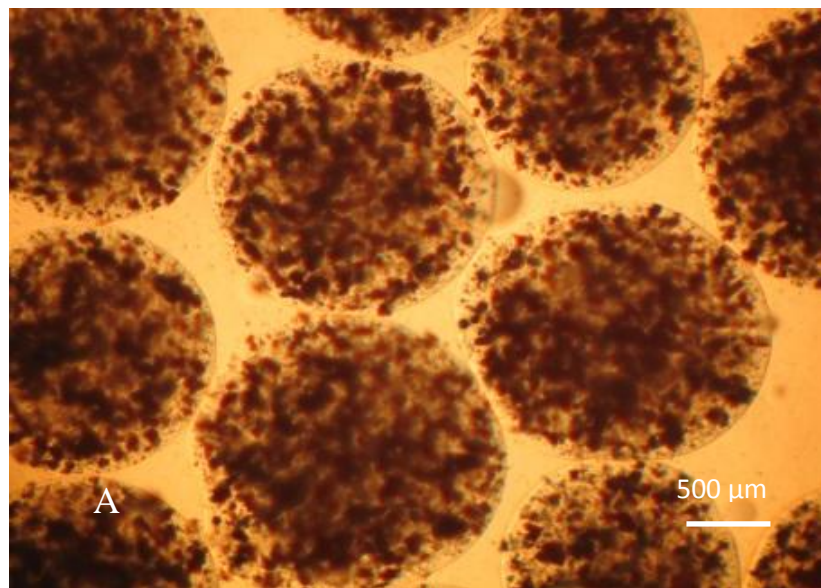
	D₁₀ (μm)	D₅₀ (μm)	D₉₀ (μm)
400 rpm	951	1294	1642
<i>St Dev</i>	105	125	189
<i>RSD (%)</i>	11.0	9.7	11.5
600 rpm	488	736	1062
<i>St Dev</i>	66	80	96
<i>RSD (%)</i>	13.5	10.9	9.0
800 rpm	181	378	602
<i>St Dev</i>	22	50.0	54
<i>RSD (%)</i>	12.1	13.2	8.9

Table 6.4 – Particle size data of the carrageenan particles produced at 400, 600 and 800 rpm showing the effect of mixing speed on the D₁₀, D₅₀ and D₉₀ particle sizes. Each value is the mean average of three independent studies ± SD.

6.6.1.2 Drug loading and encapsulation efficiency

The loading of the drug delivery particles into the carrageenan spheres was investigated by light microscopy (Figures 6.7 and 6.8) and the DL and EE of the PIP system was determined by UV spectroscopy (Tables 6.5 and 6.6). From the light microscope images, it was seen that the drug delivery particles were uniformly distributed within the embolic carrageenan

particles. They did however appear to be encapsulated in a clustered fashion which was due to the initial clustered morphology of the drug delivery particles caused during their production. Carrageenan made an attractive choice as the embolic agent since the drug delivery particles can be effectively encapsulated uniformly throughout the spheres due to the fast gelation process. Also since the particles are transparent, the uniformity of the encapsulated particles is easily viewed under a standard light microscope.



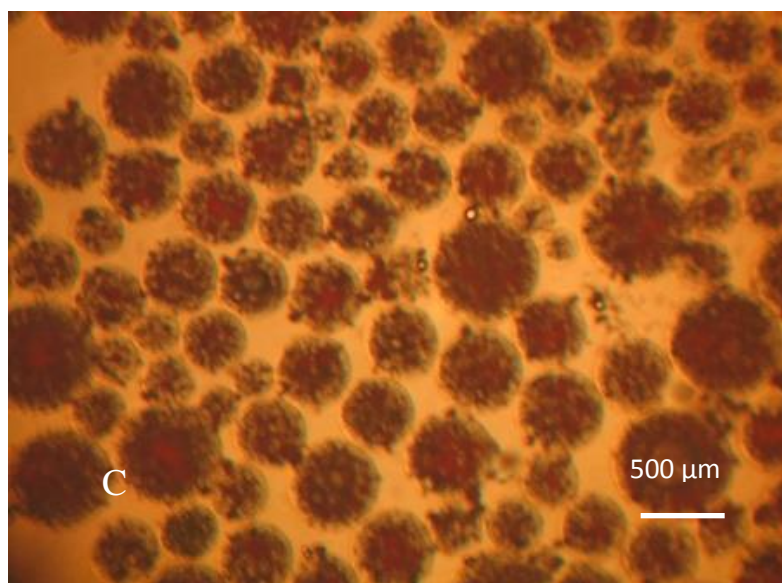


Figure 6.7 – Light microscope images of the carrageenan PIP system produced at (A) 400, (B) 600 and (C) 800 rpm. All embolic particles were loaded with 2% w/v drug delivery particles.

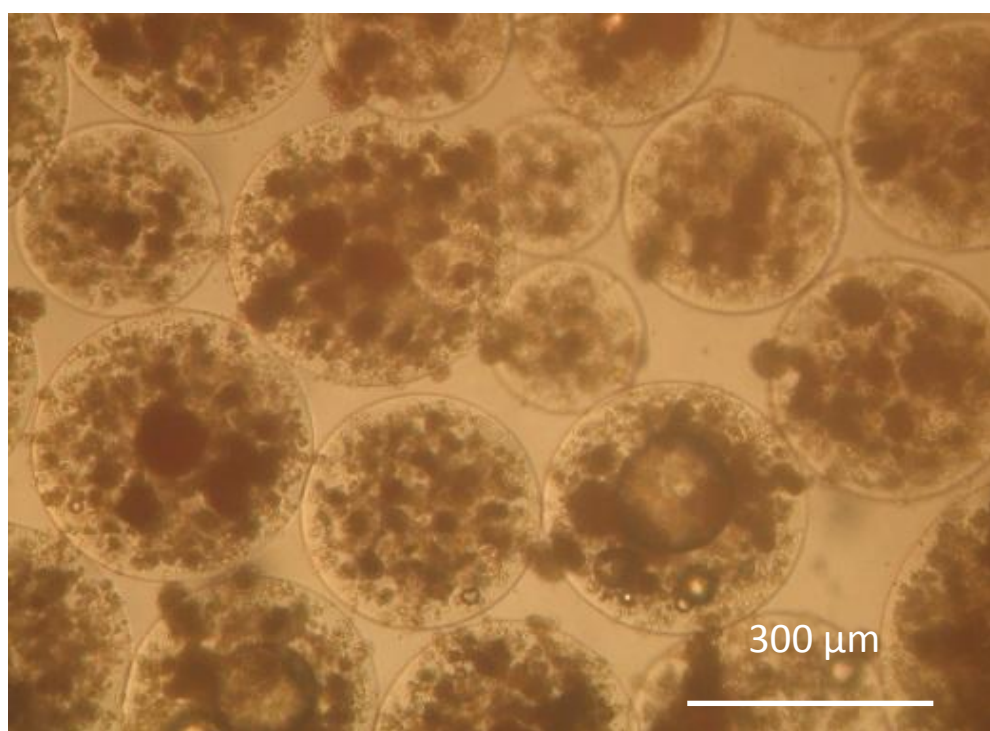


Figure 6.8 – The embolic carrageenan particles produced at 800 rpm under a higher magnification.

An important feature of the PIPs for TACE is for the particles of each size to have identical drug loadings, allowing the same dose of drug to be administered to patients with various blood vessel widths. For the Drug delivery particle loadings of 2 %, similar DLs of 3.2 %

3.3 % and 2.7 % were obtained for PIPs produced at 400, 600 and 800 rpm respectively. Likewise for 5 % drug delivery particle loadings, similar DLs of 5.4 %, 5.1 % and 4.8 % were determined for mixing speeds of 400, 600 and 800 rpm respectively. Since the production method is quick with a rapid gelation process, this allows the drug loss to be kept to a minimum where particles produced at 800 rpm has a slightly lower DL due to the faster mixing speed, and possible higher masses of drug loss during the washing process.

The EE value is less significant in producing a suitable system for TACE however the EE saw a slight decreases with increasing mixing speeds. EEs for 2 % drug delivery particles were 77.7 %, 77.7 % and 67.1 % where the 5 % drug delivery particles gave EEs of 82.3 %, 78.2 % and 72.1 %. This general decrease was believed to be due to the increased in shear created with higher mixing speeds resulting in small masses of particles being lost to the continuous phase of the emulsion before the gelation of carrageenan occurs. Also, the o-w emulsion is known to generally suffer the disadvantage of requiring multiple washing stages to ensure all surface oil is removed which can result in a higher drug loss.

	400 rpm	600 rpm	800 rpm
DL (%)	3.2	3.3	2.7
<i>St Dev</i>	0.7	0.5	0.7
<i>RSD (%)</i>	21.9	15.6	33.3
EE (%)	77.7	77.7	67.1
<i>St Dev</i>	18.5	12.9	17.6
<i>RSD (%)</i>	24.1	16.6	26.2

Table 6.5 – Drug loading and encapsulation efficiency of the PIP system produced at 400, 600 and 800 rpm.

2 % w/v of the drug delivery particles was loaded. Each value shows the mean average of three independent studies \pm SD.

	400 rpm	600 rpm	800 rpm
DL (%)	5.4	5.1	4.8
<i>St Dev</i>	1.0	0.8	0.7
<i>RSD (%)</i>	18.5	15.7	14.6
EE (%)	82.3	78.2	73.1
<i>St Dev</i>	15.1	12.8	11.7
<i>RSD (%)</i>	18.3	16.4	16.0

Table 6.6 – Drug loading and encapsulation efficiency of the PIP system produced at 400, 600 and 800 rpm.

5% particle loadings were used. Each value shows the mean average of three independent studies \pm SD.

6.6.1.3 Drug release from PIP system

The PIP systems were subject to in-vitro release in PBS where the effects of particle size and particle loading were investigated (Figures 6.10 and 6.11). By increasing the particle loading, a higher mass of drug was released due to the higher initial loading of drug particles into the embolizing spheres. A fundamental property of the PIPs is for the effect of particle size to be decoupled from the drug release rate, allowing PIPs of different sizes to display the same release pattern. No real significant changes in drug release were observed in particles produced at mixing speeds of 400, 600 and 800 rpm, indicating that PIP size had no significant effect on the drug release pattern, allowing the effect to be decoupled. PIPs loaded with 2 % particles saw release of 64 % <p 0.43>, 73 % <0.61> and 72 % <p 0.62> of the drug within the first two hours, then 95 % <p 0.89>, 92 % <p 0.85> and 96 % <p 0.82> after 4 hours for mixing speeds of 400, 600 and 800 respectively. Also, PIPs loaded with 5 % particles saw release of 45 % <p 0.45>, 59 % <p 0.63> and 62 % <p 0.53> in the first two hours followed by release of 85 % <p 0.52 >, 94 % <p 0.62 > and 96 % <p 0.65> after 4 hours for mixing speeds of 400, 600 and 800 rpm respectively showing similar release patterns for the various sized PIPs.

Carrageenan was chosen since it is a thermoresponsive polymer that forms strong gels even without addition of potassium ions to reinforce the double helical junction zones formed

during the crosslinking, which can potentially allow the particles to be more permeable than chemically crosslinked gels. Also, since the large beads investigated in the initial material screening experiments in chapter 3 released the encapsulated drugs instantly, it was hypothesized that they would make ideal embolizing materials since their porous microstructures could have the potential to allow the production of PIPs that allow the effect of particle size on drug release rate to be decoupled. However, despite the similar release rates being achieved, the release profile was fairly short and the PIPs may not display similar release profiles for drugs that have a release period of 1-2 weeks. It would therefore be worthwhile investigating if similar results can be obtained from PIPs containing a hydrophobic drug, since their poor water solubility can potentially allow a 1 – 2 week release period to be achieved.

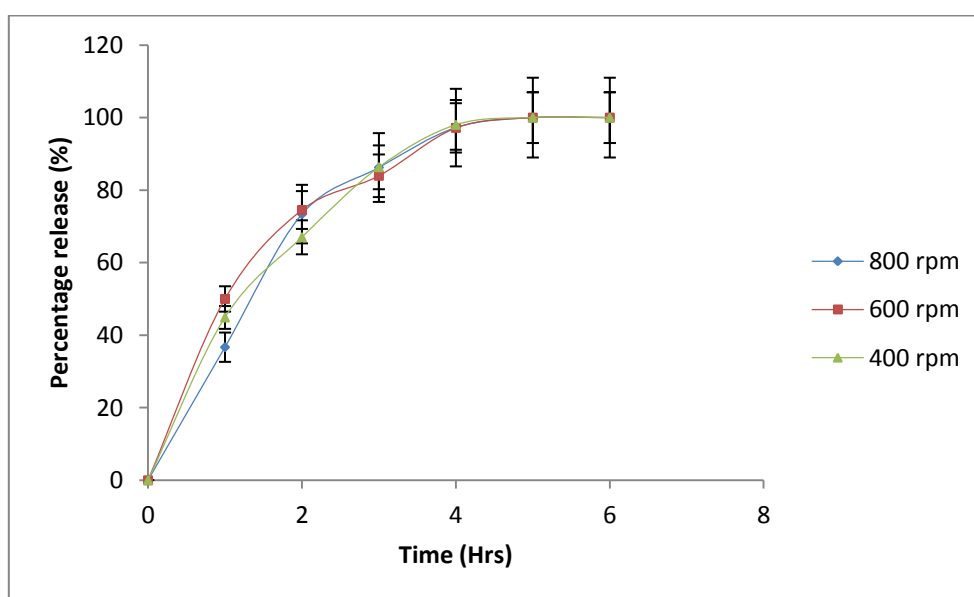


Figure 6.9 –Percentage drug release profiles of the PIP system produced at 400, 600 and 800 rpm. A 2 % drug delivery particle loading was used. Each data point shows the mean average of three independent studies \pm SD.

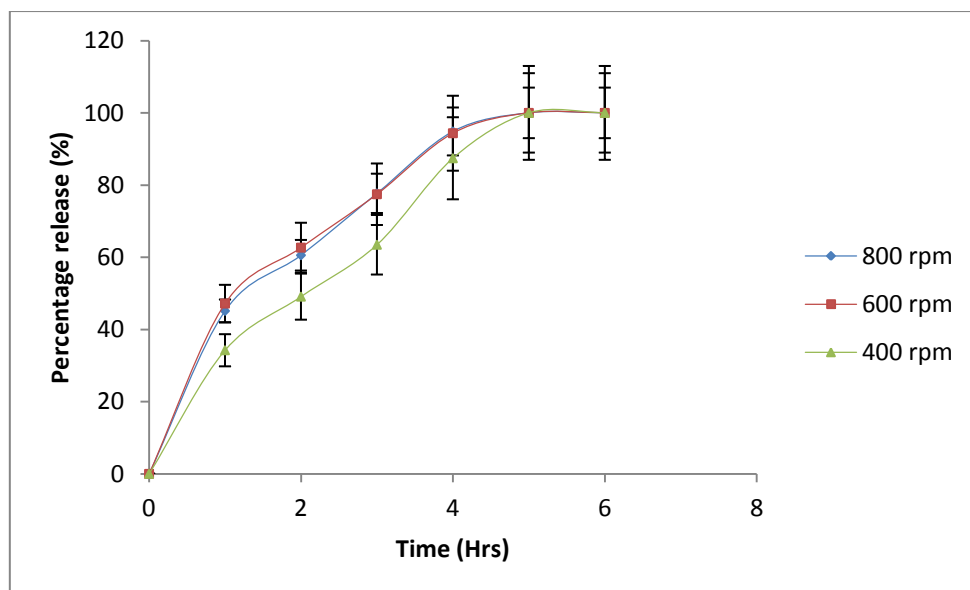


Figure 6.10 – Percentage drug release profiles of the PIP system produced at 400, 600 and 800 rpm. A 5% drug delivery particle loading was used. Each data point shows the mean average of three independent studies \pm SD.

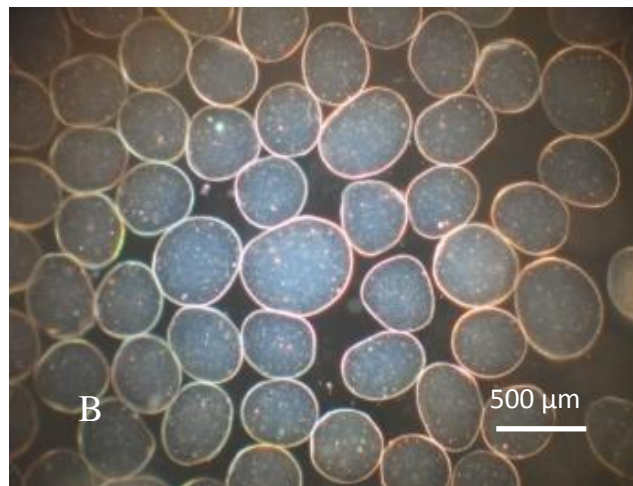
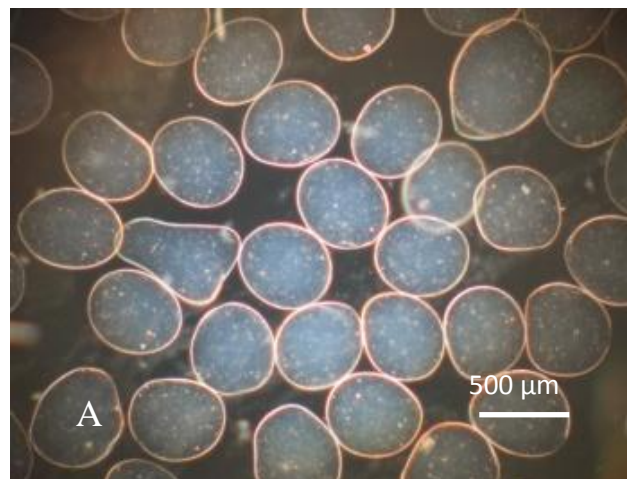
6.6.2 Production of the embolic particles by a nozzle vibration method

A second method for producing the embolizing particles was also investigated based on the principle of nozzle vibrating. This method allows particles with a uniform size to be produced by applying a superimposed vibration to a flowing polymer jet, and passing through a nozzle of a desired size. An electrostatic charge is then applied, causing the droplets to repel where they are then collected in a hardening bath.

6.6.2.1 Effect of vibration frequency on microsphere production

The effect of vibration frequency on the microspheres was investigated by light microscopy and particle sizing (Figures 6.12 and 6.13 and Table 6.7). By increasing the vibration frequency, smaller particles were obtained where average sizes of 576, 496 and 435 μm were determined for vibration frequencies of 1000, 1500 and 2000 Hz respectively. By increasing the frequency, a higher vibration is applied to the flowing polymer jet, breaking it down in to more droplets resulting in a decrease in the particle size and also allows more droplets to be produced per second. With the increasing nozzle sizes, lower vibration frequencies were

chosen. Lower frequencies are required to allow optimum droplet formation for spheres produced with larger nozzles where Weber added effects of nozzle diameter into his equations for optimum droplet formation since less agitation is required to form the larger droplets (Equation 6.2).



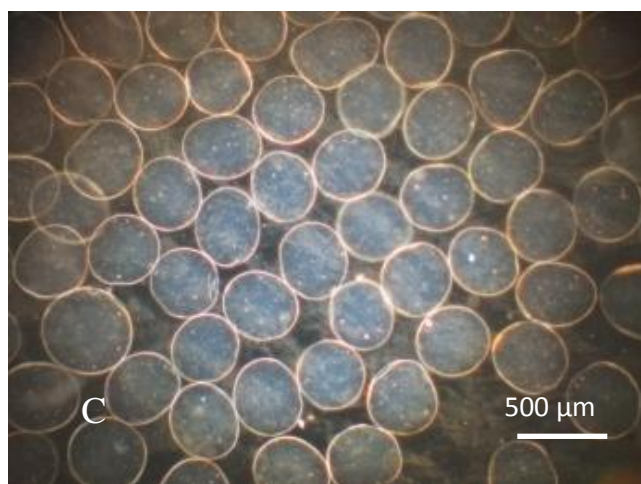


Figure 6.11 – Light microscope images of the alginate microspheres illustrating the effect of vibrating frequency on particle form. The investigated frequencies were (A) 1000, (B) 1500 and (C) 2000 Hz. The operating flow rate, electrode strength and nozzle size were 10 mL/min, 1500 V and 300 μm respectively.

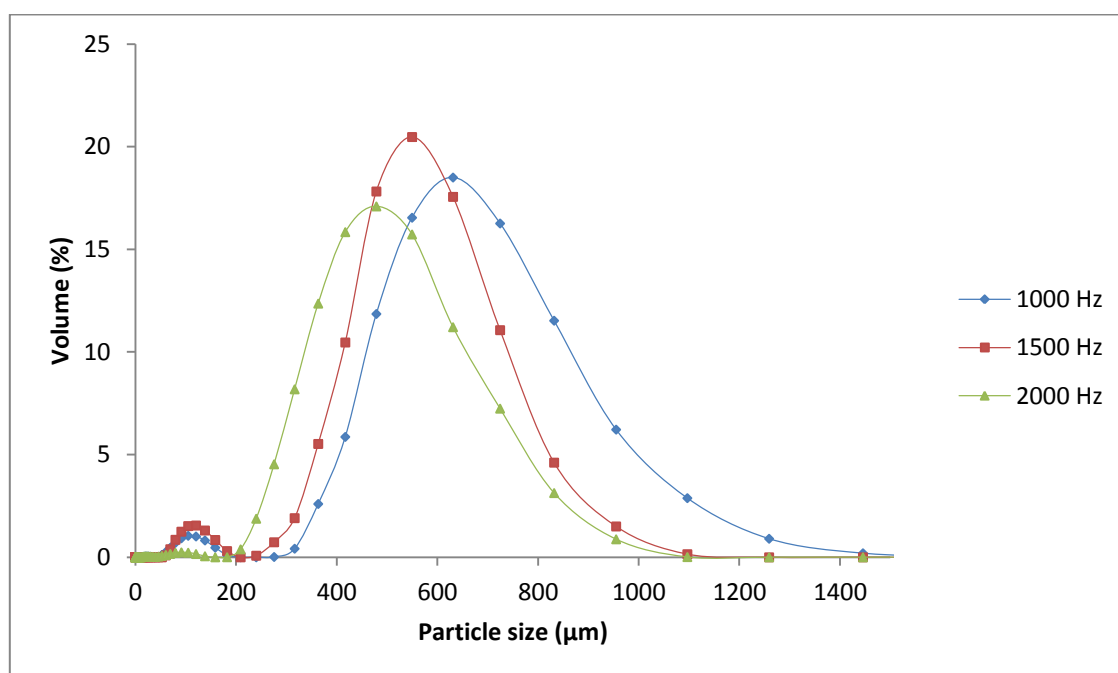


Figure 6.12 – Particle size distribution of the alginate microspheres illustrating the effect of the vibrating frequency on the size distribution. The investigated frequencies were 1000, 1500 and 2000 Hz. The flow rate, electrode strength and nozzle size were 10 mL/min, 1500 V and 300 μm respectively.

	D₁₀ (µm)	D₅₀ (µm)	D₉₀ (µm)
1000 Hz	373	576	834
<i>ST Dev</i>	25.2	33.5	38.4
<i>RSD (%)</i>	6.8	5.8	4.6
1500 Hz	303	496	684
<i>St Dev</i>	12.4	22,9	33.1
<i>RSD (%)</i>	4.1	4.6	4.8
2000 Hz	285	435	643
<i>St Dev</i>	13.4	20.5	34.7
<i>RSD (%)</i>	4.7	4.7	5.4

Table 6.7 – Particle size data for the alginate particles produced at vibrating frequencies of 1000, 1500 and 2000 Hz showing its effect on the D₁₀, D₅₀ and D₉₀ particle sizes. Each value is the average of three independent studies ± SD.

6.6.2.2 Effect of electrode voltage on particle production

The effect of the electrode voltage was investigated by light microscopy and laser sizing (Figures 6.14 and 6.15 and Table 6.8). By increasing the voltage applied to the electrode, the particle size decreases and the size distribution narrows where particle sizes of 776.8, 506 and 436 µm were determined from voltages of 1000, 1500 and 2000 V respectively.

The application of the electrode on the nozzle vibrating device applies a charge to the surface of the droplets to prevent droplets aggregating allowing beads with high degrees of sphericity and narrow size distributions to be produced. By increasing the voltage applied to the electrode, higher charges are applied to the surface of the droplets allowing them to be repelled a greater distance. This increase in the distance between droplets prevents aggregation, resulting in a decrease in particle size where the population has a narrower size range. Higher voltages are required for particles produced with larger nozzles due to the increased weight of the droplet and act of gravitational forces so that the droplet stream can be effectively repelled and avoiding aggregation upon crosslinking.

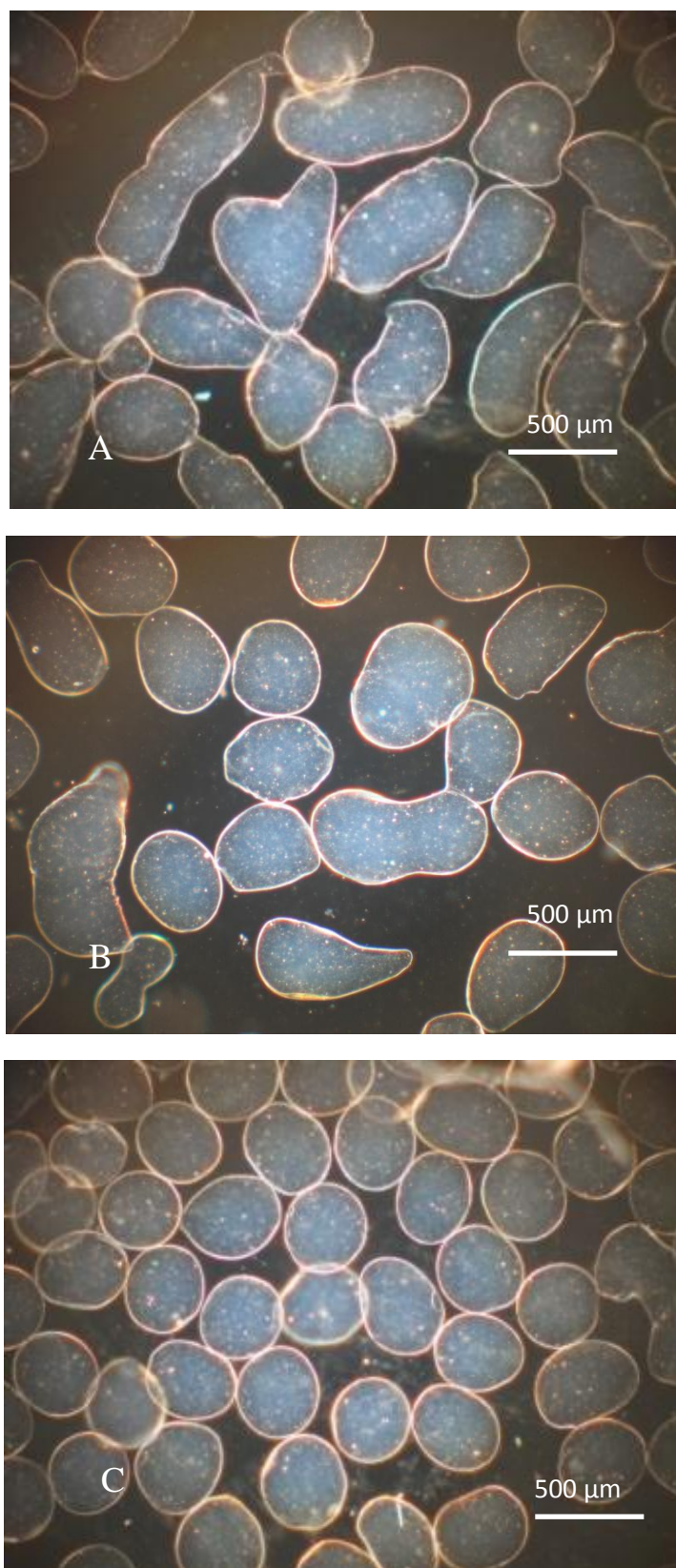


Figure 6.13 – Light microscope images of the microspheres illustrating the effect of electrode voltage on particle form. The investigated voltages were (A) 1000, (B) 1500 and (C) 2000 V. The vibrating frequency, flow rate and particle size were 1500 Hz, 10 mL/min and 300 μm respectively.

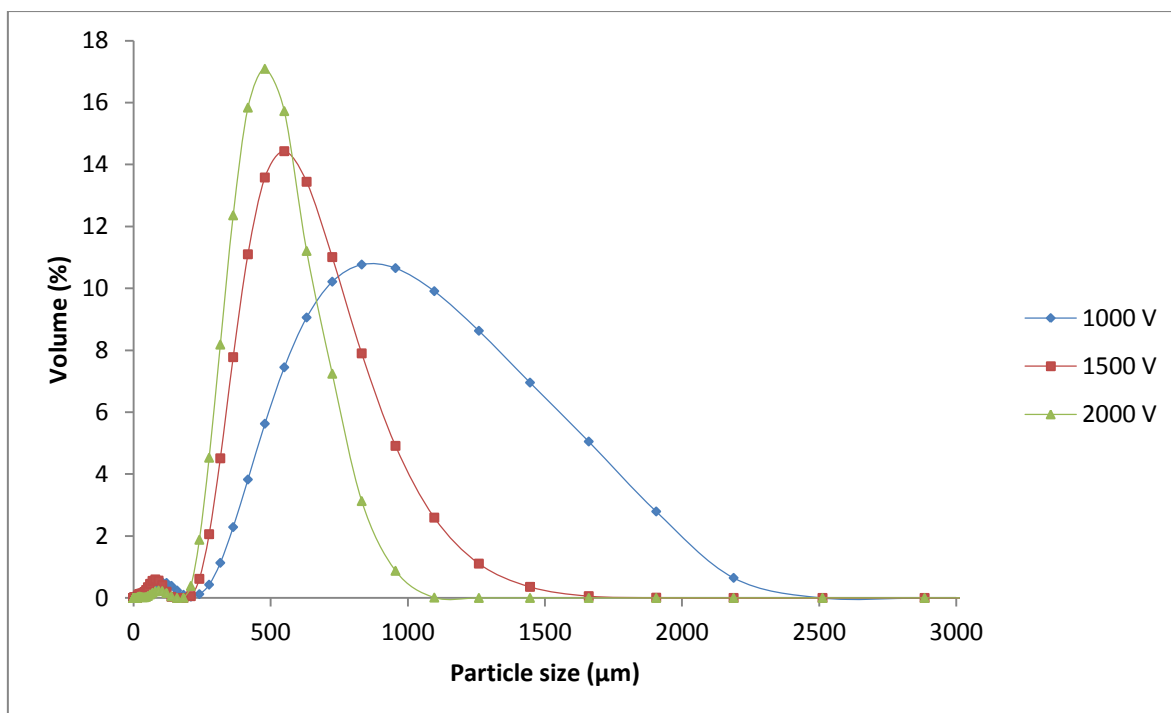


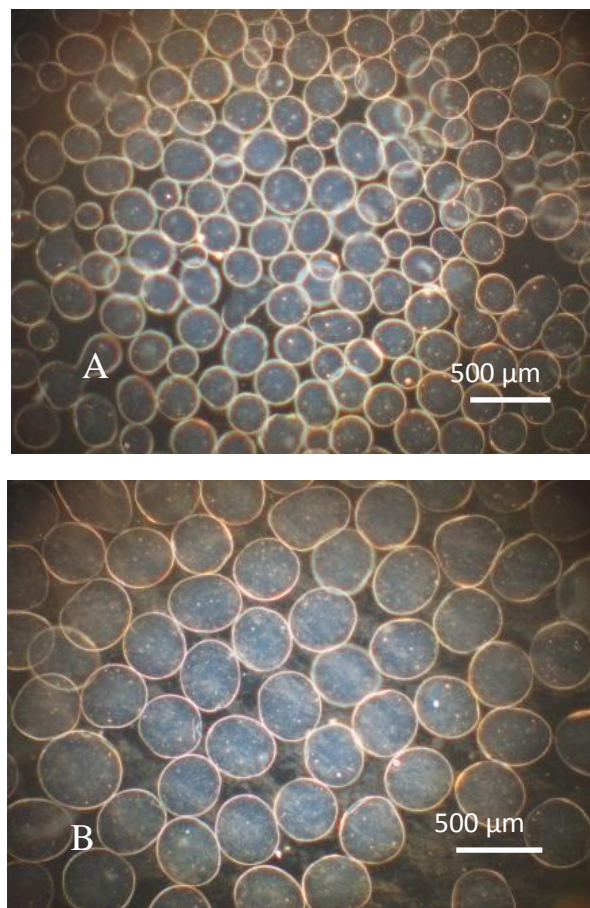
Figure 6.14 – Particle size distribution of the microspheres illustrating the effect of electrode voltage on the size distribution. The investigated voltages were 1000, 1500 and 2000 V. The vibrating frequency, flow rate and particle size were 1500 Hz, 10 mL/min and 300 μm respectively.

	D₁₀ (μm)	D₅₀ (μm)	D₉₀ (μm)
1000 V	387	776	1398
<i>St Dev</i>	18.4	39.5	78.9
<i>RSD (%)</i>	4.8	5.1	5.6
1500 V	302	506	815
<i>St Dev</i>	13.9	27.3	40.8
<i>RSD (%)</i>	4.6	5.4	5.0
2000 V	285	435	643
<i>St Dev</i>	16.1	23.5	34.8
<i>RSD (%)</i>	5.6	5.4	5.4

Table 6.8 – Particle size data for the microspheres produced at electrode voltages of 1000, 1500 and 2000 V showing their effects on the D₁₀, D₅₀ and D₉₀ particle sizes. Each value is the average of three independent studies \pm SD.

6.6.2.3 Effect of nozzle size on particle production

The effect of the nozzle size on particle formation was investigated by light microscopy and laser diffraction (Figures 6.16 and 6.17 and Table 6.9). By increasing the nozzle size the particle size also increased where average sizes of 251, 496 and 836 μm were determined for nozzles of 150, 300 and 450 μm respectively. As expected the size of the particles increases due to the increased nozzle diameter. The diameters of the particles produced with a particular nozzle size are approximately twice that of the nozzle where the size can vary depending on the alginate flow rate, vibration frequency and electrode strength used during production allowing microspheres on a wide size scale to be produced.



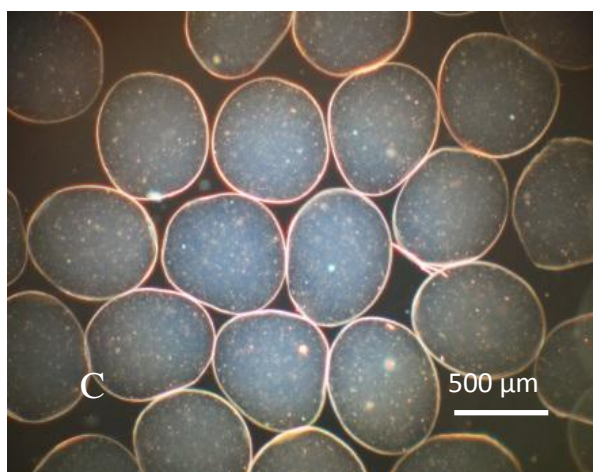


Figure 6.15 – Light microscope images of the microspheres showing the effect of nozzle size on particle size.

The investigated nozzle sizes were (A) 150, (B) 300 and (B) 450 μm . The electrode voltage, vibrating frequency and flow rate were 1500 V, 1500 Hz and 10mL/min respectively.

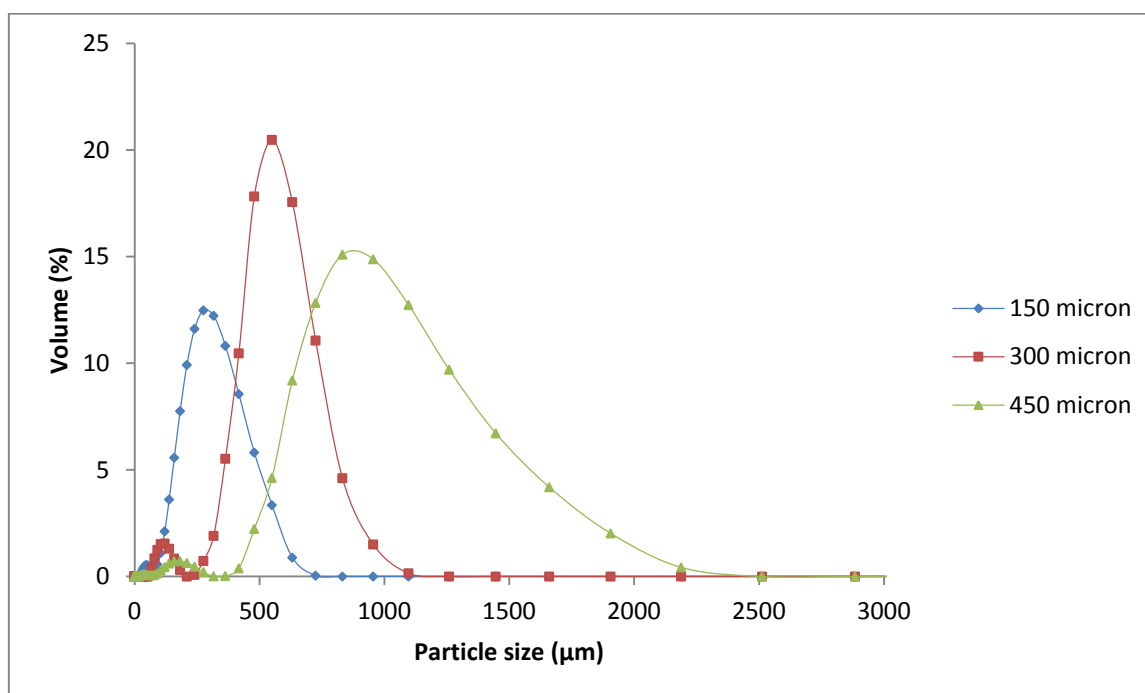


Figure 6.16 – Particle distribution of the microspheres showing the effect of nozzle size on the particle size distribution. The investigated nozzle sizes were 150, 300 and 450 μm . The electrode voltage, vibrating frequency and flow rate were 1500 V, 1500 Hz and 10 mL/min respectively.

	D₁₀ (µm)	D₅₀ (µm)	D₉₀ (µm)
150 µm	133	251	417
<i>St Dev</i>	6.3	10.4	19.3
<i>RSD (%)</i>	4.7	4.1	4.6
300 µm	303	496	648
<i>St Dev</i>	17.8	23.5	33.2
<i>RSD (%)</i>	5.9	4.7	5.1
450 µm	521	836	1339
<i>St Dev</i>	53.9	44.4	88.6
<i>RSD (%)</i>	10.3	5.3	6.6

Table 6.9 – Particle size data for the alginate particles produced with the various nozzle sizes showing their effect on the D₁₀, D₅₀ and D₉₀ particle sizes. Each value is the mean average of three independent studies ± SD.

6.6.2.4 Drug loading and encapsulation

Loading of the drug delivery particles into the microspheres was investigated however, due to their clustered and aggregated morphology, their encapsulation was not possible, even with the largest nozzle with a 1 mm diameter. For successful encapsulation by nozzle vibrating, it is believed particles of a smaller size preferably, on the nanoscale, or a semisolid system such as a liposomal based system would be required in order for the dispersion to flow freely through the nozzles. However, in order to make use of this process for a potential drug delivery system, the alginate-sodium silicate mixture was formed into a microparticle system. The effects of alginate concentration, sodium silicate concentration and nozzle size on DL and EE were investigated where 1 % verapamil hydrochloride was loaded into all formulations (Tables 6.10 – 6.12).

A decrease in DL of 14.2 %, 11.5 % and 9.3 % and increase in EE of 42.8 %, 57.5 % and 71 % was determined by increasing the alginate concentration from 1 – 3 % w/v due increase in material mass previously discussed. Similar effects on increasing sodium silicate concentration on the DL and EE were seen as to those reported in the previous chapters. The effect of nozzle size saw an increase for both DL and EE on increasing nozzle diameter, where DL of 8.3 %, 10.1 % and 13.6 % and EE of 41.8 %, 50.6 % and 67.1 % were

determined for nozzles of 150, 300 and 450 μm respectively. This was due to the effect of particle size on drug diffusion/loss during the crosslinking period. Due to their higher surface area, smaller particles will tend to lose higher masses of drug during production resulting in lower loadings and encapsulation rates.

	1 % Alginate	2 % Alginate	3 % Alginate
DL (%)	14.2	11.5	9.3
<i>St Dev</i>	0.5	0.2	0.2
<i>RSD (%)</i>	3.5	1.7	2.2
EE (%)	42.8	57.5	71
<i>St Dev</i>	1.4	1.3	1.8
<i>RSD (%)</i>	3.3	2.3	2.5

Table 6.10 – The DL and EE of the alginate-sodium silicate microspheres showing the effect of alginate concentration on DL and EE. The sodium silicate and nozzle size were 3 % and 300 μm respectively. Each value is the mean average of three independent studies \pm SD

	1 % Silicate	2 % Silicate	3 % Silicate
DL (%)	13.3	11.8	10.5
<i>St Dev</i>	0.8	0.6	1.2
<i>RSD (%)</i>	6.0	5.1	1.1
EE (%)	40	47.3	52.6
<i>St Dev</i>	2.5	2.6	3.7
<i>RSD (%)</i>	6.3	5.5	7.0

Table 6.11 – The DL and EE of the alginate-sodium silicate microspheres showing the effect of silicate concentration on DL and EE. The alginate concentration and nozzle size were 2 % and 300 μm respectively.

Each value is the mean average of three independent studies \pm SD

	150 μm	300 μm	450 μm
DL (%)	8.3	10.1	13.6
<i>St Dev</i>	0.4	0.4	1.4
<i>RSD (%)</i>	4.8	3.9	10.3
EE (%)	41.8	50.6	67.1
<i>St Dev</i>	1.4	1.6	5.2
<i>RSD (%)</i>	3.3	3.2	7.7

Table 6.12 – The DL and EE of the alginate-sodium silicate microspheres showing the effect of nozzle size on DL and EE. The alginate concentration and sodium silicate concentration were 2 % and 3 % respectively.

Each value is the mean average of three independent studies \pm SD

6.6.2.5 Drug release

The microspheres were subject to in-vitro release in PBS. The effects of alginate concentration, sodium silicate concentration and particle size on drug release rate were investigated (Figures 6.18 – 6.20). By increasing the alginate concentration, the release rate of the beads decreased. The initial burst in the first 2 hours saw a release of 80 % $\langle p 0.06 \rangle$, 40 % $\langle p 0.04 \rangle$ and 35 % $\langle p 0.02 \rangle$ of the drug in alginate concentrations of 1 %, 2 % and 3 % respectively, followed by a steady release rate over the rest of the study. The effect of sodium silicate concentration once again had a large effect on the drug release rate. Concentrations of 1 % resulted with a rapid release rate with the majority of the drug being fully released in the first 2 hours while the 3 % sodium silicate released approximately 45 % $\langle p 0.03 \rangle$ of the drug in the first two hours followed by a steady release rate over the rest of the study.

Increasing nozzle size, as expected increased the particle size. This study also shows how particles of varying diameters can display various release rates. Particles produced with the 150 μm nozzle released 85 % of the drug within the first 5 hours of the study. The 300, and 450 μm nozzles produced larger particles which has a significant effect on the drug release rate, where only 55 % $\langle p 0.03 \rangle$ and 15 % $\langle p 0.02 \rangle$ of the drug was released within the first 5

hours. Smaller particles are liable to faster release rates than larger particles due to their higher surface areas and lower distance for water molecules to penetrate in and drug molecules to diffuse out of the microparticle. Although the particles produced with the microencapsulator do not meet the aim of this project by decoupling particle size on drug release rate, it did however provide a good alternate to producing spherical embolization spheres that can encapsulate a range of drugs, making it an attractive application for TACE.

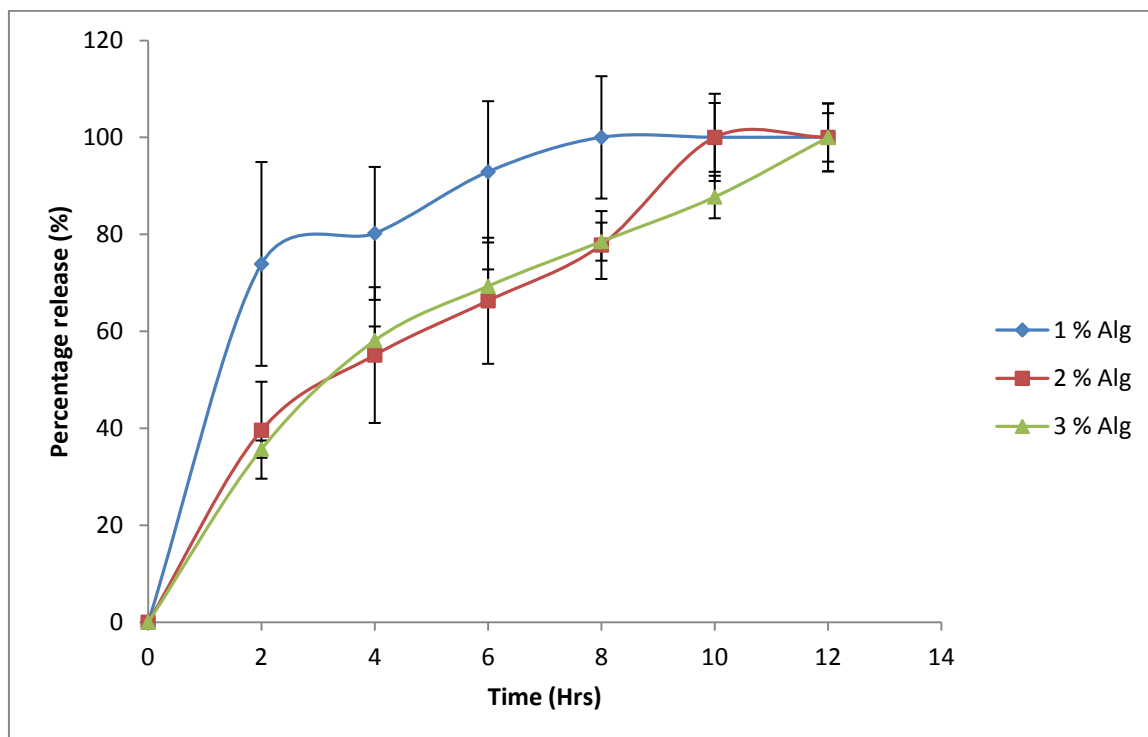


Figure 6.17 – Percentage drug release of the microspheres illustrating the effect of alginate concentration on drug release rate. Each point is the mean average of three independent studies \pm SD.

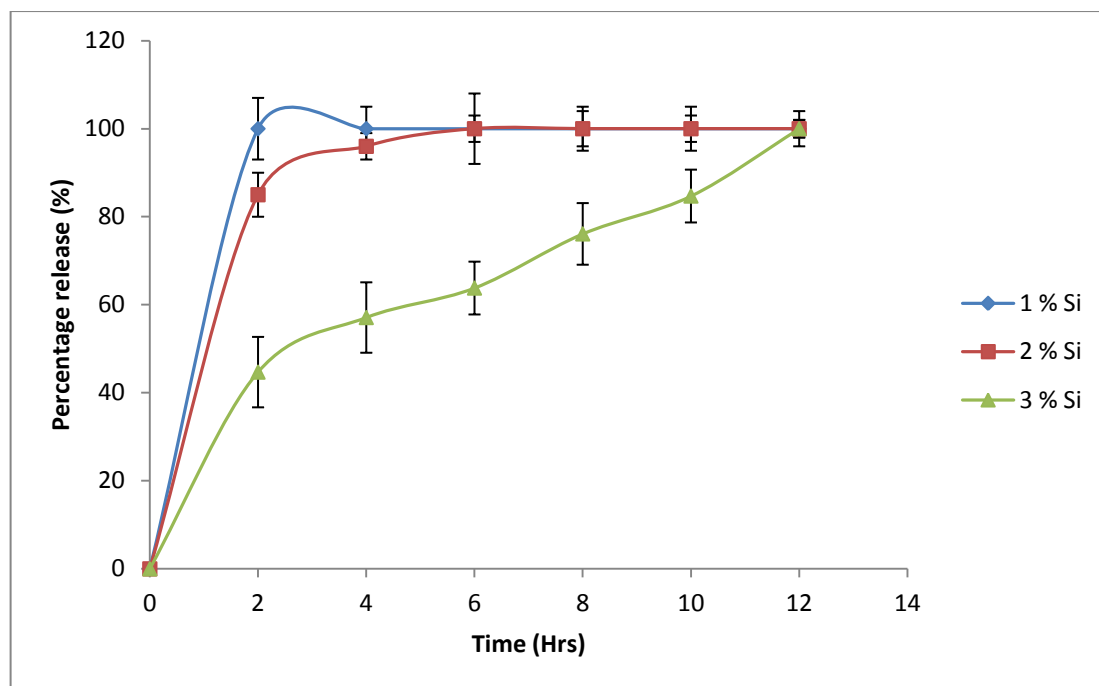


Figure 6.18 – Percentage drug release of the microspheres illustrating the effect of sodium silicate concentration on drug release rate. Each point is the mean average of three independent studies \pm SD.

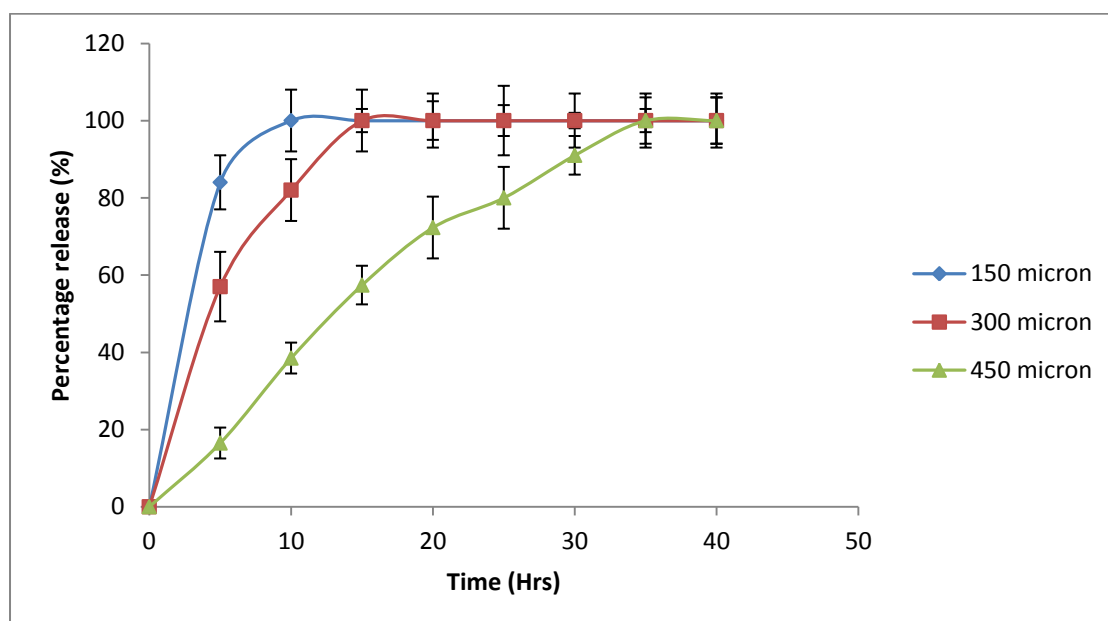
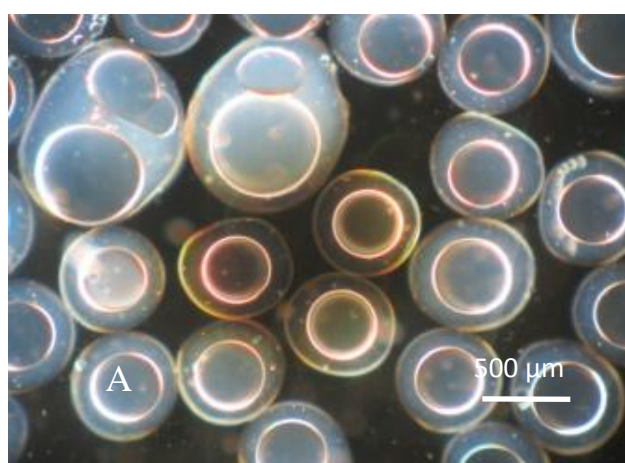


Figure 6.19 – Percentage drug release of the microspheres illustrating the effect of nozzle size on drug release rate. Each point is the mean average of three independent studies \pm SD.

6.6.2.6 Microcapsule formation

The microencapsulation unit also allowed production of microcapsules, where oils could be encapsulated within an alginate shell. Formation of alginate capsules containing mineral oil where the effect of the alginate and mineral oil flow rate on capsule formation was investigated by light microscopy (Figures 6.21 and 6.22). The effect of shell nozzle size was also investigated by light microscopy and laser diffraction (Figures 6.23 and 6.24 and Table 6.13).

By increasing the oil flow rate from 5, 10 and 20 mL/min the morphology of the oil cores drastically changed. An optimum flow rate of 10 mL/min yielded spherical cores encapsulated inside the alginate shells. The flow rate of 5 mL/min was not sufficient enough to pump the oil though in a continuous motion resulting in the oil trickling throughout the alginate solution where alginate shells containing multiple cores were produced. On the other hand, the flow rate of 20 mL/min gave flow rates that were too rapid for the alginate to effectively encapsulate to oil flow where large multiple cores were encapsulated within disordered alginate shells.



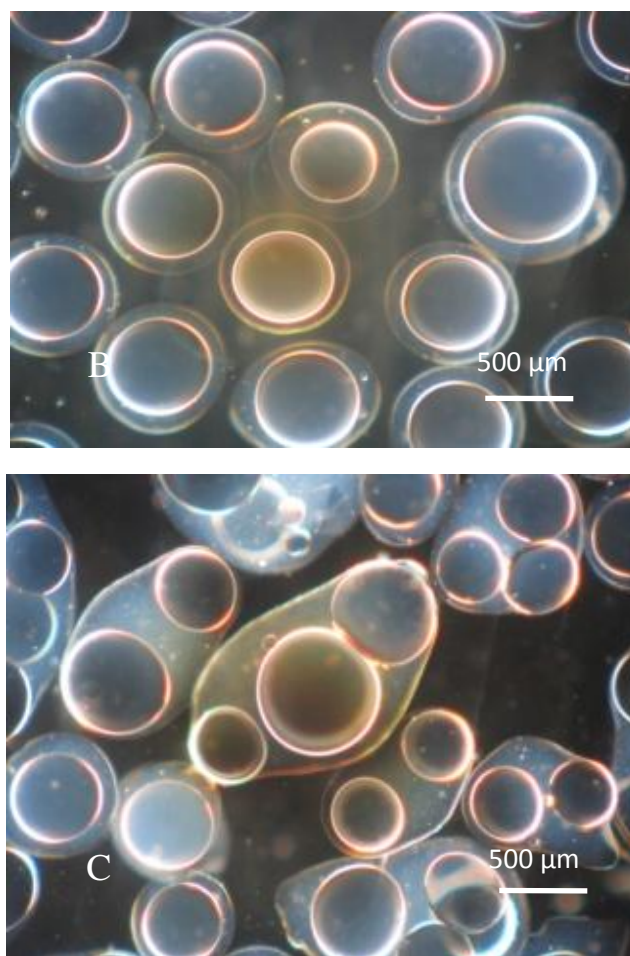
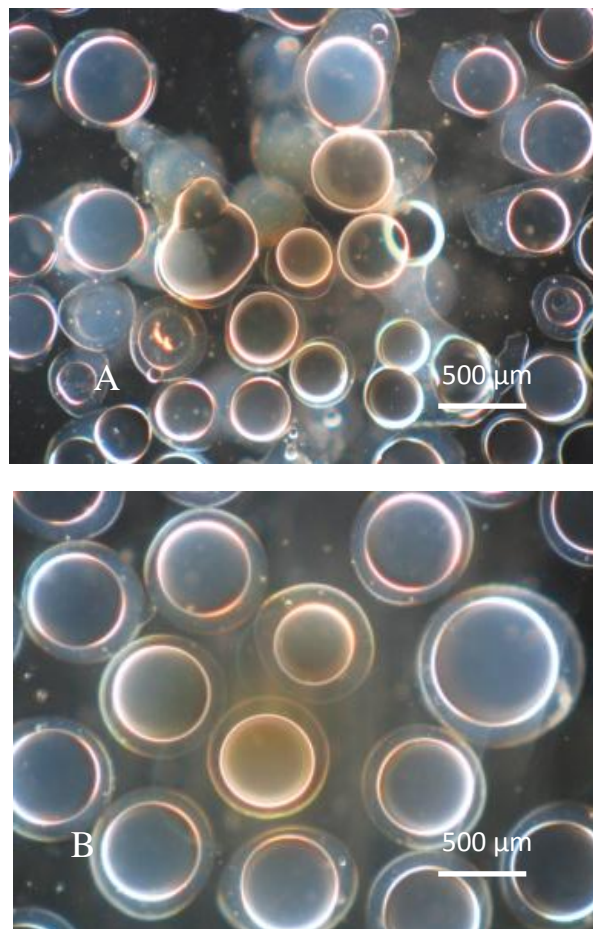


Figure 6.20 - Light microscope images of the microcapsules produced showing the effect of the oil flow rate on particle formation. Oil flow rates of (A) 5, (B) 10 and (C) 20 mL/min were investigated. The shell flow rate, vibrating frequency, electrode voltage, shell nozzle and core nozzle were 175 mbar, 800 Hz, 2500 V, 400 μm and 200 μm respectively.

The alginate flow rate, controlled by a pressure bottle, was investigated where pressures of 150, 175 and 200 mbar gave various results. The operating pressure of 175 mbar gave an optimum production process where spherical alginate shells with a single oil core were obtained. A pressure of 150 mbar gave an ineffective alginate flow rate to encapsulate the oil where disordered formations were produced with some empty shells due to the high oil flow rate causing the alginate droplets to rupture. The flow rate of 200 mbar was too rapid for capsule formation since large aggregated alginate forms with multiple oil cores were

produced. Also the higher flow rate prevented the droplet spray from being produced yielding aggregated products.

Along with the correct vibration and electrode conditions, the oil and water flow rates must be carefully controlled so that the oil can be effectively encapsulated, with single spherical cores held inside spherical shells. A general principle, according to the manufacturer is the core flow rate should be approximately 20 % of the shell flow rate.



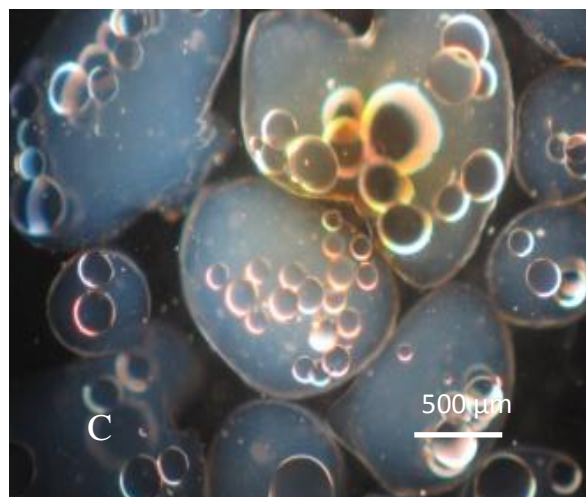


Figure 6.21 - Light microscope images of the microcapsules showing the effect of the shell pressure on particle formation. Pressures of (A) 150, (B) 175 and (C) 200 mbar were investigated. The oil flow rate, vibrating frequency, electrode voltage, shell nozzle and core nozzle were 10 mL/min, 800 Hz, 2500 V, 400 μ m and 200 μ m respectively.

Microcapsules produced with shell nozzles of 300, 200 and 500 μ m were produced where all shell nozzles were fitted with a core nozzle of 200 μ m under the optimum operating conditions for the selected shell nozzle size. With increasing shell size, the capsule size increased as expected, where the oil cores saw a slight variation in their size distribution. The microcapsules made an interesting choice for the embolizing device since if the drug loaded particles could be encapsulated into the oil cores, this could potentially allow minimal loss of drug during storage and possibly extend the drug release rate of the hydrophilic compound due to the drugs poor solubility in lipophilic media. However, since the drug delivery particles could not be encapsulated by this method this investigation was not possible to pursue.

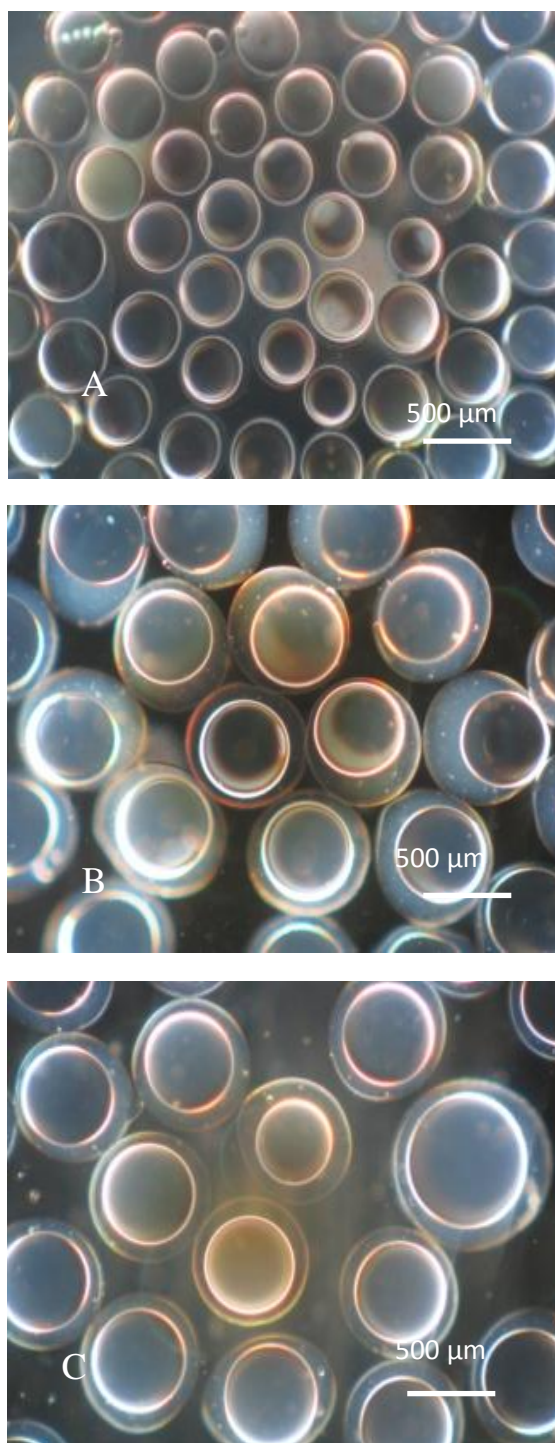


Figure 6.22 - Light microscope images of the microcapsules showing the effect of shell nozzle size on particle formation. Nozzles of (A) 300, (B) 400 and (C) 500 μm were investigated. The shell flow rate, core flow rate, vibrating frequency and electrode voltage and core nozzle were 175 mbar, 10 mL/min, 800 Hz, 2500 V and 200 μm respectively.

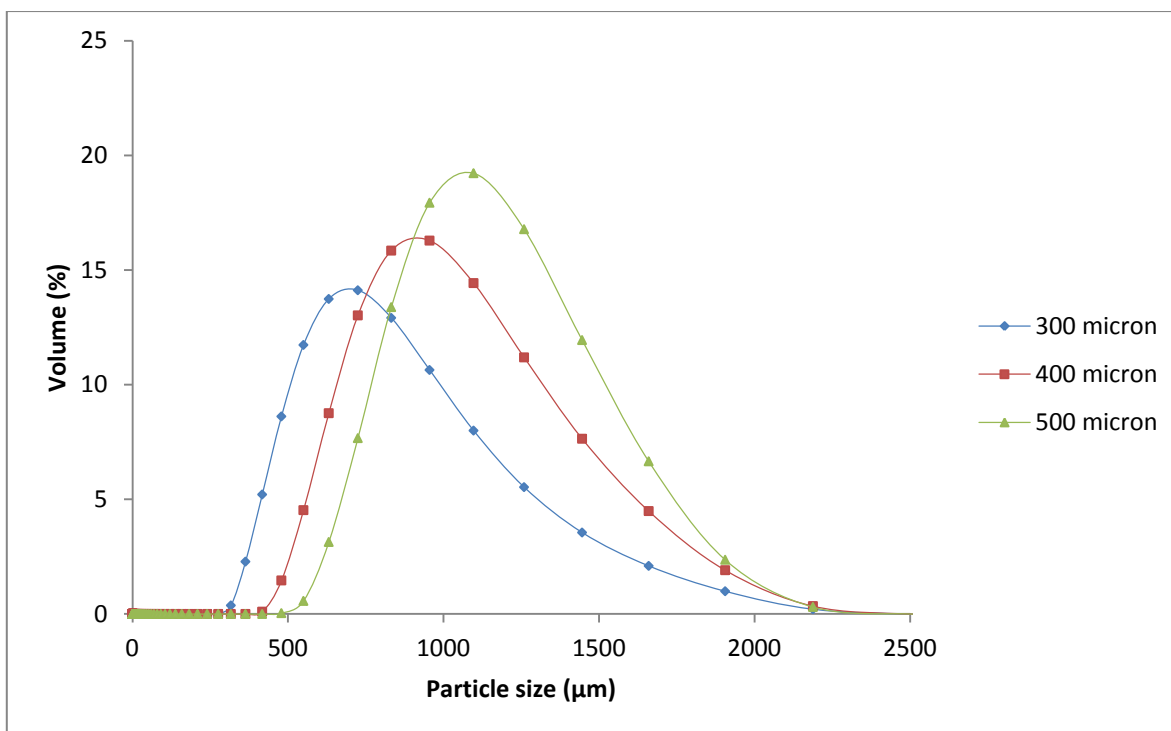


Figure 6.23 – Particle size distribution of the microcapsules produced showing the effect of shell nozzle size on the size distribution. Nozzles of 300, 400 and 500 μm were investigated. The shell flow rate, core flow rate, vibrating frequency and electrode voltage and core nozzle were 175 mbar, 10 mL/min, 800 Hz, 2500 V and 200 μm respectively.

	D₁₀ (μm)	D₅₀ (μm)	D₉₀ (μm)
300 μm	438	682	1155
<i>St Dev</i>	50.2	62.5	130
<i>RSD (%)</i>	11.5	9.2	11.3
400 μm	589	876	1352
<i>St Dev</i>	67.3	97.3	173.0
<i>RSD (%)</i>	11.4	11.1	12.9
500 μm	710	1005	1431
<i>St Dev</i>	59.7	115.0	115.1
<i>RSD (%)</i>	8.4	11.4	8.4

Table 6.13 – Particle size data for the microcapsules produced at the various nozzle sizes showing their effects on the D₁₀, D₅₀ and D₉₀ particle sizes. Each value is the mean average of three independent studies \pm SD.

6.7 Conclusion

This section investigated production of the embolic particles and incorporation of the drug delivery particles producing the PIP system for TACE. PIP systems by the w-o emulsion gave particles of a broad size range within the TACE range, where the drug delivery particles were successfully encapsulated uniformly throughout the spheres. Also, the PIP system produced allowed the aim of decoupling the effect of particle size on release rate to be achieved due to the high porosity of the carrageenan spheres. However, due to the short release period and un-even drug loadings caused by the clustery drug delivery particles, further investigation is required to draw stronger conclusions.

A new microencapsulation device yet to be explored within the literature was also explored for embolic particle production. Critical process parameters of vibrating frequency, electrode strength and nozzle size were investigated where particle formation was seen to be dependent on selection of an adequate electrode voltage to effectively repel the spray so that droplets avoided aggregation upon crosslinking. Particle size could be controlled by choice of the desired nozzle and adjustment of the vibrating frequency. Microcapsules were also formed where formation of capsules containing single oil cores in spherical spheres were dependent on selection of appropriate processing parameters. Despite being an ideal method for embolic sphere production, the drug delivery particles could not be encapsulated due to their clustery morphology. The method was however investigated to produce microspheres for the alginate-sodium silicate complex. By variation of the alginate, silicate and nozzle size parameters, release rates from instant release to over 48 hours were achieved. This method allowed production of particles under mild operating conditions where a range of microparticle sizes displaying controlled release could be produced. Combining this new method with the alginate-sodium silicate blend studied throughout this thesis, this single

technique allows great possibility not only for TACE but also other controlled drug delivery applications.

CHAPTER 7

CONCLUDING REMARKS AND FUTURE WORK

This thesis investigated the development of a new drug delivery system for the treatment of intermediate staged HCC. A frequently used treatment for this condition is TACE, a non-surgical method where DEBs have proven to show increased survival and improve patient well-being for those suffering with this non-curable disease. Of the current DEBs, the DC Bead has been a popular choice due to its ability to load and control the release of doxorubicin, where the particles show smooth hydrophilic surfaces with spherical geometries that can be calibrated to a particular blood vessel size. Despite their advantages, DEBs are limited to drugs that can bind to their functional groups, where in the DC bead, doxorubicin is held tightly by sulfonate groups. Also, since the particles are to be calibrated to a specific blood vessel size, patients with small blood vessels will require smaller particles to those with larger blood vessels. This variation will result in varying release rates where smaller particles will release their contents faster due to their increased surface area where some patients can potentially be exposed to peaks in the drugs toxicity.

The drug delivery system designed in this thesis sought to overcome these issues by use of a PIP system. Small drug delivery particles were designed to load and release a desired drug, where they would then be encapsulated into larger particles to act as an embolization device. By using this PIP system, a drug delivery system that is more versatile to a wider range of drugs can be produced. Also, the effect of particle size on drug release rate can then be decoupled by encapsulating the particles into larger embolizing particles that possess porous microstructures, allowing the release characteristics of the drug delivery particles to be retained.

The initial experiments investigated various polymer based materials and their capability to control the release of small molecular weight hydrophilic drugs, where verapamil hydrochloride was used as a model compound, since it displayed similar chemistry to doxorubicin. Polymers that displayed negative charges allowing interaction with the positive charge of the drug were of interest. Carboxylated polymers such as alginate, pectin and gellan showed effective DL and EE however, were ineffective as controlled release materials. By introducing stronger polymer-drug interactions by use of the sulfonated polymer carrageenan, higher DL and EE were achieved however, the gels still resulted in an instant release of the drug. A system composed of alginate and sodium silicate, a water soluble inorganic compound, allowed strong gels to be produced by the silica's interaction with the alginate crosslinking mechanism. This allowed strong gels where the silica reduced the degradation and porosity of the gel beads, enabling the release rate of the drug to be controlled. By varying the concentration of silica incorporated into the gel beads, release rates from hours to several weeks could be produced, making this blend of materials an attractive choice for encapsulation of water soluble drugs.

The alginate-sodium silicate blend was developed into a microparticulate drug delivery system where two methods were investigated, the w-o emulsion and spray drying. In the w-o emulsion method, effects of polymer concentration, mixing speed, surfactant concentration and alginate: sodium silicate on particle size and formation were investigated by microscopy and particle sizing. By increasing the polymer concentration, the particle size increased due to the increase in polymer viscosity. Also, with increasing surfactant concentration and mixing speed, both of these parameters saw the particle size decreased due to the decreased surface tension and increased shear respectively. Also, by increasing the crosslinking concentration, higher calcium ion concentrations were available to crosslink the polymer chains, enabling fine particulate powders which spherical geometries to be produced. Despite

fine particles being produced, no drug loaded particles could be produced due to the migration of drug into the oil phase during the manufacturing process.

The spray drying method was investigated due its ability to produce particles with high DL and EE. Processing parameters of polymer concentration, inlet temperature, polymer flow rate and alginate: silicate and their effects on particle formation were once again investigated. Along with these, effects of alginate concentration, drug concentration and alginate: silicate on DL/EE and drug release rate of the particles was also investigated. With increasing alginate concentration and flow rate, the particle size increased due to increasing in viscosity and flow rate making atomization less efficient. Varying the inlet temperature had no effect on the size of the particles however particles produced at low temperatures resulting in aggregated products due to inefficient drying. Particles produced by this method required crosslinking post-production where the particles took on aggregated formations due to their high surface areas which increased when the ratio of silicate: alginate increased. As for the DL/EE and drug release, all formulations gave controlled release over a 4 hour period where little effect of varying the process parameters was seen due to the particles small size and high surface area. Despite this, the particles produced did offer an attractive improvement over pure alginate particles that suffer limited loaded and instant release rates.

Once an optimum drug loaded microparticulate system was obtained, production of the PIP system was explored. Initially, methods for production of large particles in the TACE size range was investigated where the w-o emulsion and nozzle vibrating methods were chosen. In the w-o emulsion, embolizing spheres were produced from kappa carrageenan where effects of the mixing speed on particle size were investigated where increased mixing speed resulting in smaller particles. Also, the temperature of the oil was an important factor in order to obtain particles of a desired size specific to TACE. These particles displayed spherical geometries however suffered from wide size distributions which could be overcome by sieving for a

desired particle size. Various concentrations of drug loaded particles were loaded into the embolic spheres where they were uniformly distributed with high loadings and entrapment efficiencies. The spheres also displayed similar release rates to that of the drug delivery particles indicating that the effect of particle size on release rate was decoupled due to the porous nature of the carrageenan spheres. Despite this conclusion, further investigation would be required since the release period was rather short and the clustery nature of the drug delivery particles resulting in larger standard deviations.

The nozzle vibration method was also investigated to produce the embolizing spheres since it is a method that is yet to be explored in the literature and also allows ideal embolizing particles to be produced under mild processing conditions. Effects of nozzle size, vibrating frequency and electrode voltage on particle formation were investigated. By increasing the vibration frequency and electrode voltage particle size decreased due to the polymer being broken down into smaller droplets and decreased aggregation of the gelling polymer droplets. By increasing nozzle size, the particle size as expected increases. As well as producing spheres, the encapsulation unit also allowed capsules to be produced where mineral oil was entrapped within alginate shells. Effects of polymer and oil flow rates along with shell nozzle size were investigated. The alginate and oil flow rates had to be carefully controlled to allow spherical capsules with a single oil core to be produced. When flow rates were to high/low, aggregated capsules with multiple/no cores were the result. Due to the clustery nature of the drug delivery particles, they could not be encapsulated into the spheres or capsules. Therefore, to make use of this method for a drug delivery application, the alginate-silicate blend was processed into microspheres. Effects of polymer concentration, alginate: silicate ration and nozzle size on DL/EE and drug release were investigated upon increasing each parameter, various loadings and release rates up to 48 hours were obtained.

Despite the range of concepts covered in this thesis, there are still many other questions to be answered and areas to left to investigate. Firstly, this system still falls short of the drug release rates when compared to the DC bead where delivery times up to 2 weeks can be achieved. By incorporation of polymers containing sulfonate groups (the functional group used in the DC bead) or perhaps sulfonating a hydroxyl/carbonyl group into the alginate backbone, this could possibly allow longer release rates of the verapamil hydrochloride in the alginate-sodium silicate blend to be achieved. Investigation into alginate with higher G content to increase the gel strength could result in improved controlled release from the large hydrogel beads and the particles produced with the microencapsulator. However this increase in gel strength from higher G content alginate may not be sufficient enough to significantly increase the release from the small drug delivery particles due to their high surface area.

Release of doxorubicin hydrochloride would also have to be investigated. The drug has a higher molecular weight and lower water solubility than verapamil hydrochloride where these chemical properties could result in slower release rates than verapamil in this thesis.

The in-vitro drug release method used also needs to be addressed. In this thesis the PIPs were simply mixed in a solution of PBS which is different to the conditions the PIPs will be exposed too once they have embolized the tumour. Blood will flow with a pulsating rate which has a higher viscosity than a PBS solution. Preforming the in-vitro release in conditions that simulate the PIPS blocking the blood vessels surrounding the tumour would allow more accurate drug delivery profiles to be obtained, perhaps by injecting the PIPs into silica tubing and constantly pumping a volume of media with the viscosity increased with a polymer.

Also investigation into other materials that could potentially prolong release rate would make an interesting study. It would be worth researching materials that can interact with the amine groups in chitosan, a positively charged polymer, allowing encapsulation and controlled release of negatively charged small molecular weight hydrophilic drugs.

Further work could have been performed to improve the morphology of the spray dried alginate-sodium silicate microparticles which were aggregated to a high degree, making their encapsulation in the microencapsulator not possible. This was believed to be due to their high surface area and cohesive forces causing them to aggregate and cluster in the crosslinking process. Assessment of their stability by assessment of their zeta potential could allow this issue to be addressed with stronger conclusions. Microparticle systems with low zeta potentials (between -30 and +30) do not have ions that allow the particles to repel and stay uniformly distributed resulting in aggregated particulate systems. When these unstable aggregated systems are crosslinked post production, the particles can bind with adjacent particles giving the highly aggregated crosslinked product opposed to a more favoured uniformly distributed population of particles. The pH of the crosslinking solution can also be having a strong influence on the particle formation where the pH of the calcium chloride solution could be decreasing the stability of the particulate dispersion even further. If the drug delivery particles were in an unstable range, addition of agents to adjust the charge of the particle could be explored. A method that has frequently been explored to adjust the charge in the bilayers in liposome drug delivery systems which could adjust the charge of the particles to produce a more stable system.

The ionic gelation method may also allow production of a more uniformly dispersed particulate system produced from the alginate-sodium silicate blend which could be reinforced with chitosan, however since dilute concentrations of polymers are needed, this

system may be incapable of controlled release, however may be an attractive method for obtaining high drug loadings.

Also, since the system is designed to be more versatile to a wider variety of drugs, other active agents such as negatively charged/no charge, hydrophobic, large molecular weight and multiple drug molecules would need to be addressed. For these other classes of drugs, it is more than likely that investigation into other materials/material blends that allow controlled release would be necessary as the alginate-silicate blend may not work as well with these other classes. Liposomes may make attractive delivery systems for multiple drugs since both hydrophilic and hydrophobic can be encapsulated in the lipid core and lipid bilayers respectively, however they tend to have issues in stability and can be inefficient for high drug loading and controlled release of hydrophilic molecules.

Finally, once produced, the PIPs would require a serialization procedure since it is to be delivered by the parental route. Therefore sterilization methods such as treatment in alcohol or radiation and their effects on the drug delivery vehicle and drug molecule insuring its activity is not altered is of great significance. However the spray drying method and microencapsulation units used in this work allows sterile production therefore can potentially allow for this step to be avoided.

REFERENCES

1. Alazawi W, Cunningham M, Dearden J, Foster G (2010) Systematic review: outcome of compensated cirrhosis due to chronic hepatitis C infection *Aliment Pharmacology Therapy* (32) 344–55
2. Assifaoui A, Bouyer F, Chamblin O, Cayot P (2013) Silica-coated calcium pectinate beads for colonic drug delivery *Biomaterials* (9) 6218 – 6225
3. Alnaief M, Alzaitoun M, García-González C, Smirnova I (2011) Preparation of biodegradable nanoporous microspherical aerogel based on alginate. *Carbohydrate Polymers* (84) 1011 - 1018
4. Billany M.R (2007) Aulton's Pharmaceutics Third Edition – The design and manufacture of Medicines. Chapter 5 Suspension and Emulsions
5. Benchabane S, Subirade M, Vanderberg G (2007) Production of BSA loaded alginate microcapsules Influence of spray dryer parameters on the microcapsule characteristics and BSA release. *Journal of Microencapsulation*. 24 (6) 567 – 576
6. Burey P, Bhandarii B, Howes T, Gidley M (2009) Gel particles from spray-dried disordered polysaccharides *Carbohydrate Polymers* (76) 206–213
7. Belghiti J, Hiramatsu K, Benoist S (2000) Seven hundred forty seven hepatectomies in the 1990s: an update to evaluate the actual risk of liver resection. *Journal of the American College of Surgeons* (191) 38-46

8. Birdi G, Bridson H, Smith A, Grover L. (2012) Modification of alginate degradation properties using orthosilicic acid. *Journal of the mechanical behaviour of biomedical materials*. (6) 181 – 187.
9. Bonferoni M, Sandri G, Gavini E, Rossi S, Caramella C. (2007) Microparticulate systems based on polymer-drug interaction for ocular delivery of ciprofloxacin – In vitro characterisation. *Journal of Drug Delivery Science and Technology*. 17 (1) 57 – 62.
10. Brannon-Peppas L. (1997) Polymers in controlled delivery. *Medical Plastics and Biomaterials Magazine* Nov 34
11. Bruix J, Sherman M (2005) Practice Guidelines Committee, American Association for the Study of Liver Diseases. Management of hepatocellular carcinoma. *Hepatology*. (42) 1208-1236
12. Barea M, Jenkins M, Lee Y, Johnson P, Bridson R. (2012) Encapsulation of Liposomes within pH Responsive Microspheres for Oral Colonic Drug Delivery *International Journal of Biomaterials* (32) 34 – 42
13. Brandenberger H, Widmer F. (1998) A new multinozzle encapsulation immobilisation system to produce uniform beads of alginate. *Journal of Biotechnology* (63) 73–80
14. Calle E, Rodriguez C, Walker-Thurmond K, Thun M. (2003) Overweight, obesity, and mortality from cancer in a prospectively studied cohort of US adults. *New England Journal of Medicine* (348) 1625–38.

15. Croswell J, Kramer B. (2010) Principles of cancer screening: lessons from history and study design issues. *Seminars in Oncology* (37) 202–215.
16. Cho A, Chun Y, Kim B, Park D. (2014) Preparation of Chitosan–TPP Microspheres as Resveratrol Carriers. *Journal of Food Science*. 79 (4) 568 – 576
17. Robinson D. (2003) Polymer relationships during preparation of chitosan-alginate and poly-l-lysine-alginate nanospheres. *Journal of Controlled Release*. 89 (1) 101–12
18. Desai H (2005). Encapsulation of vitamin C in tripolyphosphate cross-linked chitosan microspheres by spray drying. *Journal of Microencapsulation* 22 (2) 179 - 192.
19. Donato F, Boffetta P, Puoti M. (1998) A meta-analysis of epidemiological studies on the combined effect of hepatitis B and C virus infections in causing hepatocellular carcinoma. *International Journal of Cancer* (75) 347-354.
20. Draget I, Skjærbæk G, Christensen E, Gæserød O, Smidsrød O. (1996) Swelling and partial solubilisation of alginic acid gel beads in acidic buffer. *Carbohydrate polymers*. 29 (3) 209 – 215.
21. Enderle J, Blanchard S, Bronzino J. (2005) Biomaterials – properties, types and applications. Introduction to biomedical engineering. Academic Press San Diego California
22. Ellis A, Jacquier J. Manufacture of food grade kappa carrageenan microspheres. *Journal of Food Engineering* (94) 316–320
23. El-Serag H. (2011) Hepatocellular carcinoma. *New England Journal of Medicine* (365) 1118–27.

24. Erinjeri J, Salhab H, Covey A, Getrajdman G, Brown K (2010) Arterial patency after repeated hepatic artery bland particle embolization. *Journal of Vascular and Interventional Radiology* (21) 522-526

25. Estevinho B, Rocha F, Santos L, Alves A. (2013) Microencapsulation with chitosan by spray drying for industry applications. *Trends in Food Science & Technology* (31) 138 - 155

26. Ferlay J, Shin H, Bran H, Forman D, Mathers C, Parkin D. (2008) Estimates of worldwide burden of cancer in 2008. *International Journal of Cancer* (127) 2893–2917.

27. Forner A, Reig M, de Lope C, Bruix J (2010) Current strategy for staging and treatment: the BCLC update and future prospects. *Seminars in Liver Disease* (30) 61-74

28. Gupta P, Vermani K, Garg S (2002) Hydrogels: from controlled release to pH responsive drug delivery. *Drug Discovery Today* 7 (10) 569 – 579.

29. Garrait G, Beyssac E, Subirade M (2014) Development of a novel drug delivery system: chitosan nanoparticles entrapped in alginate microparticles *Journal of Microencapsulation* 31 (4) 363 – 372

30. Gaudio P, Colombo P, Colombo G, Russo P, Sonvico F. (2005) Mechanisms of formation and disintegration of alginate beads obtained by prilling. *International Journal of Pharmaceutics* (302) 1–9

31. Gilberto C, Iannuccelli V, Leo E, Bernabei M, Cameroni R. (2001) Chitosan-Alginate Microparticles as a Protein Carrier. *Drug Development and Industrial Pharmacy* 27 (5) 393–400
32. Graziadei I, Sandmueller H, Waldenberger P (2003) Chemoembolization followed by liver transplantation for hepatocellular carcinoma impedes tumor progression while on the waiting list and leads to excellent outcome. *Liver Transplant.* (9) 557-563.
33. Hasheminya M, Singhania R, Sabarinath C, Pandey A. (2003). Fermentative production of gellan using *Sphingomonas paucimobilis*. *Process Biochemistry* (38) 1513-1519.
34. Hassan A, Sapin A, Lamprecht A, Emond E, Ghazouani F, Maincent P (2009) Composite microparticles with in vivo reduction of the burst release effect. *European Journal of Pharmaceutics and Biopharmaceutics* (73) 337–344
35. Hoffman S (2002). Hydrogels for Biomedical Applications. *Advance Drug Delivery Reviews* 54 (1) 3 – 12
36. Hasheminya S, Dehghannya J, (2013) An overview on production and applications of gellan biopolymer. *International Journal of Agriculture and Crop Sciences.* 5 (24) 3016 – 3019
37. Imamura H, Matsuyama Y, Tanaka E (2003) Risk factors contributing to early and late intrahepatic recurrence of hepatocellular carcinoma after hepatectomy. *Journal of Hepatology* (38) 200-207.

38. Jose S, Prema M, Chacko A, Thomas A, Souto E. (2011) Colon specific chitosan microspheres for chronotherapy of chronic stable angina *Colloids and Surfaces B: Bio interfaces* (83) 277–283
39. Kim M, Kim J, Lee H, Kim J, Yang J. (2005) Release property of temperature-sensitive alginate beads containing poly(N-isopropylacrylamide). *Collids and Surfaces* (46) 57–61
40. Kaye R, Purewal T, Alpar H. (2008) Simultaneously Manufactured Nano-In-Micro (SIMANIM) Particles for Dry-Powder Modified-Release Delivery of Antibodies. *Journal of Pharmaceutical Sciences* 98 (11) 4055 – 4068
41. Kishore N, Unnikrishnan D, Govindaraj R, Devendiran R, Celladurai K, Pully N. (2012) Effect of Formulation Variables on Rifampicin Loaded Alginate Beads. *Iranian Journal of Pharmaceutical Research* 11 (3) 715-721
42. Kao C, Matsuno-Yagi A, Yagi T (2004). Subunit proximity in the H⁺-translocating NADH-quinone oxidoreductase probed by zero-length crosslinking. *Biochemistry* 43 (12) 3750-3755
43. Kashyap N, Kumar N and Kumar R. (2005) Hydrogels for Pharmaceutical and Biomedical applications. *Critical reviews in Therapeutic Drug Carrier systems* 22 (2) 107 – 149
44. Kunal P, Paulson A, Rousseay D. (2009) Modern Biopolymer Science – Chapter 16 Biopolymers in controlled-release delivery systems.

45. Liang L, Hu S, Ni Y, Wu H, Chen F, Liao J. (2006). Effect of hydrocolloids on pulp sediment, white sediment, turbidity and viscosity of reconstituted carrot juice. *Food Hydrocolloids*. (20) 1190-1197.
46. LinShu L, Marshall L, Joseph K, Hicks K. (2003) Pectin-based systems for colon-specific drug delivery via oral route. *Biomaterials*. (24) 3333–3343.
47. Liu H, Elliott S, T Webster. (2006) Less harmful acidic degradation of poly(lactico-glycolic acid) bone tissue engineering scaffolds through titania nanoparticle addition. *International Journal of Nanomedicine*. 1 (4) 541–545
48. Lovino M, Cardinal F, Zubiri V, Bernik L. (2005) Electronic nose screening of ethanol release during sol–gel encapsulation: a novel non-invasive method to test silica polymerisation. *Biosensors and Bioelectronics* (21) 857– 862
49. Lee J, Chung D, Lee H. (2008) Preparation and characterization of calcium pectinate gel beads entrapping catechin-loaded liposomes. *International Journal of Biological Macromolecules* (42) 178–188
50. Lee H, Park O, Park J, Yang J (1996) Continuous Production of Uniform Calcium Alginate Beads by Sound Wave Induced Vibration. *Journal of Chemical Technology and Biotechnology*. (67) 255-259
51. Lam V, Chok K. (2008) Risk factors and prognostic factors of local recurrence after radiofrequency ablation of hepatocellular carcinoma. *Journal of American Collage of Surgeons* (207) 20 – 29

52. Laurent A, Beaujeux R, Wassef M (1996) Trisacryl gelatin microspheres for therapeutic embolization, I: development and in vitro evaluation. *American Journal of Neuroradiology* (17) 533–540
53. Laurent A, Wassef M, Chapot R (2004) Location of vessel occlusion of calibrated tris-acryl gelatin microspheres for tumor and arteriovenous malformation embolization. *Journal of Vascular and Interventional Radiology* (15) 491–496
54. Laurent A, Wassef M, Saint Maurice J (2006) Arterial distribution of calibrated tris-acryl gelatin and polyvinyl alcohol microspheres in a sheep kidney model. *Investigate Radiology* (41) 8–14
55. Lencioni R (2012) Chemoembolization in patients with hepatocellular carcinoma. *Liver Cancer* (1) 41–50.
56. Liapi E, Lee L, Georgiades C (2007) Drug-eluting particles for interventional pharmacology. *Techniques in Vascular and Interventional Radiology* (10) 261–269
57. Livraghi T, Goldberg S, Lazzaroni S, Meloni F, Solbiati L, Gazelle G (1999). Small hepatocellular carcinoma: treatment with radio-frequency ablation versus ethanol injection. *Radiology* (210) 655 - 661.
58. Lencioni R (2012) Chemoembolization in patients with hepatocellular carcinoma. *Liver Cancer* (1) pgs 41–50.

59. Llovet J, Fuster J, Bruix J (1999) Intention-to-treat analysis of surgical treatment for early hepatocellular carcinoma: resection versus transplantation. *Hepatology*. (30) 1434-1440.
60. Liu W, Liu J, Liu W, Li T, Liu C. (2013) Improved Physical and in Vitro Digestion Stability of a Polyelectrolyte Delivery System Based on Layer-by-Layer Self-Assembly Alginate–Chitosan-Coated Nanoliposomes. *Journal of Agricultural Food Chemistry* (61) 4133–4144
61. Lorenzo-Lamosa M, Lopez C, Vila-Jato J, Alons M. (1998). Design of microencapsulated chitosan microspheres for colonic drug delivery. *Journal of Controlled Release* 52 (12) 109 – 118
62. Liang L, Hu S, Ni Y, Wu H, Chen F, Liao J. (2006). Effect of hydrocolloids on pulp sediment, white sediment, turbidity and viscosity of reconstituted carrot juice. *Food Hydrocolloids*. (20) 1190-1197.
63. LinShu L, Marshall L, Joseph K, Hicks K. (2003) Pectin-based systems for colon-specific drug delivery via oral route. *Biomaterials*. (24) 3333–3343.
64. Liu H, Elliott B S, T J Webster. (2006) Less harmful acidic degradation of poly(lactico-glycolic acid) bone tissue engineering scaffolds through titania nanoparticle addition. *International Journal of Nanomedicine*. 1 (4) pgs 541–545
65. Lovino M, Cardinal F, Zubiri V, Bernik L. (2005) Electronic nose screening of ethanol release during sol–gel encapsulation: a novel non-invasive method to test silica polymerisation. *biosensors bioelectronics* (21) 857– 862

66. Madhav N, Kala S (2011) Review on Microparticulate Drug Delivery System
International Journal of Pharmaceutical Technology Research 3 (3) 1242-1254
67. Mladenovska K, Cruaud O, Richomme P, Belamie E, Raicki E (2007) 5-ASA loaded chitosan–Ca–alginate microparticles: Preparation and physicochemical characterization. *International Journal of Pharmaceutics* 3 (45) 59–69
68. K. Mobus, J. Siepmann, R. Bodmeier. (2012) Zinc–alginate microparticles for controlled pulmonary delivery of proteins prepared by spray-drying. *European Journal of Pharmaceutics and Biopharmaceutics* (81) 121–134
69. Mahesh C, Ayman K, Yogesh P, Hitesh H, Jayanth P. (2007) Polymer surfactant nanoparticles form controlled release of hydrophilic drugs. *Journal of Pharmaceutical sciences*. 96 (12) 3379 – 3389
70. Mayur G, Sankalia C, Jolly M, Viljay B. (2006) Physicochemical Characterization of Papain Entrapped in Ionotropically Cross-Linked Kappa-Carrageenan Gel Beads for Stability Improvement Using Doehlert Shell Design. *Journal of Pharmaceutical Sciences* (95) 1994–2013
71. Mitra J, Leila B, Farhad B. (2014) Preparation of Chlorpheniramine Maleate-loaded Alginate/Chitosan Particulate Systems by the Ionic Gelation Method for Taste Masking. *Journal of National Pharmaceutical Products*. 9 (1) 39-48.
72. McBride A, Price D, Lamoureux L, Elmaoued A. (2013) Preparation and Characterization of Novel Magnetic Nano-in-Microparticles for Site-Specific Pulmonary Drug Delivery. *Molecular Pharmaceutics* (10) 3574–3581

73. Moffat L, Marra G. (2004) Biodegradable poly-(ethylene glycol) hydrogels crosslinked with genipin for tissue engineering applications. *Journal of Biomedical Materials and Research* 71b (1) 181 – 187
74. Mrunalini N, Praveen S, Atmaram P (2010). Stomach-Specific Controlled Release Gellan Beads of Acid-Soluble Drug Prepared by Ionotropic Gelation Method. *American association of pharmaceutical sciences*. 11 (1) 267 – 277
75. Mazzaferro V, Regalia E, Doci R (1996) Liver transplantation for the treatment of small hepatocellular carcinomas in patients with cirrhosis. *New England Journal of Medicine* (334) 693-699.
76. Makuuchi M, Sukigara M, Mori T (1985) Bile duct necrosis: complication of transcatheter hepatic arterial embolization. *Radiology* (156) 331–334
77. Maluccio M, Covey A. (2012) Recent Progress in Understanding, Diagnosing, and Treating Hepatocellular Carcinoma *American Cancer Society* 62 (6) 394 – 399
78. Maeda N, Osuga K, Higashihara H (2010) In vitro characterization of cisplatin-loaded superabsorbent polymer microspheres designed for chemoembolization. *Journal of Vascular and Interventional Radiology* (21) 877–881
79. Nagasawa N, Yagi T, Kume T, Yoshii F. (2004) Radiation crosslinking of carboxymethylstarch. *Carbohydrate Polymers* (58) 109-113
80. Ostberg T, Lund E M and Graffner C. (1994) Calcium alginate matrices for oral multiple unit administration: IV release characteristics in different media. *International Journal of Pharmaceutics*. (112) 241-248.

81. Osuga K , Maeda N, Higashihara H, Hori S, Nakazawa T, Tanaka K (2012) Current status of embolic agents for liver tumor embolization. *International Journal of Clinical Oncology* (17) 306–315
82. K. Osuga, H. Anai, M. Takahashi (2009) Porous gelatin particles for hepatic arterial embolization; investigation of the size distribution and fragmentation before and after microcatheter passage. *Journal of Vascular and Interventional Radiology* (36) 437–442
83. Parkin D, Bray F, Ferlay J (2001) Estimating the world cancer burden. *International Journal of Cancer* (94) 153-156.
84. Padalkar N, Shahi S, Thube M. (2011) Microparticles: An approach to betterment of drug delivery system. *International Journal of Pharmaceutical Development* 3 (1) 99 – 115
85. Pasparakis G, Bouropoulos N (2006). Swelling studies and in vitro release of verapamil from calcium alginate and calcium alginate–chitosan beads. *International Journal of Pharmaceutics* (323) 34–42
86. Peppas A. (1987) Hydrogels in medicine and Pharmacy. CRC Press, Boca Raton, FL, Vols I – III
87. Pouponneau J, Leroux G, Soulez L, Gaboury S. (2011) Co-encapsulation of magnetic nanoparticles and doxorubicin into biodegradable microcarriers for deep tissue targeting by vascular MRI navigation. *Biomaterials* (32) 3481 – 3486

88. Petite H, Frei V, Huc A and Herbage D. (1994). Use of diphenylphosphorylazide for crosslinking collagen based biomaterials. *Journal of Biomedical Materials Research* 28 (2) 159 – 165.
89. Parikh S, Hyman D. (2007) Hepatocellular Cancer: A Guide for the Internist. *The American Journal of Medicine* (120) 194-202
90. Rajaonarivony M, Vauthier C, Couarraze G, Puisieux F, Couvreur P. (1993) Development of a new drug carrier made from alginate. *Journal of Pharmaceutical Science* (82) 912–918
91. Richardson J, Harker J, Backhurst J (2002). Chemical Engineering Volume 2 – Particle Technology and Separation Processes 5th Edition – Chapter 16 Drying
92. Roberto J, de Souza R, Feitosa J, Ricardo R. (2013) Spray-drying encapsulation of mangiferin using natural polymers. *Food Hydrocolloids* (33) 10 – 18
93. Sherman M. (2010) Hepatocellular carcinoma: epidemiology, surveillance, and diagnosis. *Seminars in Liver Disease* (30) 3–16.
94. Singal A, Volk M, Waljee A. (2009). Meta-analysis: surveillance with ultrasound for early-stage hepatocellular carcinoma in patients with cirrhosis. *Aliment Pharmacology Therapy* (30) 37–47.
95. Shiina S, Tateishi R, Arano T (2012) Radiofrequency ablation for hepatocellular carcinoma: 10-year outcome and prognostic factors. *American Journal of Gastroenterology*. (107) 569-577.

96. Sone M, Osuga K, Shimazu K (2010) Porous gelatin particles for uterine artery embolization: an experimental study of intra-arterial distribution, uterine necrosis, and inflammation in a porcine model. *Cardiovascular Interventional Radiology* (33) 1001–1008
97. Stampfl U, Radeleff B, Sommer C (2011) Midterm results of uterine artery embolization using narrow-size calibrated embosphere microspheres. *Cardiovascular Interventional Radiology* (34) 295–305
98. Stabler C, Wilks K, Sambains A, Constantinidis I. (2001) The effects of alginate composition on encapsulated bTC3 cells. *Biomaterials* (22) 1301–1310
99. Sugawara I, Otagiri M. (1994) The controlled release of prednisolone using alginate gel. *Pharmaceutical Research*. (11) 272-277.
100. Surajit D, Ka-yun N. (2010) Resveratrol-Loaded Calcium-Pectinate Beads: Effects of Formulation Parameters on Drug Release and Bead Characteristics. *Journal of Pharmaceutical Sciences*. (99) 2 - 12
101. Soni M, Kumar M, Namdeo K. (2010) Sodium alginate microspheres for extending drug release: formulation and *in vitro* evaluation. *International Journal of Drug Delivery*. (28) 64 – 68
102. Taleb A. (2008). Radiation synthesis of polyampholytic and reversible pH responsive hydrogel and its application as drug delivery system. *Polymer Bulletin* 61 (3) 341 – 351

103. Tahtat D, Mahlous M, Benamer S, Khodja A, Oumehdi H, Laraba-Djebari H. (2013) Oral delivery of insulin from alginate/chitosan crosslinked by Glutaraldehyde. *International Journal of Biological Macromolecules*. (58) 160 – 168
104. Tavakol M, Ebrahim V and Sameereh H. (2013) The effect of polymer and CaCl₂ concentrations on the sulfasalazine release from alginate-N,Ocarboxymethyl chitosan beads. *Progress in Biomaterials*. (2) 10 – 22
105. Vaidya A, Jain A, Khare P, Jain K. (2009) Metronidazole Loaded Pectin Microspheres for Colon Targeting. *Journal of Pharmaceutical Sciences* (98) 4229–4236
106. Vanbever R, Wang J, Nice J, Chen D, Langer R, Edwards D (1999) Formulation and Physical Characterization of large porous particles for inhalation. *Pharmaceutical Research* 16 (11) 1735 – 1742
107. Varma S, Sadasivan C. (2014) A long acting biodegradable controlled delivery of chitosan microspheres loaded with tetanus toxoide as model antigen. *Biomedicine and pharmacotherapy*. (68) 225 – 230
108. Vauthier C, Bouchemal K (2009) Methods for the preparation and Manufacture of Polymeric Nanoparticles. *Pharmaceutical Research* 26 (5) 1025 – 1058
109. Wong W, Chan W, Lee A. (2002) Release characteristics of pectin microspheres prepared by an emulsification technique. *Journal of Microencapsulation*. (4) 511 – 522.

110. Wang J, Chen J, Zong J, Zhao D, Li F, Zhuo R, and Cheng S. (2010) Calcium Carbonate/Carboxymethyl Chitosan Hybrid Microspheres and Nanospheres for Drug Delivery. *Journal of Physical Chemistry*. (114) 18940–18945
111. Willatt J, Francis I, Novelli P, Vellody R. (2012) Interventional therapies for hepatocellular carcinoma *International Cancer Imaging Society* (12) 79 – 88
112. Xu Y, Zhan C, Fan L, Wang L, Zheng H. (2007) Alginate chitosan blend gel beads and in vitro controlled release in oral site-specific drug delivery systems. *International Journal of pharmaceutics* 3 (36) 329–337
113. Yan K, Chen K, Yang W (2008) Radiofrequency ablation of hepatocellular carcinoma:long-term outcome and prognostic factors. *European Journal of Radioology* (67) 336-347.Zhang B, Yang B, Tang Z. (2004) Randomized controlled trial of screening for hepatocellular carcinoma. *Journal of Cancer Research and Clinical Oncology* 130 (7) 417-422.